Acid Deposition Research Program

Compressor Exhaust Chemistry and Wake Diffusion

by

R. J. VET
N. W. REID
E. ALP
S. J. DIEHL

A Concord Scientific Corporation Report

Alberta Petroleum Industry Government Environmental Committee

COMPRESSOR EXHAUST CHEMISTRY

AND WAKE DIFFUSION

Final Report To Alberta Petroleum Industry

Government Environmental Committee

Prepared By

R.J. Vet
N.W. Reid
E. Alp
S.J. Diehl

Concord Scientific Corporation

Report Number: 67-1

April 1982

TABLE OF CONTENTS

		Page
Executive Summary		v
Acknowledgements		xi
List of Figures		xii
List of Tables		xiv
1. Introduction		1
2. Background Information		5
2.1	Compressor Station Emissions	6
2.2	NO_x Chemistry Related to Compressor Station Emissions	8
2.3	Flow and Dispersion in the Vicinity of Buildings	12
2.4	Mathematical Modelling of Building Effects	32
2.4.1	Huber-Snyder Model	35
2.4.2	Briggs' Model	39
2.4.3	NRC Model	43
2.4.4	Dual Plume Model	48
2.4.5	Model Comparisons	59
3. Modelling of NO_2/NO_x Dispersion in the Wake of Gas Compressor Buildings		65
3.1	Description of the Compressor Station Chemistry Model	66

TABLE OF CONTENTS (Con't)

			Page
3.1.1	Dispersion Calculation.		66
3.1.2	Chemical Reaction Rate Module		67
3.1.3	Combination of Dispersion and Chemistry		74
3.1.4	Limitations of the CSC Model.		80
3.1.5	Computer Program.		90
3.2	Model Performance and Testing		92
3.2.1	Model Inputs and Conditions		92
3.2.2	Results		99
3.2.3	Model Characteristics		105
	3.2.3.1	Background Ozone Concentrations.	105
	3.2.3.2	In-Stack Ratio of NO_2 to NO_x.	107
	3.2.3.3	In-Stack NO_x Concentration and NO_x Mass Emission Rate	109
	3.2.3.4	Solar Intensity	110
	3.2.3.5	Atmospheric Stability . . .	112
	3.2.3.6	Stack Velocity.	113
	3.2.3.7	Wind Speed.	114
	3.2.3.8	Stack Height.	115
	3.2.3.9	Plume Rise.	116
	3.2.3.10	Summary	118

TABLE OF CONTENTS (Con't)

Page

3.3 Application of Model to Stack Design. 119

3.4 Application of the CSC Model to the Pendant D'Oreille Compressor Station. 127

3.5 Recommendations for Model Use and Improvement 133

4. Field Measurement Program 138

4.1 Required Measurements 140

4.2 Measurement Techniques. 147

4.2.1 Concentrations of NO and NO_2. 148

4.2.2 Model Input Variables 154

4.2.3 Model Parameterizations 156

4.2.4 Support Measurements. 157

4.2.5 Other Measurements. 158

4.3 Field Program Design. 159

4.3.1 Model Validation Study. 159

4.3.2 Model Verification Study. 167

4.4 Summary 169

5. Conclusions and Recommendations 171

References. 175

Appendix A: Data for an Alberta Compressor Station . . . 182

Appendix B: Typical Model Output 184

EXECUTIVE SUMMARY

This report reviews the three-stage work program carried out to fulfill Phase I of the Compressor Exhaust and Wake Diffusion Study. The objectives of the work program were:

- to determine the relationship between NO_2 and NO_x concentrations in the plume of a gas compressor facility.

- to determine the effects of air flow distortion by a compressor building on ground-level concentrations and NO to NO_2 conversion.

The first stage of the work program consisted of a detailed literature review, which indicated that:

1. Compressor emissions are highly variable from day to day, and from engine to engine to engine, and measured emissions are often different from those given in the manufacturer's specifications.

2. Traditional concepts of flow and diffusion around buildings do not incorporate many of the complexities recently observed by several investigators. The traditional view of flow about buildings is presented in Figure 1. It shows a region of aerodynamic distortion about the building which consists of flow zones - the displacement zone, the cavity and the

far wake. The displacement zone refers to the large area of displaced flow about the building; the cavity refers to the relatively steady-state recirculating flow zone immediately downwind of the building; the far wake refers to the zone of reduced wind speeds and enhanced turbulence immediately downwind of the cavity. Based on this concept, the movement of pollutants from the cavity to the far wake was thought to be due solely to turbulent transfer at the cavity boundary.

3. The more recent concept of flow about buildings is illustrated in Figure 2. The displacement zone, cavity and far wake are still considered to exist but the cavity is thought to be more variable and complicated in size and structure and the movement of pollutants from the cavity to the far wake is considered to be due, also, to flow streamlines and upper and lower level vortices crossing the cavity boundary. These mechanisms for material transfer out of the cavity and the existence of organized vorticity in the far wake have significant effects on ground level concentrations in the vicinity of gas compressor buildings.

4. Field studies of NO/NO_2 chemistry near compressor stations published to date have been limited in scope, and have not yielded conclusive results. A number of questions concerning chemistry in building wakes therefore remain unanswered.

5. One wake diffusion model, the Dual Plume Model, was most suitable for use in later portions of the work program, because it is able to treat explicitly trapping of all or part of the plume in the building cavity. This, in turn, provides a better framework for modelling the chemical reactions in the trapped and untrapped portions of the plume.

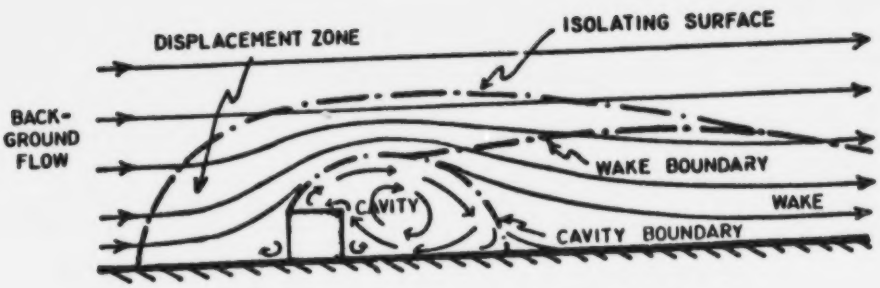

(a) SIDE VIEW

(b) PLAN VIEW

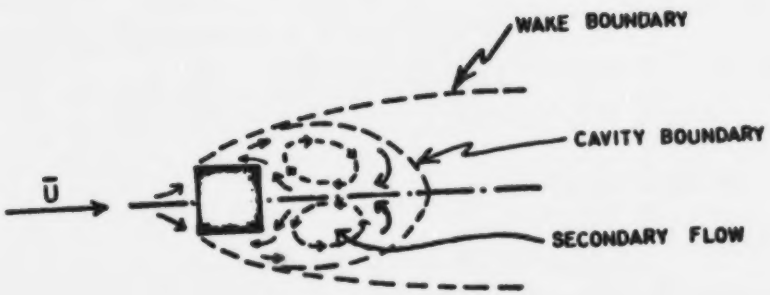

Figure 1: Original Concept of Flow About Buildings

(From Halitsky, 1968)

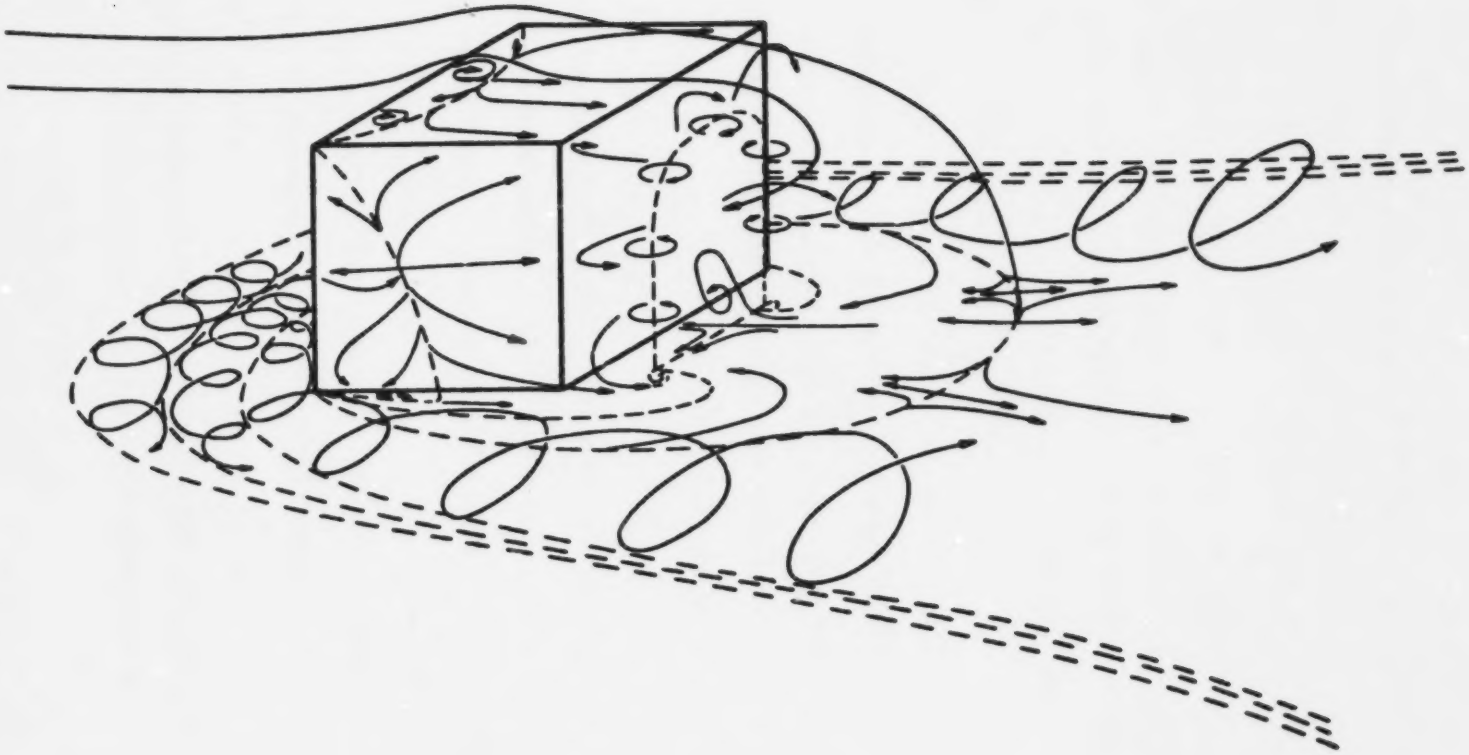

Figure 2: Current Concept of Flow About Buildings

(From Woo, et al, 1977)

The second part of the work program consisted of selecting, modifying and testing models to incorporate both NO/NO_2 reactive chemistry and wake diffusion (Note that $NO_x = NO + NO_2$). The Compressor Station Chemistry Model (CSCM) was developed as a tool to determine required stack heights. It uses a combination of the American Gas Association's Dual Plume Model for wake diffusion and Concord Scientific's expanding box model for wake chemistry.

The CSCM was used to carry out a series of calculations to predict ground level concentrations of NO and NO_2 downwind of a 'typical' compressor station for Alberta under 'typical' operating and atmospheric conditions. Stack heights were also designed using the model. The calculations indicated the following:

1. For typical isolated compressors (approximately 1150 KW) emitting up to 4.2 g NO_2/s stack heights seldom need to exceed 1.5 times the height of the building to prevent air quality exceedences;

2. Maximum concentrations of NO_2 tend to occur in the building cavity region except under light wind conditions, and

3. Maximum ground-level concentrations of NO and NO_2 generally occur within 50 m of each other but are not necessarily coincident.

The following recommendations were made:

1. Caution should be exercised in applying the results of the model calculations to full-scale compressor stations until the model can be verified experimentally (i.e. in Phase II of the Compressor Exhaust and Wake Diffusion Study).

2. The CSCM should be further refined to improve several of its current limitations; or a new Lagrangian model should be developed to eliminate these limitations altogether.

The final stage of the work program consisted of designing a field measurement program to answer many of the questions about wake diffusion and NO/NO_2 chemistry. In doing this, the measurement program should also evaluate and verify the predictive capability of the CSCM so that it can be used as a tool for designing compressor station stack heights. The field program was, therefore, designed with the CSCM as the framework for determining which measurements were to be carried out. The program was designed to consist of two field studies - a model evaluation study and a model verification study. The purpose of the former is to provide data to assess the predictive capability of the model and to adjust the model using empirical results to increase its predictive accuracy; the purpose of the latter is to quantify the predictive accuracy of the evaluated model using an independent data set. The design of both studies called for concurrent measurements of ground level NO and NO_2 concentrations, source emission rates and meteorological, building and background chemistry parameters. Other specialized measurements were

also designed into the studies to provide more information on the accuracy of the physical foundations of the CSCM. Actual measurement methods and field sampling protocols were presented for both studies.

ACKNOWLEDGEMENTS

The authors would like to express their thanks to Mr. R.P. Angle (Alberta Environment) and Dr. H.F. Thimm (Energy Resources Conservation Board) for their direction, comments and helpful discussions during the course of this study. Thanks are extended, also, to the other members of APIGEC-SCAGE for their comments on the draft report.

LIST OF FIGURES

		Page
1.	Original Concept of Flow About Buildings (from Halitsky, 1968).	vii
2.	Current Concept of Flow About Buildings (from Woo, et al., 1977)	viii
3.	Huber-Snyder Model Flowchart	38
4.	Briggs Model Flowchart	42
5.	NRC Model Flowchart.	47
6.	Dependence of α on h_s/H_B and $V_s/\bar{U}$ (from Engineering-Science, 1980b).	55
7.	Dual Plume Model Flowchart	57
8.	Comparison of Full and 2-Step Mechanisms	73
9.	Dual Plume Formulation as Used in Compressor Station Chemistry Model.	75
10.	Configuration of the Buildings Modelled.	94
11.	Model Input Conditions	98
12.	Variation of NO_2 Concentration with Downwind Distance: Case 1.	101
13.	Dependence of Maximum Ground Level NO_2 Concentration on Stack Height: Case 7.	121
14.	Dependence of Maximum Ground Level NO_2 Concentration on Stack Height: Cases 2, 10 and 12.	122
15.	Dependence of Maximum Ground Level NO_2 Concentration on Stack Height: Worst Likely Case.	123
16.	Dependence of Maximum Ground Level NO_2 Concentration on Stack Height: Downwind of Cavity: Cases 1, 3 and 4.	126

LIST OF FIGURES (Con't)

		Page
17.	Pendant D'Oreille Compressor Station Plot Plan.	128
18.	Proposed Sampling Array.	149
19.	Field Organization of Measurements	163
20.	Variation of NO_2 Concentration with Downwind Distance: Case 1	186
21.	Variation of NO_2 Concentration with Downwind Distance: Case 2	188
22.	Variation of NO_2 Concentration with Downwind Distance: Case 3	190
23.	Variation of NO_2 Concentration with Downwind Distance: Case 4	192
24.	Variation of NO_2 Concentration with Downwind Distance: Case 7	195
25.	Variation of NO_2 Concentration with Downwind Distance: Worst Likely Case.	205

LIST OF TABLES

		Page
1.	Nomenclature for Model Summaries.	33
2.	Comparison of Models.	59
3.	Model Evaluation Summary.	61
4.	Chemical Reaction Mechanism	69
5.	Exponents in the Expression $V = \beta t^m + 1$.	78
6.	Dependence of NO_2/NO_x on Exponent in $V = \beta t^m + 1$ . . .	82
7.	Values of the Two Terms Involved in In-Plume Ozone Production.	86
8.	Effect of Different Adjustments for One Hour Averaging Time.	90
9.	Sample of Model Output: Case 1	100
10.	Effect of Increased Ambient Ozone Concentration . . .	106
11.	Effect of Decreased In-Stack NO_2/NO_x Ratio.	108
12.	Effect of Reduced Solar Intensity	111
13.	Effect of Reduced Plume Rise.	117
14.	Source Conditions for Pendant D'Oreille Compressor Station.	127
15.	Model Results for Pendant D'Oreille Compressor Station: V_s = 50 m/s	130
16.	Model Results for Pendant D'Oreille Compressor Station: V_s = 24 m/s	131
17.	Source Characteristics.	103

1. INTRODUCTION

Concord Scientific Corporation was contracted in June, 1981 by Alberta Environment and The Energy Resources Conservation Board acting on behalf of the Alberta Petroleum Industry Government Environmental Committee (APIGEC) to carry out a study entitled "Compressor Exhaust Chemistry and Wake Diffusion - Phase I". The objectives of this study were twofold:

1. To determine the relationship between NO_2 and NO_x concentrations in the plume of a gas compressor facility.

2. To determine the effects of air flow distortion by a compressor building on ground-level concentrations and NO to NO_2 conversion.

These objectives reflect concern of APIGEC over the potential impact of gas compressor emissions on local air quality. APIGEC estimates that compression facilities in Alberta emit roughly 40% of the total provincial NO_x emissions constituting approximately 135,000 t/y NO_x (APIGEC, 1981). Although emissions from individual compressor facilities are relatively small (1.5 to 15 g/s NO_x), local air quality can be jeopardized if the emissions are not sufficiently diluted by the time they reach ground level. It is therefore necessary to construct exhaust stacks at the appropriate height to keep ground level concentra-

tions below Alberta's ambient air quality objective, which is 400 $\mu g/m^3$ NO_2 as an hourly average. Because the objective is written in terms of NO_2 while emissions are predominantly in the form of NO at release and because dispersion of the emissions is complicated by aerodynamic distortion around the compressor building, it was necessary, in the past, to adopt a non-traditional design method for compressor station stacks. This included (1) setting a minimum stack height equal to 1.5 times the building height (based on the assumption that this would be sufficient to prevent entrainment of the plume into the building wake) and (2) assuming 40% of the emitted NO_x exists in the form of NO_2. However, industry estimated that implementation of the stack designs based on this method would cost roughly $20 million. Considering these financial implications, it was reasonable to question the accuracy and suitability of the design method. Hence APIGEC issued the contract to Concord Scientific Corporation with the aforementioned objectives. To meet these objectives, a work program consisting of three parts was designed. They were:

1. To examine critically all research and literature related to compressor emissions, atmospheric NO/NO_2 chemistry, flow and dispersion in the vicinity of buildings and building wake dispersion models.

2. To select, modify, and test models which incorporate both NO/NO_2 reactive chemistry and wake diffusion (note that $NO_x = NO + NO_2$). The model should ultimately be used as a tool for determining required stack heights.

3. To design a field measurement program to answer many of the key questions about NO/NO_2 chemistry and wake diffusion and, in doing so, provide data for assessing the predictive capability of the stack design model.

The first part of the work program, the critical examination of literature was designed to provide a comprehensive understanding of the state-of-the-art in all areas related to chemistry, dispersion, and modelling in the vicinity of compressor stations. It consisted of producing an annotated bibliography of all literature available on these subjects.

Because of the length of the bibliography, it has been published under separate cover and is available from APIGEC. However, the most important findings in the areas of compressor emissions, NO/NO_2 chemistry, flow and dispersion about buildings and dispersion models of building effects are summarized in Chapter 2 of this report. Also included is a brief evaluation of the best models for use in the next stage of the work program.

The second part of the work program, the design, development and testing of a dispersion and chemistry model for application to compressor station stack design is presented in Chapter 3 of this report. The model, known as the Compressor Station Chemistry Model (CSCM), consists of a chemistry module developed at Concord Scientific and a dispersion module chosen from those currently-available as most suitable for this application. The dispersion module is actually the Dual Plume Model developed for application to gas compressor stations by Engineering-Science under contract to the American Gas Association. The model testing presented in Chapter 3 consists of a series of calculations based on "typical" and "worst case" conditions expected for Alberta. These calculations provided sufficient information to assess the sensitivity of the model to its design parameters.

The final portion of the work program, the design of a field measurement program for Phase II of the Compressor Exhaust Chemistry and Wake Diffusion Study is presented in the last chapter. It was designed to answer many of the questions about chemistry and diffusion in the wake of gas compressor buildings and to validate and verify the predictive capability of the Compressor Station Chemistry Model.

2. BACKGROUND INFORMATION

This chapter presents a state-of-the-art review of current research and literature covering the areas of compressor emissions, NO/NO_2 atmospheric chemistry, flow and dispersion in the vicinity of buildings and models of diffusion in the wake of buildings. It constitutes the first phase of the overall Compressor Exhaust Chemistry and Wake Diffusion Study and provides the background information necessary to understand and carry out the succeeding portions of the work program. The reviews in each of the aforementioned areas are based on the annotated bibliography published under separate cover (Concord Scientific Corporation, 1981).

At the end of this chapter, a brief evaluation is given of the dispersion models reviewed in the bibliography and a rationale is provided for selecting the model used in later portions of the work program.

2.1 Compressor Station Emissions

A substantial body of information now exists on emissions from gas compressor stations. The major part of this is derived from the work of the Southwest Research Institute (Dietzmann and Springer, 1974; Urban and Springer, 1975; and Fanick and Dietzmann, 1980).

Dietzmann and Springer (1974) have presented the results of emission measurements made on 59 reciprocating engines (up to 8000 hp.) and 9 gas turbines (up to 20,000 hp.). A number of measurements were made on each engine, and for each test the following quantities were listed:

Date

Time

Barometric pressure

Ambient temperature

Relative humidity

Engine speed

Horsepower

Scavenging air pressure

Ignition timing

Fuel specific gravity

Fuel high heat value

Orifice constant

Fuel temperature

Orifice drop and static pressure

Fuel flow

Heat flow

Air flow

Air/Fuel ratio

Brake Specific Fuel Consumption

NO_x, NO_2, NO, CO_2, total hydrocarbon and O_2 concentration in exhaust

Ratio NO/NO_x

Ratio non-methane/total hydrocarbons

NO_x, CO and hydrocarbon emissions in lb/hr, lb/mil. BTU and gr/hp. hr

Variation of emissions with altered operating conditions were also investigated. However, a number of parameters required in modelling compressor station emissions were not included. This situation was redressed by Fanick and Dietzmann (1980), in the second phase of the emission survey. In this study, measurements were made on 55 reciprocating engines and 11 gas turbines, and the additional parameters reported were:

Inlet manifold temperature

Exhaust velocity

Exhaust temperature

Exhaust flow

Exhaust H_2O content

The measurement techniques used in the survey were described in a separate report (Dietzmann, 1976), and some supplementary data

were gathered in a literature survey (Urban and Springer, 1975).

Additional data on compressor station emissions may be obtained from McGowin (1973), Salvesen et al. (1978), Milligan et al. (1979) and Hunter and Cherry (1980). However, these data are generally more of a background nature, and do not include the details required for any modelling work. From this point of view the report by Fanick and Dietzmann (1980) is by far the most important.

However, it should be pointed out that the variability reported in their results is very high. For example five measurements taken on one engine during the course of less than 3 hours give NO_x concentrations of 879, 402, 987, 867 and 701 ppm (Engine test 128). At another site (test site 11), tests made on three examples of the same engine gave mean NO_x concentrations of 1079, 930, and 1062 ppm respectively, with very large variability in the second measurement. It seems advisable for measurements to be taken at the actual site which is to be modelled, rather than relying on representative data for a particular engine.

2.2 NO_x Chemistry Related to Compressor Station Emissions

Field studies relevant to NO_x chemistry at compressor stations are very limited in number and, in many cases, in quality.

Angle et al (1979) studied the emissions from a compressor station in rural Alberta, and found an NO_2/NO_x ratio which increased steadily from an in-stack value of 0.03 to 0.15 at 20 seconds to 0.2 at 70 seconds (the longest time considered). The scatter in the data was considerable.

Davis and Kolb (1980) carried out an environmental assessment relative to the operation of six large diesel engines in an urban environment (Jersey City). They did not set out to study NO to NO_2 conversion rates, but one of the authors (Davis, 1981) indicated that they were of the same order as those reported by Angle et al.

Measurements made at a large installation in Texas were described by Bilsky et al (1980). They found an initial (i.e. in-stack) NO_2/NO_x ratio of 0.11, which increased to 0.14 at a downwind distance of 1.2 km. Unfortunately this paper contains serious flaws, which call all the results into question. For example:

1. The quoted NO concentration at the stack exit is 1.5 ppm, which must be in error by at least a factor of 1000. The validity of the quoted NO_2/NO_x ratios is therefore uncertain.

2. The NO_2/NO_x ratio was measured at 6 points up to 2.4 m, then only at 580 m and 1158 m. Travel times were not estimated.

3. There is no indication of the background ozone concentration.

Engineering-Science carried out a study during 1981 on NO_x chemistry in compressor station plumes, working under contract to the American Gas Association (AGA, 1981). However, the project has been extended for a further year, since the results obtained to date have proved inconclusive.

It is apparent that the details of the physical and chemical interactions in the vicinity of compressor stations have not been clearly established by actual measurement. This is a deficiency in our current state of knowledge. However, experimental work in other environments, both laboratory and field, has provided sufficiently detailed knowledge that some general observations can be made about the chemistry of emissions from compressor stations.

The only pollutants which need be considered are NO_x and hydrocarbons: particulates and SO_2 are essentially absent from the exhaust gas stream. Further, approximately 95% (or more) of the emitted hydrocarbons will be methane (Fanick and Dietzmann, 1980), which can be assumed to be inert on the short time scales appropriate to the compressor station situation (i.e. times up to about four minutes).

Given these simplifications, a number of reactions are known, or believed, to be important (Demerjian et al, 1974; Derwent and Hov,

1980). These are listed in Table 4 (see section 3). The possible reaction scheme divides essentially into three parts: a) oxidation of NO to NO_2, b) photolysis of NO_2, and c) oxidation of NO_2.

a) Oxidation of NO. In polluted atmospheres this proceeds by reaction with O_3, HO_2 and organic peroxy radicals written as RO_2. However, compressor stations are generally rurally sited, so that concentrations of HO_2 and RO_2 will probably be low and oxidation by ozone is expected to predominate.

b) Photolysis of NO_2 proceeds very rapidly, producing NO and an oxygen atom, which combines almost instantaneously with an oxygen molecule to produce ozone. On the time scales considered here it is not expected that a photostationary state in ozone will be reached. This contention has been confirmed in the course of this modelling study.

c) Oxidation of NO_2. In the virtual absence of reactive hydrocarbons the only oxidation path open to NO_2 is $NO_2 + OH \rightarrow HNO_3$. Combining the known rate constant for this reaction (Anastasi and Smith, 1976), with a typical ambient OH concentration of 5×10^6 radicals per cubic centimetre (Calvert, 1981) one can calculate that approximately half of one percent of an initial

amount of NO_2 will react in one minute in a closed reactor (ignoring depletion of the OH). Under the plume conditions considered here this reaction will therefore be negligible.

To summarize, the important chemical reactions in a compressor station plume occur as follows. Relatively rapid initial oxidation of NO to NO_2 by ambient ozone takes place. As NO_2 is produced, its net rate of production decreases, because it is subject to photolysis, recreating NO and ozone. At some distance downwind the rates of production and removal will become equal, resulting in a stationary state, or "pseudo-equilibrium", but this will generally occur beyond the regions which are of interest in this study. At night no photolysis can occur, so the reaction between NO and O_3 will go to completion. This will generally result in local removal of the ozone.

The actual rates of the various reactions are determined by the concentrations of the species, and thus by the dynamics of plume dilution.

2.3 Flow and Dispersion In The Vicinity of Buildings

This section provides a review of current information on the flow and dispersion in the vicinity of buildings.

Halitsky (1968) presented one of the earliest summaries of flow characteristics in the vicinity of buildings or structures. He

indicated the following: The introduction of a structure into a flow field results in a region of aerodynamic distortion around and downstream of the body. This region can be broken down into three distinct zones which are shown in Figure 1. The first zone, called the displacement zone, is formed by the displacement of fluid around the structure and is enclosed by an imaginary isolating surface separating undisturbed and disturbed flow. The second zone, referred to as the 'cavity' or 'separation bubble' begins at the leading edge of the building and extends downwind roughly 2 to 4 building heights. It is characterized by low pressure and recirculating flow and is delineated by a separation streamline starting at the leading edge of the building and reattaching to the ground at some distance downwind. The reattachment point is known as the stagnation point and has a zero mean longitudinal velocity. Inside the cavity, the flow velocities are less than mean background velocities and, at lower levels, are negative as the flow returns from the downwind stagnation point to the rear face of the structure, then along the roof and sides to the leading edge. In plan view, flow separation at the leading side edges of the building result in the formation of two counter-rotating vortices symmetrical about the building centre-line. Material caught in the cavity exits from it by turbulent diffusion through the layer of strong shear flow which encloses the bubble.

Downstream of the cavity is the third zone known as the wake or far wake. In it, mean flow velocities remain less than background values while turbulence levels are enhanced over background due to

building-induced mechanical turbulence. At some point downwind, roughly 10 to 20 building heights, the velocity and turbulence fields return to background levels.

Since this description was first published, the concept of flow in the vicinity of buildings has changed - becoming considerably more complicated. The new picture is based on both wind tunnel (Woo et al, 1977; Castro, 1973; Castro and Robins, 1975) and full-scale (Frost et al, 1977) experimental work specifically designed to investigate flow and turbulence fields in the vicinity of buildings. In addition, experimental programs on dispersion in the vicinity of buildings have produced a great deal of new information on turbulence and flow (Start et al, 1980; Vincent, 1977; Vincent, 1978; Thuiller et al, 1980) as have theoretical studies (Hunt et al, 1978a, 1978b).

Almost all current work has been comprehensively summarized in Hosker (1980a) and Hosker (1980b). The former is a draft chapter of the book Atmospheric Science and Power Production, D. Randerson, editor (U.S. Department of Energy). It covers, in great detail, work carried out on all shapes of structures, e.g. cylinders, flat plates, 2-D fences, spheres and bluff bodies in all types of flows e.g. uniform free, uniform bounded, boundary layer neutral and boundary layer non-neutral stratified flow. It also gives a summary of research directly applicable to flow and dispersion about buildings. The general description which follows is based on that reference as well as information in the annotations of the individual publications reviewed.

The new, more-complicated concept of flow about buildings is illustrated in Figure 2. It illustrates the flow pattern about a block building immersed in a deep boundary layer oriented at 0^{o} to the mean wind direction. It is suggested that this diagram be referred to throughout the forthcoming discussion.

The first characteristic of note is that the velocity gradient in the upwind flow induces a downward flow on the front face of the building. At ground level, this flow moves upwind, away from the building, causing the approach flow to separate from the ground at some distance upwind and resulting in a standing vortex in front of the building. The size and strength of this vortex depends upon both the curvature of the wind speed profile relative to the building height and the width to height ratio (W/H_B) of the building. Wind tunnel work suggests that for wide buildings, the main flow contacts the face of the building above the vortex between 0.5 and 0.8 H_B with 0.6 H_B the most commonly observed value. For W/H_B roughly equal to unity, the vortex height is roughly 0.75 H_B and, for tall narrow buildings, the vortex reaches a height of about W. The distance upwind of the building at which the flow separates from the ground because of the standing eddy has been observed to vary from 0.9 H_B (Frost et al, 1977) to 1.3 H_B (Wilson and Netterville, 1978).

The size of the upwind vortex is quite variable because it depends on aerodynamic force balances. Hence perturbations are caused by both atmospheric turbulence and unsteadiness in the incident flow. This means the upwind vortex is generally rather unsteady.

It is now recognized that the vortex not only affects the flow in front of the building, it also affects flow beside and downsteam of it. It does so by interacting with the incident flow to wrap around the building and trail off downwind. This behaviour was noted by Castro (1977) and Woo et al (1977) and has been called the 'horseshoe vortex' because of its horseshoe, wrap-around shape. Wind tunnel work has shown that the horseshoe vortex may actually consist of a system of several counter-rotating vortices; however, full-scale work suggests that only one vortex exists. It is worth noting that fluctuations in the strength and location of the horseshoe vortex can lead to fluctuations in the downwind wake which, in turn, causes feedback to the upwind vortex.

Downwind of the building's front face, the cavity region is formed. At the leading edges of the building, the flow cannot turn sharply enough to follow the roof and sides and therefore separates from the leading edge. The air in the separated zones in the vicinity of the roof and sides moves upwind to produce recirculating flow. The boundary between the recirculating and undistrubed flow is a turbulent shear layer which curves in towards the body. If the building is long enough, the shear layer reattaches to the roof and sides. This generally occurs for structures with L/H_B ratios equal to or greater than one if the building is not too wide. To illustrate this, Vincent (1977) found reattachment of the separated boundary layer on the roof and sides in uniform flow when the parameter $\Lambda = V_e/\bar{U}H_B > 2.5 \times 10^{-3}$ where q and V_e are the characteristic turbulence and velocity scales and $\bar{U}$ and H_B have

their usual meanings. If this criterion also holds for boundary layer flows, then there is a strong possibility that flows will reattach on buildings with $L/H_B = 1$ in the atmosphere and in wind tunnels. Castro and Robins (1977) showed that this was the case in their wind tunnel experiments for a cube in a neutral boundary layer. However, Hosker (1979) uses the criterion that reattachment occurs for $L/H_B \geq 2$ unless otherwise noted by investigators. It should be noted that the forgoing discussion applies to flat-roofed buildings only.

If the width to height ratio of the building is large, then reattachment may be delayed or may not occur at all. Wilson (1979) examined the roof recirculation zone in detail and found that it extends downwind a distance $X \approx 0.9\ R$ from the upwind edge where $R = \zeta_b^{2/3}\ \xi_b^{1/3}$ and ζ_b is the smaller of H_B and W and ξ_b is the larger.

Immediately downwind of the building the flow situation becomes very complex and the earlier concept of a relatively simple recirculating cavity or bubble bounded by a turbulent shear layer appears to be inadequate. Figure 2 shows the more recent concept of the near wake flow field based mostly on the work of Woo et al (1977) and Hunt et al (1978a). The work shows that the counter-rotating horseshoe vortices already referred to trail off behind and to the sides of the building. Also, in the lee of the building near its lateral edges are a pair of vertical vortices which interact with the main flow near roof level and trail off downwind as an elevated counter - rotating pair. The existence of these vortices had not been noted before but were again seen quite clearly by Hatcher et al (1978). Two facts are of special

note in this new picture, namely: (1) the flow streamlines bounding the cavity are not the separation streamlines and (2) transfer of material into and out of the cavity is not only due to turbulent transfer across the bounding shear layer but is also due to the advection of material into the recirculation zone along the entering streamlines and removal through the rising spiral vortices generated near the lateral lee edges of the obstacle. Vincent (1978) suggests that in a deep turbulent boundary layer, the simpler cavity concept may be adequate since turbulent transfer probably dominates over advective transport. This is still a controversial point.

Information on the horseshoe vortex is rather sparse but Woo et al (1977) indicate that it was almost undetected by $X/H_B = 4.69$ in their wind tunnel experiments. Information on the elevated vortex pair produced by the interaction of the mean flow with the front corner near roof level is also sparse. Frost and Shahabi (1977) indicate the presence of these vortices in smoke visualization tests in the atmosphere but even a qualitative description of their behaviour and interaction with the incident and cavity flows is not available.

The size of the cavity zone in the X, Y and Z directions is known to be quite variable, even for similar shaped buildings. Hosker (1979) examined available data for the longitudinal extent of the cavity, X_r, from the rear face of the building for <u>uniform</u> flow and suggested the relation $\frac{X_r}{H_B} = \frac{A - (W/H_B)}{1 + B(W/H_B)}$ where A and B are weakly dependent on L/H_B. In the case where flow does not reattach to the roof, A = 2.0 + 3.7

$(L/H_B)^{-1/3}$ and B = -0.15 + 0.305 $(L/H_B)^{-1/3}$ and, in the case where it does reattach, A and B are constants equal to 1.75 and 0.25 respectively. If the flow separates at the leading edge of the roof and reattaches to it, the cavity then forms at the downwind edge of the building and smaller vertical and horizontal cavity dimensions result.

The above equations were applied to boundary layer flows and were found to provide less accurate but reasonable predictions of the cavity extent. It is of note that the maximum cavity extent occurs for large W/H_B ratios for which the relation predicts $(X/H_B)_{max}$ → 7 if reattachment occurs and even more if it does not occur. Hosker's equation for non-reattached flow provides a better comparison with data than is suggested because the experimental results of Frost and Shahabi (1977) were found, as part of this work program, to be in error.

The maximum height of the cavity is equal to H_B if the flow reattaches and 1.5 to 2.5 H_B if it does not reattach. Roof slope seriously affects this value.

Cavity width is also seriously affected by reattachment. If it occurs, then the maximum cavity width is W. If it does not occur, Hosker (1980) suggests that the maximum width is equal to approximately 1.1 W + 1.7 W exp (-0.55 W/H_B) but indicates that this relation needs field validation.

Finally, it is worth noting that the size and structure of the cavity region in the atmosphere is highly variable because of

fluctuations in the speed, direction and turbulence levels of the incident flow. This is often not reflected in wind tunnel measurements and the implications on mass transfer out of the cavity region are important.

Turning our attention to the shear layer bounding the cavity, Woo et al (1977) indicate that from the building edges outward, the cavity velocity defect decreases in absolute magnitude, finally becoming an excess. The excess velocities reach a peak value in the bounding shear flow before returning to background flow values. If the maximum velocity excess is considered to be the outer boundary of the shear layer, it is shown to grow as $Z/H_B = A\ (X/H_B)^{0.1}$ and $Y/(W/2) = B(X/H_B)^{0.1}$ for a short squat building.

For orientations other than 0^o, flow separation does not occur on the roof. Instead, a counter-rotating vortex pair is shed from the front roof corner and separation occurs at the trailing roof edge. Separation from the building sides occurs at the corners across the flow. The vertically oriented vortex pair immediately behind the building is larger in this orientation than in the 0^o orientation.

Downstream of the recirculating cavity zone is the region known as the wake or far wake. It also has a mean velocity defect and a turbulence intensity enhancement. Woo et al (1977) indicate that the wind speed defect decays with distance downwind as $(X/H_B)^{-3/2}$ for buildings oriented at 0^o to the flow. This agrees well with the theoretical value of Hunt (1973) for flow with no organized vorticity in it.

Woo et al also observed that the turbulent intensity excess decayed as $(X/H_B)^{-2}$ and that the horseshoe vortices both sides of the building could be seen as bumps on the velocity defect and turbulence intensity excess profiles (to a distance of 12 to 14 H_B downwind).

In general, wakes appear to extend 10 to 20 H_B downwind and wide low buildings tend to have a much slower return to background conditions than narrow ones. In the experiments of Woo et al (1977), the turbulent intensity excess and the velocity deficit extended downstream at least 25 H_B and 40 H_B respectively.

The orientation of the building to the flow has a significant effect on the far wake. For example, the upwind roof edges of a building at an angle to the incident flow can generate a vortex pair similar to wing-tip vortices from an airplane. These vortices are shed from the upwind corner of the building and are most significant at distances greater than roughly 10 to 15 H_B downwind where momentum effects of the building have begun to die away. Woo et al (1977) noted that these vortices cause a velocity excess near the top of the wake because of mixing of higher velocity upper air downward by the vortices. Hansen and Cermak (1975) show that velocity excesses due to roof tip vortices can be observed in the wake to at least 80 H_B downwind.

When the incident flow is moderately stable, even block-like structures normal to the wind can generate wakes influenced by vortices. Kothari et al (1979) observed vortex-dominated wakes to at least 60 H_B downwind. In addition to a velocity excess, a temperature excess can

be produced by roof tip and horseshoe votices as they transfer the stable warm air aloft down towards the wake centre-line. Kothari et al (1977) found that the volocity excess persisted farther downwind and decayed more slowly than the turbulence excess.

Hosker (1980a) provides an excellent summary of the status of present understanding of the far wake behind three-dimensional buildings. It is as follows: in wakes where organized vorticity is unimportant, the mean velocity defect decays roughly as $(X/H_B)^{-3/2}$ and the turbulence intensity excess decays as $(X/H_B)^{-2}$. The cross-wind velocity defect profile is approximately bell-shaped and the wake extends typically 10 to 20 H_B downwind but this depends on the building W/H_B ratio. Higher W/H_B ratios result in increased longitudinal wake extent.

When organized vorticity becomes important in the wake (this applies to hemispheres, block buildings inclined to the incident flow and block buildings in stable flow), the wake can assume a vortex character. The vortices can induce a velocity excess in the wake that can persist to large distances downwind and is predicted to decay slowly as $(X/H_B)^{-1/2}$. Horseshoe vortices in this case tend to rise slowly from the ground and spread gradually from the wake centre-line. The measureable wake can extend to 50 or 100 H_B downwind depending on the ambient turbulence level. A wake temperature excess can be produced if the incident flow is stable.

Hosker also points to a number of caveats to the foregoing description:

1. Most experiments have been done in wind tunnels rather than in the atmosphere. Most workers have noted a sensitivity of their results to the ratio of the building height to incident boundary layer depth, H_B/δ. However, the effect of this factor is not quantified.

2. The processes of vortex generation and decay are known to be Reynolds number dependent and the Reynolds numbers in wind tunnel experiments are much lower than in the atmosphere. This is even more of a problem in modelling stable flows where Reynolds numbers are smaller than normal to account for thermal scaling in the flow.

Finally, the author indicates that more full-scale experimentation is necessary and that it should include cross-wind and down-wind meteorological measurements as well as measurements using remote sensing devices.

It is clear from the foregoing discussion that flow in the up-wind region, the cavity region and the far wake region is far more complicated than first conceived. In fact, many of the flow characteristics (such as the vertical vortex pairs immediately behind buildings)

affect more than one flow region and are still very poorly understood. For example, Figure 2, taken directly from Woo et al (1977), does not present a clear picture of how the vortices and streamlines cross the free shear layer which bounds the cavity - a very important characteristic as noted by Hosker (1980a). It is also not clear how often and under what conditions organized vorticity is important in the wake region under atmospheric flow situations.

In general, our understanding of flow in the vicinity of buildings is advancing significantly but there are still many questions to be answered. Based on this current picture of flow near buildings, it is now reasonable to focus on dispersion characteristics in the vicinity of buildings.

Hosker (1980a) and (1980b) both present good summaries and evaluations of dispersion characteristics; both are used in conjunction with the references in the bibliography to provide the following summary and evaluation of dispersion in the wake of buildings. It will be noted that the summary looks at several situations, i.e. sources upwind of buildings, sources on or near buildings and pays special attention to concentrations in the near wake and far wake region.

a) Source Upwind Of A Building

The standing vortex formed upstream of the front building face has a major effect on pollutants released upwind of it. The rising flow in the front portion of the vortex

tends to divert pollutants upward while the downwash along the building face directs pollutants downward thereby causing increased ground level concentrations in front of the building. As mentioned earler, the height of the vortex has been shown to be roughly two thirds of the building height and it extends upstream to distances as great as 1.3 H_B, thereby influencing the ground level concentration fields to that distance (see Wilson and Netterville, 1978, and Frost and Shahabi, 1977). It was also shown in the former reference that the centre-line of a plume released at Z = 1 H_B can be forced higher by the building.

Some of the material entrained into the frontal vortex and carried to ground level can trail off downwind in the horseshoe vortex. This material will be reasonably well-mixed so that concentrations on the rear face of the building will be relatively uniform. This was also shown in Wilson and Netterville (1976).

If the building is long in the downwind direction, then the flow that has separated from the top leading edge can reattach on the roof bringing the pollutant down and causing high concentrations on the building faces.

If the building is not long, then the flow will not reattach and the plume will be deflected above roof level. The resulting concentrations on the roof will be similar to

those on the rear face because both are caused by recirculation of the material entrained into the cavity. Hence, the effect of a building on pollutants emitted upwind is to induce rapid enlargement and dilution of the incident plume. Near the building, the concentrations will be higher than if it was not there but further downwind the concentrations will be lower.

b) Source On Or Near A Building

For sources roughly flush with the front surface of the building, the standing frontal vortex is very important. If the emission occurs in the lower half to two thirds of the building, the pollutants will be carried to ground level and swirled past the building sides in the horseshoe vortex. Some of it will enter the downwind cavity region by advection and turbulent diffusion while the balance will be advected into the far wake.

Material emitted into the upper third of the building's front face is forced upward and sideward with the flow which then separates from the leading edges of the building. This drives the effluents out and away from the building surfaces.

However, if L/H_B is greater than 1 or 2 (see Hosker, 1979), the separated flow reattaches to the roof and sides driving the effluent closer to the building.

Material emitted within the separated flow areas (e.g. from flush vents on the roof) will be trapped within the recirculating flow zone and can cause high concentrations on the building surfaces and in the cavity region. This is particularly important for building ventilation intakes which are located in the separated flow region.

If the building is at an angle to the wind, the flow will not separate from the most exposed face and may or may not separate and reattach to the less exposed face. On the roof, the counter-rotating vortex pair generated from the upwind corner will transport air from above to the roof level. A roof cavity does not form so that effluents from roof vents will be advected downwind rapidly.

Considering the area immediately downwind of the building, the conventional view has been that a closed re-circulation cavity or bubble bounded by a turbulent shear layer is formed (see Section 3.1). The work of Woo et al (1977) has shown that this concept is not totally correct; however, Vincent (1977) suggests that it may be a reasonable approximation for predicting ground level concentrations in the area. Hosker points out that the possiblility of direct advection into and out of the cavity must be recognized and that a leaky bubble concept should be considered. Frost and Shahabi (1977) indicate that the cavity is non-stationary

and depends highly on the incident flow structure and direction.

For material emitted into the cavity at low levels, the flow carries it up the lee face of the building and, in the case of separated flow, onto the roof. While this material is generally rapidly mixed throughout the cavity, there is some evidence (Start et al, 1980) that the cross-wind distribution of material has a maximum near the centre-line which suggests incomplete mixing. This was also seen by Hatcher et al (1978) and Huber and Snyder (1976) who found that ground level releases in the wake of structures tend to have enhanced dispersion in the vertical and horizontal while elevated releases are enhanced only in the vertical. This behaviour is probably due to the large counter-rotating vortices in the cavity forcing the material from elevated releases towards the centre-line.

The curvature of the shear layer bounding the cavity induces a downwash of the outer flow. Therefore material released above the cavity near this flow will be brought close to the ground causing higher concentrations than if the building was not present.

Downwind of the cavity is the far wake region. While wind tunnel work (e.g. Woo et al, 1977) indicates that organized vorticity can cause this region to exist to great dis-

tances downwind, e.g. X = 40 to 50 H_B, full-scale experiments (e.g. Hatcher et al, 1980) indicate that the velocity and turbulence levels return to background levels at a distance of roughly 15 H_B downwind. Whether this implies a lack of significant vorticity effects in the atmosphere, as suggested by Vincent (1978), or whether it reflects a specific flow situation is not clear. Snyder et al (1976) produced a new set of dispersion coefficients based on this enhancement. Other authors (e.g. Gifford, 1960 and Thuillier et al, 1980) considered that the effect of the building was to increase σ_z at the building's lee face by a value equal to some constant, C, times the building area normal to the flow. This constant was suggested to range from 0.5 to 1. Thuillier et al (1980) indicate that this approach has problems as C was found to vary with downwind distance.

Finally, the work of Start et al (1980) shows that effluents emitted into a building wake in the atmosphere often exhibit very unusual behaviour. For instance, these authors found that tracers often took a multimodel cross-wind concentration distributions instead of Gaussian distributions. Also, they often encountered the situation where the effluent would lift off the ground to produce an elevated concentration maximum in the far wake region. Unfortunately, there was no attempt made to relate this effect back to the atmospheric stability or the dominant flow

characteristics at the time of the experiment.

The effect of stratification seems to be to increase concentrations in stable conditions and decrease them in unstable conditions (Hatcher et al, 1978). However, there is some question about this in the far wake region since Start et al (1980) showed that the effluent transferred out of the cavity zone can actually lift-off the ground and form an elevated, intact plume with very low ground level concentrations.

The design of proper stack height to avoid or minimize building effects on effluent dispersion has conventionally been approached using the '2 1/2 times' rule of thumb. This states that the stack exit should be 2.5 times the highest flow obstacle in the vicinity, thereby allowing the effluent to be emitted into undisturbed flow and diffuse as if no building was present. In actual fact, the building induced distortions to the near field flow are often significantly lower than the rule would suggest. For instance, Snyder et al (1976) show that the 2 1/2 times rule was justified for the case of a low building with $W/H_B = 2$ but was unnecessarily conservative for a tall building with $W/H_B < 1$. It was shown that Briggs' (1973) proposed alternative to the 2 1/2 times rule was reasonable for a tall thin building and a stack height of 1.5 H_B would be adequate. This means

careful consideration of the source-building configuration should be given in designing stack heights.

One topic which was not discussed explicitly in any of the literature reviewed was the effect of turbulence levels and streamline displacement on plume trajectory and final height. Obviously, plume rise and growth in the displacement zone about a building will depend upon the orientation of the flow and the enhancement of turbulence in that zone. For example, if the flow in the wake region has a downward component as suggested in Figure 1, the plume rise will be inhibited and final rise will be reduced. Unfortunately, the literature tends to concentrate on the effect of wake flow on final ground level concentrations and does not focus on plume-flow interaction. This is clearly an area requiring further study.

In summary, the foregoing review of flow and dispersion in the vicinity of buildings has produced a very complicated picture. While the basic understanding of this picture is growing rapidly, it appears that a great deal of further work is needed. In particular, future field studies should be designed to study the flow characteristics about the building in great detail while concurrently studying the dispersion characteristics. Two subjects which need special attention and study are the mechanisms by which pollutants are transferred from the cavity region to the far wake region and plume rise - flow streamline interaction.

2.4 Mathematical Modelling Of Building Effects

Fourteen mathematical models for the prediction of pollutant concentrations in the vicinity of buildings were reviewed for their application to gas compressor station stack design. The models were:

1. Huber-Snyder (1976), Huber (1977)
2. Briggs (1973)
3. Nuclear Regulatory Commission (U.S. NRC 1979)
4. Dual Plume (Engineering Science 1977, 1980c)
5. Industrial Source Complex (ISC) Model (Engineering Science 1980a; High, 1980)
6. Ontario Hydro, Moroz et al (1981)
7. Wilson (1976)
8. Wilson (1977)
9. Wilson and Netterville (1976)
10. Barry (1963)
11. Halitsky (1977)
12. Hunt et al (1973, 1978)
13. Puttock (1979)
14. Puttock et al (1979)

Of these models, the first four - Huber-Snyder, Briggs, NRC and Dual Plume were considered to be the most applicable to gas compressor stack design based on physical representativeness, technical soundness, suitability for application to near and far wake regions and to stack design. In addition, these particular models are cur-

rently accepted by the scientific and regulatory communities for modelling dispersion in the wake of buildings.

This section describes each of the four models in detail, summarizes all current literature on the performance of each and provides an assessment of the best model for application to compressor station stack design. Table 1 summarizes the nomenclature used in the model descriptions.

Table 1. Nomenclature for Model Summaries

A	-	building cross-sectional area	m^2
D	-	internal stack diameter	m
C	-	constant of O(1)	-
F	=	$\frac{-\Delta \cdot g \cdot V_s \, D^2}{4}$ buoyancy flux of source	$\frac{m^4}{s^3}$
h	-	effective stack height	m
h_a, h'	-	stack height modified by downwash	m
H_B	-	building height	m
h_m	-	stack height modified by building	m
h_s	-	actual stack height	m
g	-	gravitational acceleration (9.8 m/s^2)	m/s^2
K	-	constant of O(1)	-
l_B	-	min (H_B, W_B)	m
Q	-	emission rate	kg/s

Nomenclature - Cont'd.

R_z, R_y	-	plume half-widths	m
$\bar{U}$	-	wind speed	m/s
U_c	=	$0.22\ C\ \sqrt{g\Delta D}$; critical windspeed	m/s
V_s	-	stack discharge velocity	m/s
W_B	-	building width	m
x	-	downwind distance	m
α	-	entrainment coefficient	-
Δ	=	$(\rho_s - \rho_a)/\rho_a$ buoyancy parameter of source	-
ρ_a	-	ambient air density	kg/m^3
ρ_s	-	stack discharge density	kg/m^3
σ_x, σ_z	-	dispersion coefficients	m
σ_y^T, σ_z^T	-	dispersion coefficients recommended by Turner	m
σ_y', σ_z'	-	enhanced dispersion coefficients	m
χ	-	ground level, centreline concentration	kg/m^3

2.4.1 Huber-Snyder Model

The Huber-Snyder model is based primarily on wind tunnel results (Huber and Snyder, 1976). It incorporates reduced plume rise, enhanced vertical Gaussian dispersion, and in some cases, enhanced horizontal dispersion due to building effects. The building effect dominates the enhanced vertical dispersion the closer the stack height is to the building height (for $h_s < 2.5\ H_B$). The stack and building must be within 2 H_B of each other for the model to apply and it is generally used between 100 m (~3 H_B) and 10 H_B downwind. Beyond this distance, the enhanced vertical dispersion coefficient is derived by adding a virtual source distance to the downwind distance and using normal Pasquill-Gifford dispersion functions.

Based on the wind tunnel results, the authors postulated that the centre-line concentration downwind of the near building source is given by

$$\chi = \frac{Q}{\pi \sigma_y \sigma_z \bar{U}} \exp\left(-\frac{1}{2}\left(\frac{H}{\sigma_z}\right)^2\right)$$

where Q = emission rate

σ_y, σ_z = dispersion coefficients

$\bar{U}$ = wind speed

H = effective stack height

with the values of σ_y, σ_z modified to account for the building wake effects. The authors recommend the following expressions for σ_y' and σ_z' where prime indicates the enhanced value.

Ground Level Source

$$\frac{\sigma'_y}{H_B} = \frac{\sigma'_z}{H_B} = 0.7\,\frac{l_B}{H_B} \qquad ; 0 < x < 3H_B$$

$$\frac{\sigma'_y}{H_B} = \frac{\sigma'_z}{H_B} = 0.7\,\frac{l_B}{H_B} + 0.067\left(\frac{x}{H_B} - 3\right) \qquad ; 3H_B < x < 10H_B$$

$$\frac{\sigma'_y}{H_B} = \frac{\sigma'_z}{H_B} = 0.115\left(\frac{x}{H_B} + 8.2\right)^{0.8} \qquad ; 10H_B < x$$

Roof Level Source

$$\frac{\sigma'_y}{H_B} = 0.115\left(\frac{x}{H_B}\right)^{0.8} \qquad ; \text{all } x$$

σ'_z as for ground level source

Cavity Level Source

$\frac{\sigma'_y}{H_B}$ as for roof level source

$$\frac{\sigma'_z}{H_B} = 0.067\left(\frac{x}{H_B}\right) \qquad ; 0 < x < 10H_B$$

$$\frac{\sigma'_z}{H_B} = 0.115\left(\frac{x}{H_B}\right)^{0.8} \qquad ; 10H_B < x$$

where l_B = min (building height, building width).

In a later paper, Huber (1977), these were modified by increasing the horizontal dispersion coefficients for roof and cavity level sources.

Roof Level Source

$$\frac{\sigma'_y}{H_B} = 0.35 \frac{l_B}{H_B} \quad ; 0 < x < 3H_B$$

$$\frac{\sigma'_y}{H_B} = 0.35 \frac{l_B}{H_B} + 0.067 \left(\frac{x}{H_B} - 3\right) \quad ; 3H_B < x < 10H_B$$

$$\frac{\sigma'_y}{H_B} = 0.115 \left(\frac{x}{H_B} + 1.6\right)^{0.8} \quad ; 10H_B < x$$

Cavity Level Source

$$\frac{\sigma'_y}{H_B} = 0.067 \left(\frac{x}{H_B} - 3\right) \quad ; 3 < x < 10H_B$$

$$\frac{\sigma'_y}{H_B} = 0.115 \left(\frac{x}{H_B}\right)^{0.8} \quad ; 10H_B < x$$

He also recommends that if the standard Pasquill-Gifford coefficients exceed the above values for a given stability condition that the un-

Figure 3: Huber-Snyder Model Flowchart

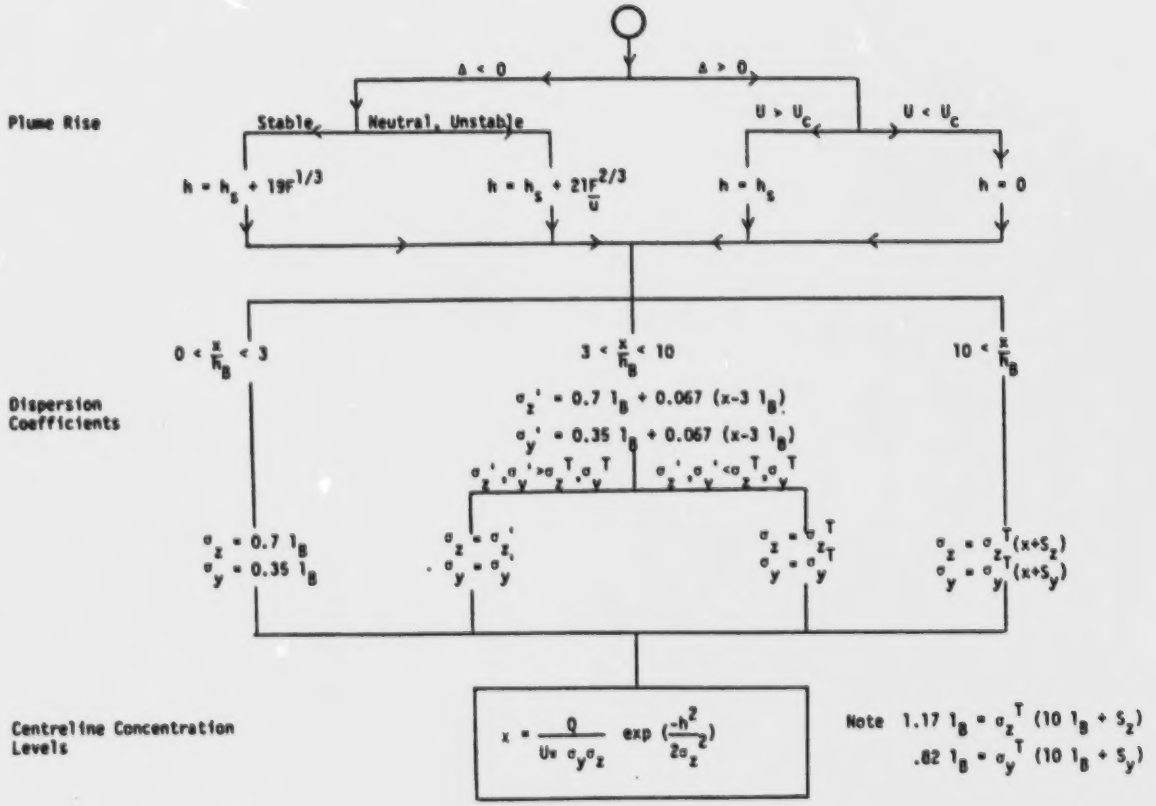

modified coefficients be used.

The flowchart of the Huber-Snyder model is given in Figure 3. It should be pointed out that the model assumes that the plume is either totally above the cavity or totally entrained into the cavity. This is not a realistic approximation for elevated releases given the transient nature of the cavity structure and the possibility of entrainment into the cavity from above.

2.4.2 Briggs' Model

Briggs' model was developed for sources with $h_s < 2.5\ H_B$ and for releases within 100 m of the building. It is based primarily on wind tunnel results and plume rise analysis. Based on certain stack and building configurations as well as wind speeds, Briggs separates the releases into elevated and ground sources. The elevated plume heights are adjusted according to the release height/building height ratio and the wind speed and plume buoyancy.

Briggs assumes that the plume cross-section downwind of the building is rectangular and contains a uniform concentration of effluent. Dispersion is calculated using plume half-widths and depths which are specified as a function of downwind distance, day-night conditions and wind speeds. The model itself is presented in detail in Briggs (1973) which is, essentially, a workbook outlining a set of rules

for dispersion calculations. These rules are based on the idea that the building will affect the plume by modifying the effective stack height. If the plume is entrained into the cavity then the plume is considered to originate from an effective ground level area source.

If the effective stack height, including aerodynamic downwash effects (but not buoyancy effects), h', is less than the building height, H_B, then the effective stack height, h'', is

$$h'' = h' - 1.5\, l_b \quad \text{where } h' = h_s + 2\,(V_s/\bar{u} - 1.5)\,D$$

where l_b is the smaller of the building height and building width. If h' is greater than H_B then the effective stack height is

$$h'' = 2h' - (H_B + 1.5\, l_b)$$

If the effective stack height, h'', is less than $l_b/2$ then it is recommended that ground level concentration, χ, be based on a dispersion formula for a ground level source emission of area l_b^2

$$\chi = \frac{Q}{U\,(l_b^2 + 2R_z\,R_y)}$$

where Q = emission rate

U = wind speed

R_z, R_y = plume half-widths

If the effective stack height, h'', is greater than $l_b/2$, then the stack height is corrected for buoyancy effects and the downwind

concentrations are based on a dispersion formula for an elevated source

$$\chi = \frac{Q}{2\bar{U} R_y (h + R_z)}$$

where h is the final corrected stack height.

If the plume is entrained into the cavity then the report recommends that the cavity concentration levels be computed using

$$\chi = \frac{KQ}{(\bar{U} l_b^2)}$$

where K is a constant between 1 and 100.

The flowchart of the model is given in Figure 4.

It should be noted that there are several important features of dispersion in building wakes which have not been accounted for in the model (except possibly in very empirical fashion). These include the enhanced turbulence levels in the wake region, and the mixed mode dispersion whereby the plume is an elevated source some of the time and a ground level source the rest of the time. Also, it is not clear whether the model is suitable for all building geometries and flow situations, because it is based on empirical information rather than the actual physics of flow and dispersion.

Figure 4: Briggs Model Flowchart

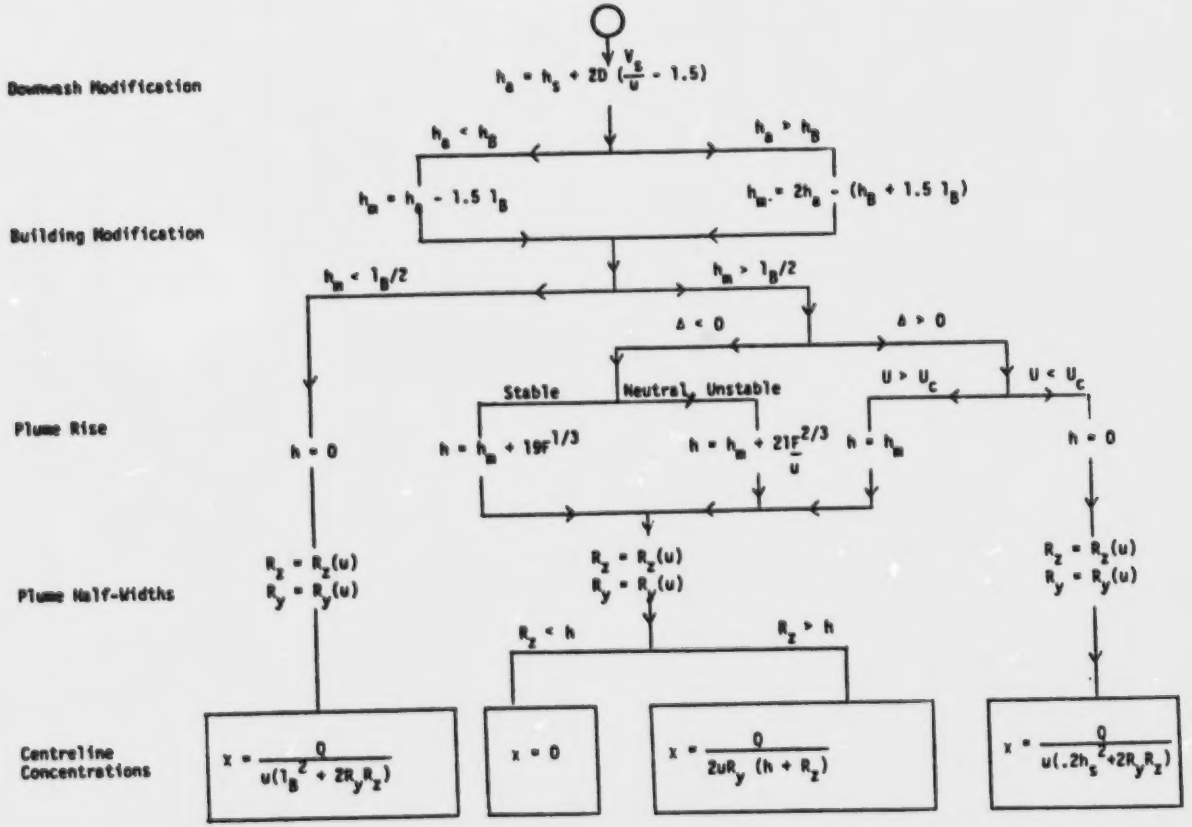

2.4.3 NRC Model

The NRC Model is based primarily on the work of Sagendorf (1974). It accounts for building downwash by determining whether the release was at ground level, at an elevated level or at an intermediate level (combined ground and elevated source). For ground sources, an adjustment is made to account for initial effluent mixing in the building wake. For intermediate releases, the fraction of the time that the plume is assumed to be a ground level release is known as the entrapment factor and is a function of the stack gas velocity to wind speed only. Ground level concentrations are calculated from the Gaussian plume equation and unenhanced Pasquill-Gifford dispersion coefficients.

Details of the NRC Model and an evaluation of it (based on an experimental field program) are given in Thuiller and Mancuso (1980). It is based on Nuclear Regulatory Guidelines 1.111 and 1.3 of the U.S. NRC. The following plume models are recommended:

$$\frac{X}{Q} = \frac{\exp(-h_e^2 / 2\sigma_z^2)}{\pi \bar{U} \sigma_y \sigma_z} \qquad (1)$$

and

$$\frac{X}{Q} = \frac{2.032 \exp(-h_e^2 / 2\sigma_z^2)}{\sigma_z \bar{U} x} \qquad (2)$$

where X = concentration

Q = source strength

h_e = effective height of plume centre-line

σ_y, σ_z = lateral and vertical dispersion coefficients

$\bar{U}$ = average wind speed

x = downwind distance

Turner's values of σ_y and σ_z are recommended.

Equation 1 is to be used for accidental releases of 0.8 hour duration. Equation 2 is a sector-averaged form of (1) used for releases longer than 8 hours. Only equation 1 is considered in the following description.

To account for stack and building downwash the following guidelines are set:

a) Elevated Releases:

If $h_s > 2\ H_B$ where h_s = height of release

H_B = building height

then $h_e = h_s + h_{pr} - h_t - C$

where h_e = effective stack height

h_{pr} = plume rise according to Briggs (1969)

h_t = terrain difference between release point and receptor

C = stack downwash correction for low exit velocity,

i.e. $C = 3\ (1.5 - U_e/\bar{U})\ d$

where $\bar{U}$ = mean wind speed at stack height

U_e = vertical exit velocity of plume.

d = stack diameter

b) Releases Other Than Elevated:

i) For $1\ H_B < h_s < 2\ H_B$, the release is considered to be elevated if $U_e/\bar{U} \geq 5.0$ and to be ground level if $U_e/\bar{U} \leq 1.0$.

ii) For $h_s < H_B$, the ground level release is assumed, i.e. $h_e = 0$.

If $1.0 \leq U_e/\bar{U} \leq 5.0$, a mixed-mode release should be assumed. In such a case, the plume is considered as an elevated release during part of the time and a ground level release the rest of the time. An entrainment coefficient, E_t is determined for these cases where

$E_t = 2.58 - 1.58\ (U_e/\bar{U})$ for $1 < U_e/\bar{U} \leq 1.5$

and $E_t = 0.3 - 0.06\ (U_e/\bar{U})$ for $1.5 < U_e/\bar{U} \leq 5.0$.

The release should be considered to occur as an elevated release $100\ (1-E_t)$ percent of the time and as a ground release $100\ E_t$ percent of the time. Each of these cases should then be

calculated separately and the concentration calculated as a fraction of the time each type of release occurs.

For elevated releases, the wind speed at the height of the release should be used; for ground releases, the wind speed at 10 m should be used.

c) Ground Level Releases (Both true ground level and mixed-mode releases).

In such cases, a building wake correction is made to the dispersion calculation. This includes an augmentation to σ_z accounting for the initial mixing of the effluent plume within the building wake, i.e.

$$\sigma_z' (x) = [\sigma_z^2 (x) + 0.5\, D_z^2/\pi] \leq \sqrt{3}\, \sigma_z (x)$$

for long-term releases (Equation 2).

For short-term releases, a correction is made to the $\sigma_y\, \sigma_z$ product, i.e.

$$[\sigma_y (x)\, \sigma_z (x)]' = [\sigma_y (x)\, \sigma_z (x) + 0.5\, A/\pi] + 3\, \sigma_y (x)\, \sigma_z (x)$$

It can be seen that the latter correction simply adds a building correction factor to the σ values equal to the building's characteristic length.

Figure 5: NRC Model Flowchart

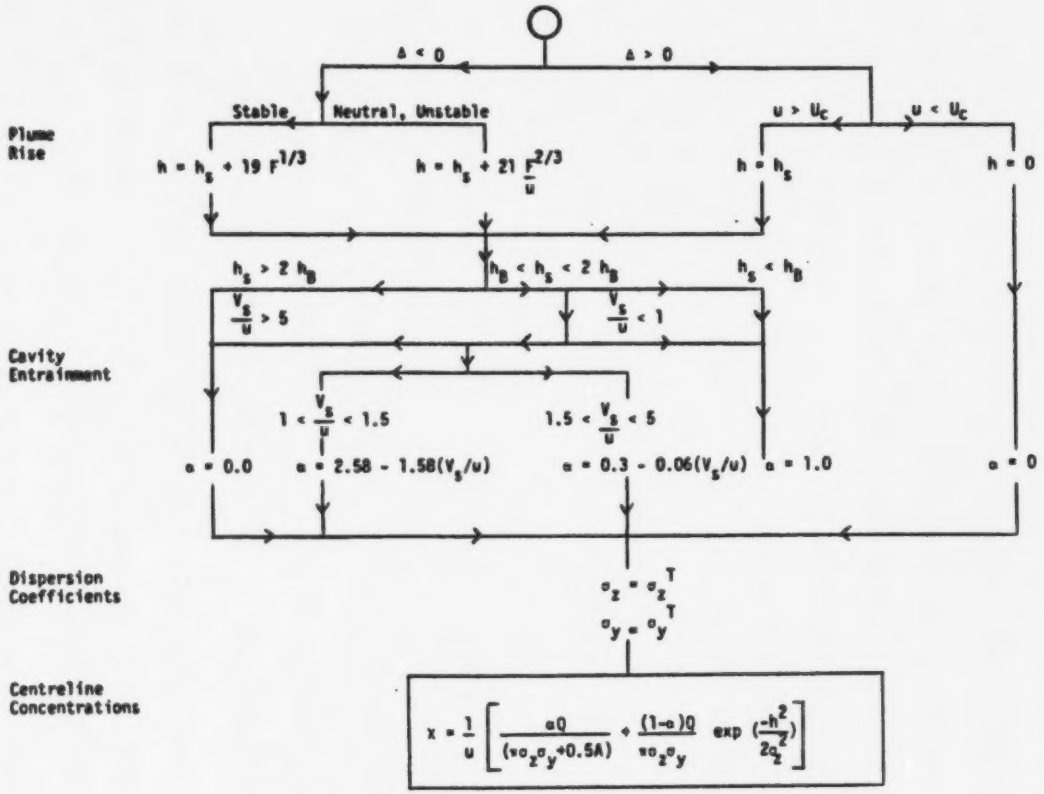

The flowchart summarizing the overall model structure is given in Figure 5.

Based on the foregoing description, the NRC model appears to account reasonably well for ground, elevated and mixed-mode releases by using the entrapment coefficient, E_t. However, E_t depends only on the ratio of the stack gas velocity to the mean wind speed. This makes the model relatively insensitive to the height of the stack and height of the building which are major considerations in the dispersion process. This appears to be the major shortcoming of the model.

2.4.4 Dual Plume Model

The Dual Plume model is very similar to the NRC model. It models ground level releases by using the standard Gaussian expression with Pasquill-Gifford σ_y and σ_z values and a constant building correction term added to the product, $\sigma_y\sigma_z$. For elevated releases which can be partially entrapped in the building cavity, the model uses both elevated and ground level release equations proportioned by an entrapment factor. This factor represents the portion of time that the plume can be considered to be either elevated or at ground level, its value depends on the stack gas velocity to wind speed ratio and the stack height to building height ratio. The latter dependence makes this entrapment factor different from that in the NRC model.

The original Dual Plume model was developed for application to gas compressor stations by Engineering-Science under contract to the American Gas Association. The original model is described in Engineering-Science (1977) and a slightly modified version, calibrated to field study results, is described in Engineering-Science (1980b).

The basic assumptions of the Dual Plume Model are:

- the portion of the plume entrapped by the cavity region can be determined for any combination of wind speed, effluent velocity, building height and release height.
- the portion of the effluent free of the cavity behaves as if the building were not present and disperses as a Gaussian plume.
- the portion of effluent captured by the cavity is subjected to initial mixing in the cavity and then disperses downwind as a Gaussian half-plume.
- the ground-level concentration downwind of the building is the sum of the concentrations resulting from the two portions.

The downwind concentrations are determined by the following equation:

$$\chi = \frac{1}{\bar{U}} \left\{ \frac{\alpha Q}{\pi \sigma_y \sigma_z + CA} + \frac{(1-\alpha)Q}{\pi \sigma_y \sigma_z} \exp(-h^2/2\sigma_z^2) \right\}$$

The first term in this equation models the dispersion of that portion of the plume entrapped in the cavity. The second term models the dispersion of the elevated portion of the plume which is dispersed without influence from the building. Both terms apply only in the region beyond the actual cavity boundary.

where χ = ground level concentration at any point beyond the building cavity ($\sim 2.5\ H_B$)

$\bar{U}$ = mean wind speed

σ_y, σ_z = horizontal and vertical dispersion coefficients

Q = source strength

A = projected cross-sectional area of the building facing the wind

C = dilution factor based on the ratio of cavity area to building area A. C generally is given between 0.5 and 2.

h = effective stack height ($=h_s + \Delta h$) where h_s = stack height and Δh = final plume rise

α = mean fraction of the plume which is entrapped within the building cavity over an hour or so. Under high wind conditions with short stacks, $\alpha = 1.0$. Under low wind conditions with high stacks, $\alpha = 0$. Under other circumstances, $0.0 < \alpha < 1.0$.

The dilution factor, C, for completely trapped plumes depends on the building orientation to the wind and the building shape. Values are given for several combinations of these factors. The maximum concentrations occur when CA is a minimum.

The dispersion coefficients, σ_y and σ_z, are taken from Turner's Workbook (1970). Stability types A to F are also taken from Turner.

The entrapment coefficient, α, depends on two factors:

h_s/H_B where H_B = building height

$V_s/\bar{U}$ where V_s = stack gas exit velocity

The variation of α with h_s/H_B and $V_s/\bar{U}$ is given in graphical form in Figure 6. It can be summarized as follows:

Tall stack → $h_s/H_B \geq 2.5$; $= 0.0$

Short stack → $h_s/H_B = 0.5$ and $3.0 < V_s/\bar{U} < 6.0$; $0.0 < \alpha < 1.0$

Short stack → $h_s/H_B = 0.5$ and $V_s/\bar{U} < 3.0$; $\alpha = 1.0$

For the completely elevated source, the effective plume height, h is equal to the stack height, h_s plus the plume rise, Δh where

$\Delta h = 19\ F^{0.33}$ for stable conditions, E and F

$\Delta h = \dfrac{21\ F^{0.67}}{u}$ for unstable and neutral conditions, A to D.

where $F = 2.6 \times 10^{-3} M \frac{(T_s - T_a)}{T_s}$ and M = stack gas mass flow rate (g/s)

T_s = stack gas temperature (K)

T_a = ambient air temperature (K).

It is useful at this point to discuss a number of points on the background and validity of these equations, as they apply to compressor station emissions.

(1) The above equations are taken from Briggs (1973) and are specific for application to small sources. They are based on Briggs original formulation for buoyancy and momentum induced plume rise and are discussed in detail in Engineering Science (1977). The assumption was made that beyond 3 stack heights, buoyancy is dominant over momentum for most sources and the basic Briggs formula for buoyancy - dominated sources. ($\Delta h = 1.6 F^{1/3} X^{2/3} / U$) should apply to elevated compressor station emissions. Based on turbulent eddy sizes and spectra as well as experimental data, the final plume rise under neutral and unstable conditions was determined by Briggs to occur at $X = 49 F^{5/8}$ for $F < 55$

$X = 119 F^{2/5}$ for $F > 55$.

Therefore the final plume rise is

$$\Delta h = \frac{21 F^{0.75}}{U} \quad \text{for } F < 55$$

$$\Delta h = \frac{39 F^{0.60}}{U} \quad \text{for } F > 55$$

Briggs suggests that for small sources, a compromise between the above equations is reasonable, that is

$$\Delta h = \frac{21 F^{0.67}}{U}$$

In a stable atmosphere, the final rise occurs at

$$X = \frac{2.4\ \bar{U}}{s^{1/2}}$$ where s is a measure of the retarding force

exerted by the stable atmosphere. Hence, final plume rise is

$$\Delta h = 2.9 \left(\frac{F}{\bar{U}\ s}\right)^{1/3}.$$

Briggs then assumes that plume rise under stable conditions is relatively unaffected by meteorological conditions and sets $\bar{U}\ s = 3.3 \times 10^{-3}$. The equation for final rise is therefore

$$\Delta h = 19\ F^{0.33}$$ where F can be expressed as ρ

$$F = 2.6 \times 10^{-3}\ M\ (T_s - T_a/T_s)$$ and $M = \pi R^2\ V_s\ \rho_e$

with $\rho_e = 1.2 \times 10^{-3}$ g/cm^3 at STP. Briggs does not indicate the magnitude of the differences between these equations and his standard equations.

(2) The validity of applying these buoyancy-dominated equations to compressor station emissions is somewhat questionable since most reciprocating compressor engine plumes have very high stack velocities and are definitely momentum-dominated instead of buoyancy-dominated. For example, the Pendant D'Oreille compressor station in Alberta (discussed in detail in Section 3.4) has a stack exit velocity of 50 m/s, a stack radius of 0.125 m, a stack gas temperature of 510 K, a momentum flux of 39 m^4/s^2 and a buoyancy flux of 3.3 m^4/S^2. Further examples can be found in Dietzmann and Springer (1974) and Fanick and Dietzmann(1980). Given this information, it appears that the most suitable plume rise equation for this application would be Briggs' standard equation combining both momentum and buoyancy effects. This would eliminate the assumption that either buoyancy or momentum were dominant and would cover the complete range of compressor engines.

However, there is even some question about the validity of applying any of Briggs' equations to compressor engine plumes. In order to address this question, the American Gas Association is funding an experimental investigation to compare experimental plume rise data with Briggs' buoyancy and momentum equation. The final report has not been published to date but preliminary results (American Gas Association, 1982) indicate that plume heights from reciprocating engines are generally higher than predicted by Briggs. Until the final results of the study are known, it is not possible to state whether any one form of Briggs' equations is more valid than any other or whether any of them is adequately accurate.

(3) The plume rise equations shown above calculate final plume rise which is then used in the Dual Plume model to calculate ground level concentrations. One can argue that the concentrations calculated by the model would be more accurate if the plume rise was expressed as a function of downwind distance instead of final height. In fact, this arguement was presented to Engineering Science at the time the Dual Plume Model was developed. As a result, Engineering Science (1977) carried out a study to compare Briggs' distance-dependent, buoyant, plume rise equation with the above final rise equations. They found no significant difference in the concentrations predicted using the two types of equations.

To summarize, the Dual Plume Model was developed using Briggs' final plume rise equations for small sources. The validity of these equations for application to compressor engine plumes can be questioned

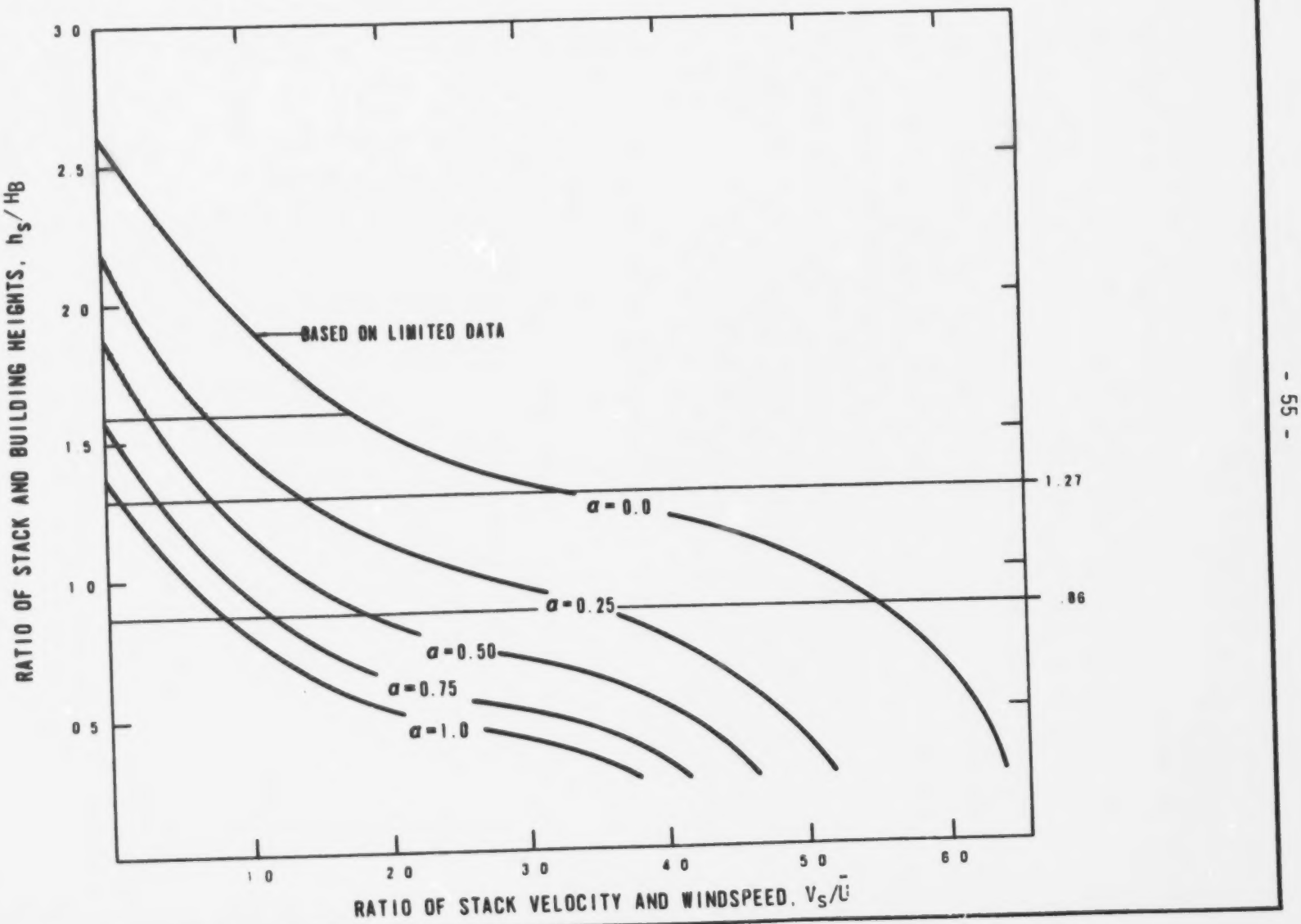

Figure 6: Dependence of α on h_s/H_B and $V_s/\bar{U}$ (From Engineering-Science, 1980b)

on the basis of (1) the accuracy of the approximations made in their development (2) the assumption of buoyancy-dominated plume rise when, in fact, it is most often momentum-dominated (3) the use of the final rise form of the equations instead of the distance-dependent form and (4) the overall accuracy of Briggs' equations for use with compressor plumes. It is worth pointing out, however, that the Dual Plume Model is calibrated using measured concentration data through the entrainment coefficient, α. Hence, any changes made in the plume rise equations would require a complete recalculation of the α values. This would be a major undertaking.

Concentrations within the cavity region cannot be handled using the above formulation. The authors suggest that a simple box model be applied whereby $\chi = \frac{K\alpha Q}{\bar{U}CA}$. Here $\alpha Q/\bar{U}CA$ represents the average concentration of an effluent released at rate αQ into a stream moving at velocity $\bar{U}$ with cross-section CA. If $h_s > 0.75\ H_B$, then $K = 1.5$. If $h_s < 0.75\ H_B$, $K = 1.5$ to 3.0.

For off centre-line concentration calculations, the concentrations are reduced by the factor:

Elevated portion of plume : $\exp(-y^2/2\sigma_y^2)$

Entrapped portion of plume: $\exp(-y^2/2\sigma_y^2)$ for $X > 10\ H_B$

$\exp[-(y-\sqrt{CA})^2 / 2\sigma_y^2]$ for $y \geq \sqrt{CA}$

$\exp[-(y+\sqrt{CA})^2 / 2\sigma_y^2]$ for $y < \sqrt{CA}$

Figure 7: Dual Plume Model Flowchart

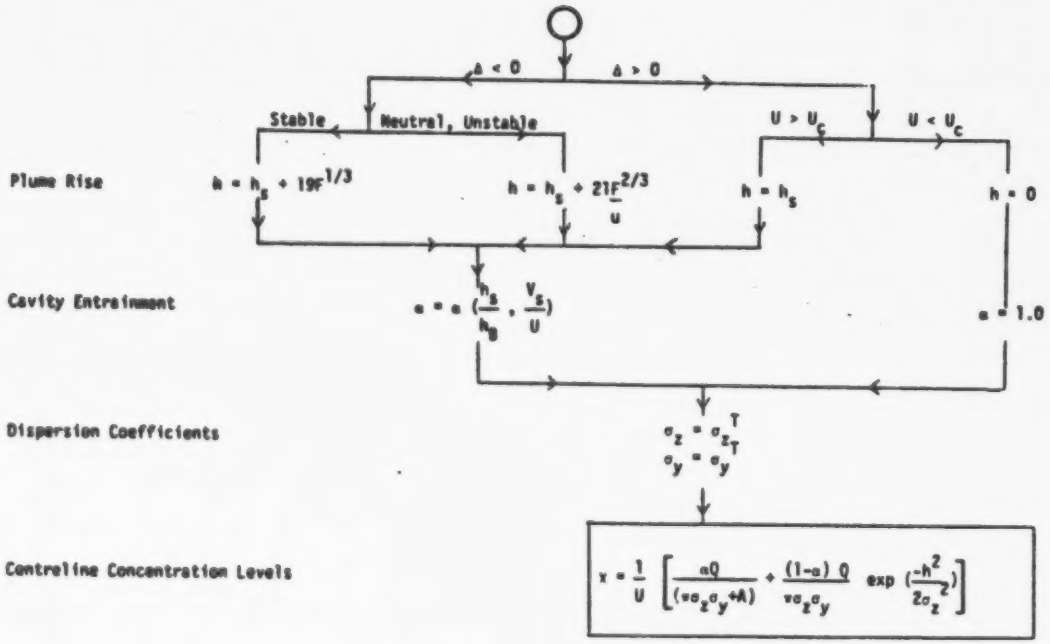

NAME	PLUME RISE FORMULA	PLUME HEIGHT	PLUME SHAPE	STABILITY TYPING	DISPERSION COEFFICIENTS	CAVITY CONCENTRATION
BRIGGS	Briggs (1969) (final rise)	- modified by building - elevated or ground release	rectangular	function of wind-speed only	plume half-widths based on Turner σ_z, σ_y	$x = \frac{KQ}{u l_B^2}$ K = 0.5-3.0
HUBER-SNYDER (ISC)	Briggs (1969) ISC uses rise as function of x	- no building modif. - elevated or ground release	Gaussian	Pasquill-Gifford function of wind-speed and solar insolation	enhanced neutral or Turner's σ_z, σ_y	$x = \frac{Q}{U\pi \cdot .245 \, {}^{1}/_{3} h_B}$
NRC	Briggs (1969) (final rise)	- no building modif. - blend elevated and ground release	Gaussian	Pasquill-Gifford	Turner's σ_z, σ_y	no recommended formula
DUAL PLUME	Briggs (1969) (final rise)	- no building modif. - blend elevated and ground release	Gaussian	Pasquill-Gifford	Turner's σ_z, σ_y	$x = \frac{\alpha KQ}{u A}$ K = 1.5-3.0

Table 2. Model Summary of Principal Models of Diffusion in Building Wakes

In the Engineering-Science 1980 report, a number of slight modifications were made to the model. The value of C was set equal to unity based on cavity visualization experiments. Based on the ground level concentration measurements, new curves for the entrapment factor, α, were determined as functions of h_s/H_B. Finally, the suitability of Briggs' final effective plume rise equations in the model were confirmed as it was noted that the varying plume rise (with downwind distance) equations made no difference in comparison with data.

The flowchart of the Dual Plume Model is shown in Figure 7.

Based on the two Engineering-Science documents, the Dual Plume model appears to be reasonable for use with gas compressor stations. Its representation of the diffusion processes is somewhat artificial in that it uses the superposition of elevated and ground level plumes to represent building-enhanced dispersion. However, the model is tuned using an empirically-determined entrapment parameter, (α). Unfortunately, the amount of data used to quantify α is relatively small.

2.4.5 Model Comparisons

In addition to the flowcharts, the four models have been summarized in comparative form in Table 2. It is apparent from the table that the Dual Plume and NRC models are quite similar in that they both use an initial building enhancement effect, an entrapment factor, and the unenhanced Pasquill-Gifford dispersion coefficients.

The major difference between the two is that Dual Plume determines the entrapment factor from both stack velocity to wind speed and stack height to building height ratios while the NRC model uses the former only.

Also, Dual Plume uses a field-calibrated initial building enhancement factor (C) of unity while NRC uses a factor of 0.5. It appears that the Dual Plume model is somewhat more realistic in its modelling of the physical situation than is the NRC model.

The Huber-Snyder model handles dispersion enhancement due to building effects in a manner different from Dual Plume and NRC, i.e. by using enhanced dispersion coefficients. It also accounts for different building geometries. It appears to also model the physical situation reasonably well.

Briggs' model is probably the most simplified as it calculates dispersion as the growth of a rectangular homogeneous plume. Also, it does not account for different dispersion characteristics for different release levels as noted by Huber and Snyder (1976) and Thuillier et al (1980). Of the four models presented, Briggs' appears to be built on the least physical grounds.

In addition to comparing the basic components of the four models in Table 2, it was possible to compare the performance of the models against experimental data and/or each other. Six publications

Table 3: MODEL EVALUATION SUMMARY

STUDY	BUILDING SITUATION	RELEASE TYPE	RELEASE LOCATION	MODEL				CONDITIONS	COMMENTS
				BRIGGS	NRC	HUBER-SNYDER	DUAL PLUME		
Engineering-Science [1980b]	Compressor Stations	Buoyant	Elevated	-	-	Overpredicted (2x)	Overpredicted (2x)	Sample time adjustments; used in concentration calculations. All stability conditions covered.	1. Setting C=1 improved modelling results 2. σ_y and σ_z close to Huber-Synder's enhanced values. 3. Dual Plume results not significantly different from H-S.
Hatcher et al (1978)	Reactor Building Complex Wind Tunnel	Passive	Ground Elevated	- -	Overpredicted (<2x) -	Overpredicted (<2x) Underpredicted (very badly)	- -	No sampling time adjustments needed. All stability conditions covered.	1. For ground level releases, NRC and H-S were roughly equivalent if NRC used C=1 (NRC performed best at C=1). 2. Ground level releases enhanced in both horizontal and vertical directions while elevated releases enhanced only in vertical.
Koziar et al (1980)	Large building	Low momentum	Elevated	Overpredicted (>>2x)	Overpredicted (>2x)	Underpredicted (~2x) (Best)	-	Time adjustments made. Neutral stability only.	1. H-S results underpredictions speculated to be due to overpredictions of plume rise. 2. NRC overpredictions speculated to be due to setting elevated releases at ground level too conservatively. 3. Briggs' large overpredictions suggested to be due to setting elevated releases at ground level too conservatively.
Miller (1981)	Large reactor building	Passive & low momentum	Ground & Elevated (not distinguished)	-	Overpredicted (>>2x)	Overpredicted (>2x) (Best)	-	No time adjustments made. All stability conditions.	1. H-S performed best for ground level releases although it overpredicted.
Thuiller et al (1980)	Large reactor	Low momentum Passive Passive	Elevated Mid building Ground	- - -	Underpredicted (>2x) Overpredicted (~2) Underpredicted (~2x)	- - -	- - -	No time adjustments indicated. All stability conditions.	1. Experiments indicated that C=0.5 was too small and C tended to increase with downwind distance. 2. Experiments indicated that the plume entrapment factor underpedicted the fraction of time the plume was entrained in the wake This was due to it being a function of V/u only when it should also account for buildings and stack configurations. It therefore accounted for the large underprediction for elevated releases.
Howroyd et al (1980)	Kiln	Low momentum	Elevated	Overpredicted (>2x)	-	-	-	3 hour and 24 hour sampling only. All stability conditions.	-

with such comparisons were reviewed -- Engineering-Science (1980), Hatcher et al (1978), Koziar et al (1980), Miller (1981), Thuiller et al (1980) and Howroyd et al (1980). The results are summarized in Table 3. It shows the type of comparison carried out, the performance of the particular models used and the conclusions of the studies. The following observations can be made from the table.

1. No one model consistently overpredicts or underpredicts except for Briggs' model which greatly overpredicted in both studies cited. This tends to confirm the assessment that Briggs' model is the least physically representative.

2. The NRC model was shown experimentally to have an inadequate value of C and an inadequate formulation of the entrapment factor. The need for the entrapment factor to reflect the physical building-stack configuration was acknowledged by Thuillier et al (1980). Both of these points suggest that the Dual Plume model is substantially better than NRC because it has a realistic value of C confirmed in two field studies and its entrapment factor does account for the building/stack configuration.

3. The Huber-Snyder model both overpredicted and underpredicted but the margins of error tended to be smaller than either the NRC or Briggs' models. The method of handling dispersion using enhanced σ_y and σ_z values was confirmed experimentally.

4. The Dual Plume model proved not to perform significantly differently from the Huber-Snyder model in the one comparison study cited. Although it is dangerous to rely solely on this one study to draw conclusions, it does seem reasonable that Dual Plume, being an improved NRC model, should be close to Huber-Snyder since Huber-Snyder is only marginally better than the standard NRC model. Also, the one study cited applies to gas compressor facilities which are of direct concern to this work program.

The information provided in this section provides the background necessary to select a wake dispersion model suitable for use in the next portion of the work program, namely, the development of a combined chemistry and wake diffusion model for application to compressor station stack design.

The choice of the most suitable model was based on three factors:

1. the physical foundations of the models
2. the performance of the models against experimental data and/or each other
3. the suitability of the model for use with an NO versus NO_2 reaction scheme.

It was shown earlier that both the NRC and Briggs models had significant shortcomings in their fundamental designs and their performances against experimental data (see Table 3). Therefore, these two models were eliminated from further consideration. The two remaining models, Huber-Snyder and

Dual Plume, were shown to be based on good physical principles and both performed equally well against measured data. The final selection was, therefore, based on each model's suitability for use with the NO/NO_2 chemistry modelling scheme. As such, the Dual Plume model was chosen for the following reasons:

- Dual Plume contains a formulation for predicting concentrations in the building cavity. Huber-Snyder has no explicit formulation.
- Dual Plume separates the effluent plume into an elevated portion and a ground level portion. The former is transported and dispersed downwind unaffected by the building presence; the latter is trapped within the building cavity and undergoes enhanced dispersion. This split plume design makes it possible to account realistically for the extra reaction time experienced by the trapped portion of the plume.

Based on these arguments, the Dual Plume model was selected for use in the remaining portions of the work program.

3.0 MODELLING OF NO_2/NO_x DISPERSION IN THE WAKE OF GAS COMPRESSOR BUILDINGS

This chapter describes the design, development and testing of a computer model for predicting ground level concentrations downwind of gas compressor stations. The model, known as the Compressor Station Chemistry Model (CSCM), consists of a dispersion module based on the aforementioned Dual Plume Model (see Chapter 2) and NO/NO_2 chemistry module developed at Concord Scientific. It was necessary to develop the CSCM because existing mathematical models treating dispersion in the wakes of buildings were able to handle, at best, only first order transformation of reactive species, while many of the models did not permit any chemical transformation at all. The CSCM provides a basis for investigating the relationship between NO/NO_2 chemistry and wake diffusion and has ultimate use as a design tool for determining compressor station stack heights.

This chapter describes the model in detail, summarizes its testing and performance and presents a series of recommendations for upgrading and improvement.

3.1 Description of the Compressor Station Chemistry Model

The Compressor Station Chemistry Model (CSCM) features a modular design, which allows separate testing of the components. The major submodules are the dispersion calculation, which is based on the Dual Plume Model (Engineering-Science, 1977), and the chemistry simulation, which is based on a simple expanding box formulation developed by Concord Scientific Corporation.

3.1.1 Dispersion Calculation

The Dual Plume Model (Engineering-Science, 1977) has been described in Section 2.4. Briefly, this model is based on the observation that emissions from a stack mounted on, or close to, a building may become partially or totally trapped in the building cavity. In general the fraction trapped is denoted by α, where α has been characterised as a function of h_S/H_B and V_S/U (ratio of stack height to building height, and stack gas exit velocity to wind speed respectively).

The fraction of emissions not trapped in the cavity, $(1-\alpha)$, is treated as a simple Gaussian plume, while the trapped portion is modelled as a Gaussian half-plume emitted by a ground level area source (the cavity). The downwind concentration at a point is the sum of the concentrations determined separately for the two parts of the plume.

It was noted in Section 2.4.4 that the Dual Plume Model utilizes a simplified form of Briggs' plume rise equation. The validity of using this form of Briggs' equation for application to compressor engine plumes can be questioned (see Section 2.4.4). In spite of this, no modification of the plume rise equations within the model was undertaken and the model was used in its published form. The reasons for this are twofold:

(1) This portion of the work program called for the incorporation of an existing dispersion model into a compressor station chemistry

model. The terms of reference of the work program clearly specified that no major modifications of the existing model were to be undertaken.

(2) Changing the plume rise portion of the Dual Plume Model would necessitate a complete recalibration of the model through recalculation of the entrainment coefficient, α. The background data to do this was not available and it was clearly beyond the scope of the work program to do it.

3.1.2 Chemical Reaction Rate Module

The calculation of chemical reaction rates within an expanding plume is based on an expanding box model which treats a portion of the plume as a closed, but expanding reactor, or box. The model is described below in terms of the chemical reactions taking place, and the dynamics of the expansion of the box.

a) Chemistry

The model describes the chemistry of the compressor station emissions in terms of the 38 step reaction mechanism given in Table 4. This scheme is based on that given by Bottenheim and Strausz (1978), but the reactions of hydrocarbons have been omitted. This assumption removes about 50 reactions from their scheme and thus greatly reduces the computational requirements of the model. It is justified on the grounds that at least 95% of the typical hydrocarbon emission from a

spark ignition engine fuelled by natural gas is normally methane (Dietzmann and Springer, 1974), which, to a first approximation, may be considered to be inert.

b) Dynamics

Preliminary results from a study of NO to NO_2 conversion sponsored by the American Gas Association (AGA, 1981) indicate that the exhaust plume from a gas compressor station will typically expand by 10,000 to 20,000 times in the first 30 seconds of travel, and by a further factor of about 5 in the succeeding 3 to 10 minutes. This rapid expansion of the plume, which is consistent both with the results of Angle et al (1979) and with a calculation based on Briggs' plume rise formulation, is predominant in determining the course of the reactions. This is because the NO concentrations are almost instantaneously reduced to the point where the rate of reaction 18

$$2NO + O_2 \rightarrow 2NO_2$$

becomes negligible by comparison with that of other reactions (since it depends on the square of the NO concentration). At the same time, the expansion results in the entrainment of ambient ozone, which brings about the oxidation of NO by reaction 22

$$O_3 + NO \rightarrow NO_2 + O_2 \quad .$$

TABLE 4

Chemical Reaction Mechanism for the Expanding Box Model

No.	Reaction	Rate Constant (k_i) ($l\ mol^{-1}\ s^{-1}$)	
1	$O_3 + h\nu \rightarrow O(^3P) + O_2$	4.8×10^{-4}	(c)
2	$O_3 + h\nu \rightarrow O(^1D) + O_2$	3.0×10^{-5}	(c)
3	$H_2O_2 + h\nu \rightarrow 2OH$	8.8×10^{-6}	(c)
4	$NO_2 + h\nu \rightarrow NO + O\ (^3P)$	7.8×10^{-3}	(c)
5	$NO_3 + h\nu \rightarrow NO_2 + O\ (^3P)$	6.3×10^{-3}	(c)
6	$NO_3 + h\nu \rightarrow NO + O_2$	0.00	
7	$HNO_2 + h\nu \rightarrow NO + OH$	2.5×10^{-3}	(c)
8	$HNO_2 + h\nu \rightarrow NO_2 + OH$	3.8×10^{-7}	(c)
9	$HNO_4 + h\nu \rightarrow NO_2 + HO_2$	8.8×10^{-6}	(c)
10	$O(^3P) + O_2 \overset{M}{\rightarrow} O_3 + M$	8.8×10^{6}	(d)
11	$O(^1D) \overset{M}{\rightarrow} O\ (^3P)$	8.5×10^{10}	(e)
12	$O(^1D) + H_2O \rightarrow 2OH$	2.1×10^{10}	
13	$OH + O_3 \rightarrow HO_2 + O_2$	5.3×10^{7}	
14	$HO_2 + O_3 \rightarrow OH + 2O_2$	3.7×10^{5}	
15	$OH + HO_2 \rightarrow H_2O + O_2$	9.3×10^{9}	
16	$2HO_2 \rightarrow H_2O_2 + O_2$	5.6×10^{8}	
17	$OH + H_2O_2 \rightarrow HO_2 + H_2O$	4.9×10^{8}	
18	$2NO + O_2 \rightarrow 2NO_2$	2.9×10^{8}	(f)
19	$O(^3P) + NO \overset{M}{\rightarrow} NO_2$	1.1×10^{9}	(d)
20	$O(^3P) + NO_2 \overset{M}{\rightarrow} NO_3$	1.2×10^{10}	(d)
21	$O(^3P) + NO_2 \rightarrow NO + O_2$	3.7×10^{9}	
22	$O_3 + NO \rightarrow NO_2 + O_2$	1.1×10^{7}	
23	$O_3 + NO_2 \rightarrow NO_3 + O_2$	2.0×10^{4}	
24	$NO_3 + NO \rightarrow 2NO_2$	5.3×10^{9}	
25	$NO_3 + NO_2 \rightarrow NO + NO_2 + O_2$	4.9×10^{9}	
26	$NO_3 + NO_2 \overset{M}{\rightarrow} N_2O_5$	2.3×10^{9}	(d)
27	$N_2O_5 \overset{M}{\rightarrow} NO_3 + NO_2$	1.2×10^{1}	(e)
28	$N_2O_5 + H_2O \rightarrow 2HNO_3$	7.7	
29	$NO + NO_2 + H_2O \rightarrow 2HNO_2$	1.6×10^{2}	(f)
30	$2HNO_2 \rightarrow NO + NO_2 + H_2O$	4.4	
31	$OH + NO \overset{M}{\rightarrow} HNO_2$	6.9×10^{9}	(d)
32	$OH + NO_2 \overset{M}{\rightarrow} HNO_3$	9.8×10^{9}	(d)
33	$OH + HNO_2 \rightarrow H_2O + NO_2$	4.0×10^{9}	
34	$OH + HNO_3 \rightarrow H_2O + NO_3$	4.9×10^{7}	
35	$HO_2 + NO \rightarrow OH + NO_2$	4.6×10^{9}	
36	$HO_2 + NO_2 \rightarrow HNO_4$	6.1×10^{8}	
37	$HNO_4 \rightarrow NO_2 + HO_2$	4.2	(g)
38	$OH + CO \overset{O_2}{\rightarrow} HO_2 + CO_2$	1.0×10^{8}	

Notes:

a) Taken from Bottenheim and Strausz (1978). Checked against values from Derwent and Hov (1980) and Baulch et al (1980

b) The value given corresponds to a temperature of 298 K.

c) Units of s^{-1}. Values are for Summer in Alberta, as given by Bottenheim and Strausz.

d) These are pseudo - second order rate constants, i.e. they are obtained by multiplying the third order rate constant by the concentration of air under ambient conditions.

e) Pseudo - first order, units of s^{-1}. This rate constant is obtained by multiplying the second order rate constant by the concentration of air under ambient conditions.

f) Units of $l^2\ mol^{-2}\ s^{-1}$

g) Units of s^{-1}.

Clearly any modelling work which neglects plume expansion is not valid, since the emphasis in the reaction scheme will be wrong, i.e. reaction 18 will then be very important, and reaction 22 much less so.

To derive the appropriate equations governing the behaviour of the plume, consider a volume of gas emitted from the stack, which is then allowed to expand, as described above. During the expansion, mass will be conserved within the volume, so that for any particular species, i, the change in mass arises solely from reactions producing or removing that species, or from entrainment of that species from the background.

Therefore:

$$\frac{dM_i}{dt} = R_i + E_i \qquad (3)$$

where M_i = mass of species i

R_i = the reaction kinetic terms affecting species i

E_i = entrainment rate of the species from ambient air.

However,

$$M_i = C_i V \qquad (4)$$

where C_i = concentration of i

V = volume.

(Thus the assumption is made of uniform concentration throughout the volume.)

Also,

$$E_i = C_b \frac{dV}{dt} \tag{5}$$

Where C_b = background concentration of this species

(This equation applies only for an expanding plume).

Then

$$\frac{d\,(C_i\,V)}{dt} = R_i + C_b \frac{dV}{dt}$$

$$\therefore \quad V \frac{d\,C_i}{dt} + C_i \frac{dV}{dt} = R_i + C_b \frac{dV}{dt}$$

$$\therefore \quad \frac{d\,C_i}{dt} = \frac{1}{V} \left(R_i + (C_b - C_i) \frac{dV}{dt} \right) \tag{6}$$

Note that R_i has units of mass per unit time. It therefore follows that $R_i^{'}$, defined by

$$R_i^{'} = R_i/V \tag{7}$$

has units of concentration per unit time, and is derived in the normal manner from the reaction scheme

$$\therefore \quad \frac{d C_i}{dt} = R_i' + \left(\frac{C_b - C_i}{V}\right) \frac{dV}{dt} \qquad (8)$$

An equation of the form of equation 8 is set up for each species in the reaction mechanism.

Initial testing of the expanding box module revealed that the two reactions,

$$NO_2 + h\upsilon \xrightarrow{O_2} NO + O_3 \qquad (4)$$

and

$$NO + O_3 \longrightarrow NO_2 + O_3 \qquad (22)$$

predominate in determining the overall reaction rate. The effect of eliminating all other reactions from the scheme was tested, using the expanding box module. The comparison between the full and abbreviated chemical mechanisms is shown in Figure 8. These results correspond to initial NO and NO_2 concentrations of 1400 and 70 ppm respectively. The expansion rate of the plume cross section was 10,000 times in 30 seconds and a further 5 times in 300 seconds.

The agreement is within 15 %at all reaction times, and similar results were obtained for initial NO_x concentrations in the range 1100 to 2000 ppm. The two step mechanism was therefore considered to be acceptable. The savings in computer time made possible by reducing the number of chemical species from 16 to 3 are considerable.

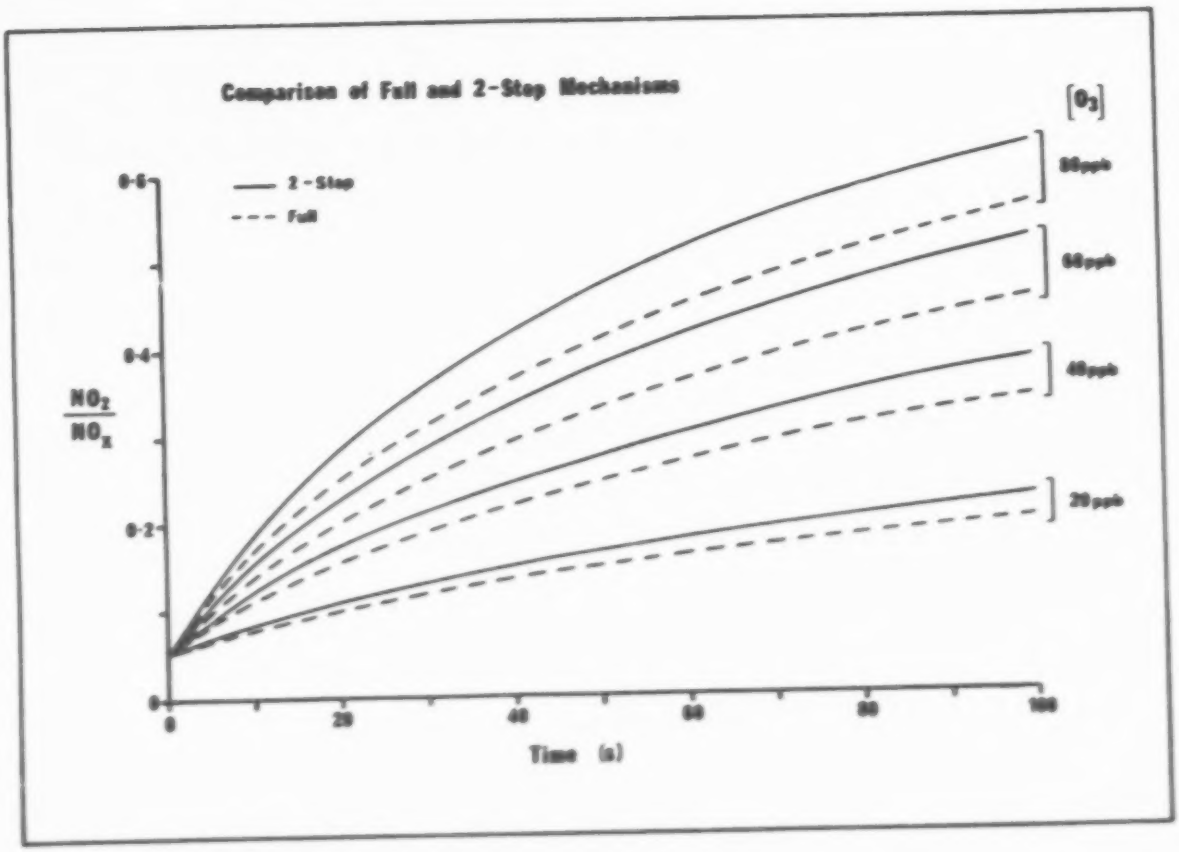

Figure 8: Comparison of Full and 2-Step Mechanisms for a plume expanding in cross section by 10,000 times in 30 seconds and a further 5 times in 300 seconds.

$[NO]_o$ = 1400 ppm

$[NO_2]_o$ = 70 ppm

3.1.3 Combination of Dispersion and Chemistry

The calculation of dispersion and chemical reaction in the CSCM are carried out on the dual parts of the plume separately. The ground level concentrations of NO and NO_2 at a point are then taken to be the sum of the concentrations found in the two parts of the plume. The details of how the calculations are carried out are as follows, and apply separately to the ground level and elevated portions of the plume.

The ground level NO_x concentration is first calculated using the Dual Plume Model equations where the plume travel time to the point of measurement is approximated as downwind distance divided by mean wind speed.

The expanding box scheme is then applied to determine what fraction of the NO_x is NO_2. Since this formulation assumes uniform concentrations within the box, it cannot be applied to the whole plume. Instead, an infinitesimally small box is assumed, which is imagined as following a trajectory from its source (the stack or the cavity respectively) to the point of measurement. This situation is depicted schematically in Figure 9.

An important quantity in the expanding box equations is the expansion term

$$\frac{1}{V}\frac{dV}{dt}$$

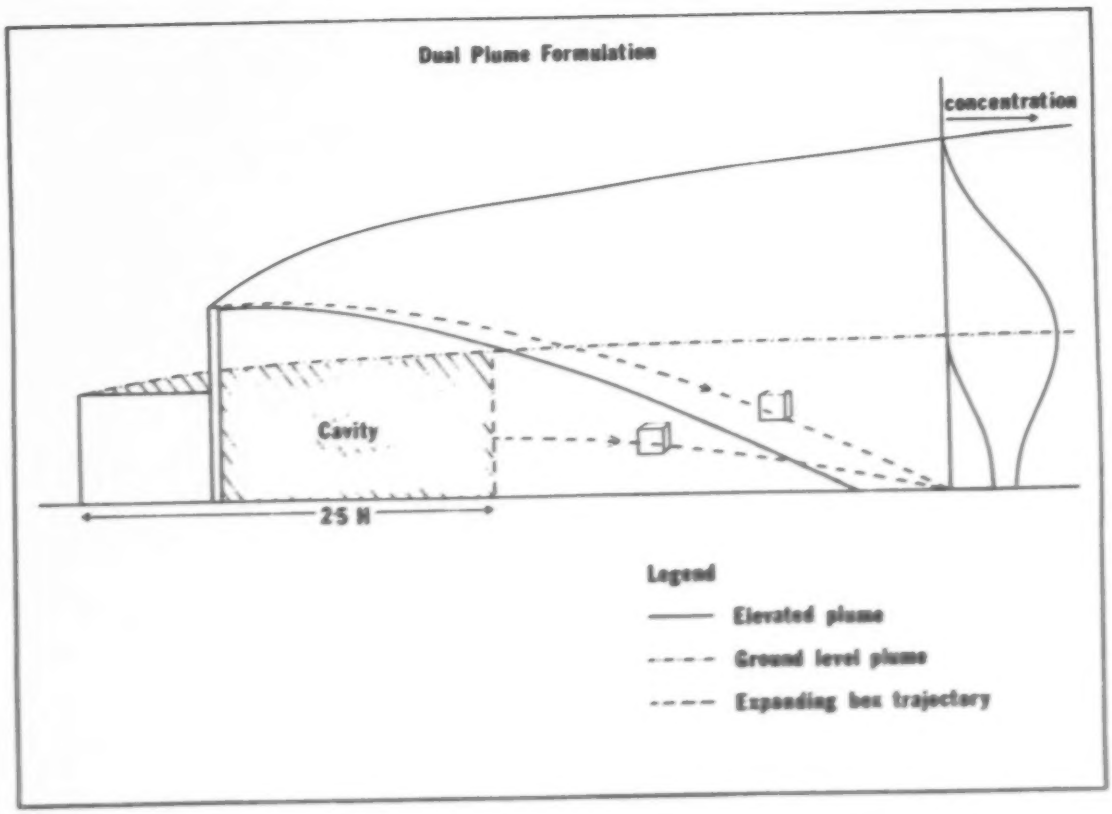

Figure 9: Dual Plume Formulation as Used in the Compressor Station Chemistry Model

which requires that the functional form of the variation of box volume with time be known. It was assumed that this functional relationship was the same as that for the plume as a whole, i.e.

$$V \propto \sigma_y \sigma_z \tag{9}$$

For ease of calculation the σ's were cast into the form

$$\sigma \propto x^n \tag{10}$$

Where x is the downwind distance, and the exponent n is dependent on atmospheric stability. Such power law relationships for σ have been given for stability classes C, D, E and F (Portelli, 1974). The σ values for stabilities A and B were given in the form

$$\sigma = \sum_{i=o}^{p} A_i \, (\ell n \, x)^i \tag{11}$$

where p = 1 or 2 depending on the stability category.

Over the relatively short distances appropriate to this study (under a kilometre) the equations represented by 11 can be very well fitted ($r > 0.998$) by the power law form of equation 10.

It then follows from equation 9 that the box volume for all stability classes is proportional to

$$x^{n_1} \cdot x^{n_2}$$

or x^m

where $m = n_1 + n_2$

and $x = \bar{U}t.$

Therefore, $V = \text{Constant}.t^m$ (12)

since wind speed, $\bar{U}$, has been assumed to be constant during a model run.

Equation 12 is not well behaved at time equal to zero, so that volume should actually be expressed by

$$V = \beta t^m + V_o \tag{13}$$

where V_o is small. The factor β is specific to a particular trajectory, and is determined from the initial in-plume NO_x concentration, $\left(NO_x\right)_i$, and the concentration at the point of measurement $\left(NO_x\right)_f$, since

$$\frac{V_f}{V_i} = \frac{V}{V_o} = \frac{\left(NO_x\right)_i}{\left(NO_x\right)_f} = R, \text{ say} \tag{14}$$

$$\therefore \frac{\beta t^m + V_o}{V_o} = R$$

$$\therefore \beta t^m + V_o = V_o R$$

$$\therefore \beta = \frac{V_o(R-1)}{t^m}$$

Because β contains V_o, as shown above, the precise value of V_o is unimportant since it cancels out in

$$\frac{1}{V}\frac{dV}{dt} = \frac{m\beta t^{m-1}}{\beta t^m + V_o}$$

For convenience we therefore set

$$V_o = 1 \qquad (15)$$

The exponents, m, used in this study are summarized in Table 5.

Table 5

Exponents in the Expression $V = \beta t^m + 1$

Stability	m
A	2.01
B	1.89
C	1.84
D	1.79
E	1.70
F	1.70

The sequence of calculations then follows as given below.

The initial and final NO_x concentrations are known from the

dispersion calculation, as is the corresponding travel time, so that β can be calculated from equation 14.

$$\frac{1}{V}\frac{dV}{dt}$$

can then be calculated at all points along the expanding box trajectory. Numerical solution of the set of partial differential equations defined by equation 8 is then carried out, yielding the NO_2 concentration at the point of measurement.

The appropriate initial concentrations are the in-stack concentration for the elevated part of the plume and the in-cavity concentration for the ground level part. The in-cavity NO_x concentration is calculated as described in Section 2.4, but it is also necessary to determine the initial fraction of NO_2. This was done by estimating the cavity residence time from a relation given by Vincent (1978).

$$\frac{t_r . \bar{U}}{h_s} = 7 \text{ to } 10 \qquad (16)$$

where t_r is the mean residence time in the cavity.

Reaction within the cavity was then estimated in two ways:

a) As a closed reactor with

$$[NO]_o = 0.90\ [NO_x]_{\text{cavity}}$$

$$[NO_2]_o = 0.10\ [NO_x]_{cavity}$$

$[O_3]_o$ = background concentration.

For typical conditions (t_r = 8 sec., O_3 = 40 ppb) it was found that an initial ratio of NO_2/NO_x of 0.10 was increased to 0.14.

b) Rapid expansion of the plume into the cavity on a time scale defined by equation 16, and with the chemistry modelled by the expanding box formulation. The expansion ratio was given by stack exit NO_x concentration divided by cavity NO_x concentration, and, again for typical conditions, the ratio of NO_2 to NO_x increased from 0.10 to 0.14.

The source conditions for the ground level portion of the plume in the CSC Model were thus set as

$$[NO] = 0.86\ [NO_x]_{cavity}$$

$$[NO_2] = 0.14\ [NO_x]_{cavity}$$

The procedure outlined above is followed for each downwind point of interest.

3.1.4 Limitations of the CSC Model

The limitations of the CSC model are comprised of those inherent in the Dual Plume Model, and the expanding box formulation,

plus additional limitations brought about by the combination of the two.

The limitations of the Dual Plume Model have been discussed in Section 2.2. Briefly, they are

- enhancement of dispersion in the wake of the building is not accounted for in the dispersion coefficients, σ_y and σ_z.

- the calculation of in-cavity concentration is based on a very simple model.

- both in-cavity and downwind concentrations depend on the cavity entrapment factor, α, which has been empirically characterized only to a limited extent.

The expanding box formulation allows the incorporation of complex chemistry, but its treatment of the dynamics of expansion and the entrainment of background gas is based on the simplifying assumption of uniform concentration throughout the box.

Since the CSC Model was created by modifying an existing dispersion model it features the decoupled simulation of dispersion and chemistry. In this formulation it is difficult to allow for the different phases of plume growth and background entrainment, i.e. initial dominance by source effects, followed by a transition period,

after which plume growth is dominated by atmospheric turbulence. The functional dependence of plume volume on travel time is different in the different regions, which could be catered for in an integrated model.

However, it has been shown by actual test that the dependence of calculated concentrations on the actual form of

$$V = V(t)$$

is relatively weak (see Table 6), so this limitation was considered to be acceptable at this stage of model development.

Table 6

Dependence of NO_2/NO_x Ratio After 30 s on Exponent m in the Formula $V = \beta t^m + 1$

m	NO_2/NO_x
0.67	0.16
1.00	0.17
1.50	0.18
2.00	0.16

Another simplification which has been introduced is that the stack gases have been assumed to cool instantaneously to ambient temperatures. This assumption causes no problems because very few of the reactions listed in Table 4 have an appreciable activation energy.

The most significant activation energy (considering its absolute magnitude, and the rate of the associated reaction) is that of reaction 22

$$O_3 + NO \rightarrow NO_2 + O_2$$

The magnitude of the activation energy is 12.06 kJ/mol , from which it can be calculated that the rate constant changes by 10% for a 5 K change in temperature from 293 K.

If the stack gas temperature is taken to be 700 K and ambient temperature is 293 K, one volume of stack gas will be cooled to 298 K on mixing with x volumes of background air, where

$$x\ (298 - 293) = 1\ (700 - 298)$$

$$\therefore \quad x = \frac{402}{5}$$

$$\simeq 80$$

If the plume expands 10,000 times in 30 seconds, the time taken to mix with this much ambient air will be approximately

$$\frac{80 \times 30}{10{,}000}$$

$$= 0.24 \text{ s.}$$

This means that the rate constant will decrease from 16 times the room temperature value (corresponding to 700 K) to 1.1 times the room temperature value within a quarter of a second. The assumption of instantaneous cooling is thus satisfactory, since the extent of reaction during

the first second or two of plume travel is small, even at the rates appropriate to the high in-stack temperatures.

A more fundamental limitation is that the dual plume formulation inherent in the CSC model has the potential for underestimating the rate of production of NO_2 by reaction 22

$$NO + O_3 \rightarrow NO_2 + O_2$$

However, careful analysis indicates that the problem does not actually arise, as is shown below.

Let the NO and O_3 concentrations in the elevated part of the plume be $[NO]_e$ and $[O_3]_e$, with the concentrations in the ground level part of the plume being denoted by $[NO]_g$ and $[O_3]_g$. The corresponding rates for reaction 22 are

$$R_e = k_{22} \ [NO]_e \ [O_3]_e$$

$$R_g = k_{22} \ [NO]_g \ [O_3]_g$$

Where the two parts of the plume overlap the model calculates a combined rate

$$R' = R_e + R_g$$

Whereas the true rate would be

$$R = k_{22} \left([NO]_e + [NO]_g \right) \left([O_3]_e + [O_3]_g \right)$$

which exceeds the model rate by

$$R - R' = k_{22} \left([NO]_e [O_3]_g + [NO]_g [O_3]_e \right)$$

However, if the predominant factor producing ozone in the plume is background entrainment we have

$$[O_3]_e = [O_3]_g = [O_3]$$

Then the model rate is

$$R' = k_{22} [NO]_e [O_3] + k_{22} [NO]_g [O_3]$$

while the true rate is

$$R = k_{22} \left([NO]_e + [NO]_g \right) [O_3]$$

which is identical.

Ozone is produced in the expanding plume by photolysis of NO_2 and by entrainment of ambient ozone. The rates of the two processes are

$$k_4 [NO_2]$$

and

$$\frac{[O_3]_{amb}}{V} \frac{dV}{dt}$$

respectively. For typical conditions, taken from runs made during the development of the model when a number of parameters were printed, the following values apply at a plume travel time of 30 seconds:

$$[NO_2]_e = 2.5 \times 10^{-3} \text{ µmol } \ell^{-1}$$

$$[NO_2]_g = 1.2 \times 10^{-3} \text{ µmol } \ell^{-1}$$

$$[O_3]_{amb} = 1.6 \times 10^{-3} \text{ µmol } \ell^{-1}$$

$$\beta_e = 1.4 \times 10^{4}$$

$$\beta_g = 4$$

$$k_4 = 7.8 \times 10^{-3} \text{ s}^{-1}$$

$$k_{22} = 11.0 \ \ell \text{ µmol}^{-1} \text{ s}^{-1}$$

The two desired terms then have the values indicated in Table 7.

Table 7

Values of the Two Terms Involved in In-plume Ozone Production

	Term 1 $k_4 [NO_2]$	Term 2 $\frac{[O_3]_{amb}}{V} \frac{dV}{dt}$
Elevated plume	2×10^{-5}	1×10^{-4}
Ground level plume	1×10^{-5}	1×10^{-4}

Units are µmol ℓ^{-1} s^{-1} .

As these figures show, entrainment is the dominant process, though the margin is not as large, particularly for the elevated plume, as is really desirable for accurate modelling.

At greater plume travel times dispersion gives rise to lower NO_2 concentrations, thus reducing term 1 and improving the approximation (term 2 changes more slowly with time). At shorter travel times the NO_2 concentrations are higher, and the approximation becomes less rigorous, but even after 5 seconds of travel the rate of entrainment of ozone exceeds its rate of production by a factor of 3 to 4 in both parts of the plume.

To summarize the above, the separate treatment of chemical reactions in the two parts of the plume could, in certain circumstances, lead to an underestimate of the rate of the reaction between NO and O_3 which is kinetically of second order. It has been shown, however, that this does not cause a serious problem in the application of the model. The effect of this approximation is to cause an underestimate in the NO_2 concentration.

The above effect is offset by a further approximation in the CSCM, which causes it to overestimate NO_2 production. This effect arises because the air entrained into the expanding box is assumed to contain ozone at ambient concentrations. However, most box trajectories will be within the plume, as illustrated in Figure 9. The appropriate ozone concentration for entrainment is thus that existing in the plume.

Table 8

Effect of Different Adjustments For One Hour Averaging Time

Downwind Distance (m)	NO_2 Concentration ($\mu g/m^3$)		Difference %
	NO_x Adjusted	NO_2 Adjusted	
150	93.5	92.8	+1
175	115.7	114.0	+1
200	119.5	121.7	-2
225	124.9	126.7	-1
250	125.3	120.8	+4
275	119.1	114.9	+4
300	111.2	109.8	+1

3.1.5 Computer Program

The CSC model described above exists as the Fortran program CSCM.FOR which runs on an Itel computer, which is IBM compatible. Installation specific features have been avoided, and it is believed that the program should be fully transportable. The only limitation is that the program uses subroutines from the International Mathematical and Statistical Library (IMSL). The availability of this library is therefore a requirement.

The main program performs input and output and subroutines take care of the calculation of effective stack height, entrainment coefficient (α) and dispersion coefficients (σ_y and σ_z). A further subroutine carries out the expanding box simulation of the chemical transformation. The integration of the differential rate equations makes use of the IMSL subroutine DGEAR, which utilizes the Gear algorithm. This algorithm is widely used in the solution of stiff systems of simultaneous differential equations (Gelinas, 1976).

The program inputs are

- Mass emission rate of NO_x (presently input as grams per hour per brake horsepower, and engine power. Note that these units were selected to be compatable with all existing compilations of engine emission data.)
- Building width and height
- Wind speed at stack height
- Stack gas temperature and exit velocity
- Ambient temperature
- Stack internal diameter
- Stability class
- Ambient ozone concentration
- Rate constants for the two reactions of the chemical mechanism.

The program has been designed to allow determination of the stack height required to avoid exceedence of the Provincial NO_2 limit, and thus allows the user to specify the range of stack heights, and the number of intermediate heights (i.e. the increment) for which the model is to be run.

The output of the program is a table for each stack height giving plume travel time, NO_x concentration, NO_2 concentration and mean NO_2/NO_x ratio as functions of downwind distance. The in-cavity NO_x concentration is also printed, as are the downwind maxima of NO_x and NO_2 and the distances at which they occur. A graph of maximum NO_2 concentration versus stack height will allow the design stack height, corresponding to a maximum ground level NO_2 concentration of 400 $\mu g/m^3$ to be read off.

A relatively simple program change would also allow output of maximum NO_x and/or NO_2 concentrations as a function of stack height.

3.2 Model Performance and Testing

The CSCM was tested using data corresponding to a representative, single-engined compressor station. A range of meteorological inputs, appropriate to Alberta conditions was considered, as was a "worst likely" case. The model was also tested against data obtained at a large compressor station. The input data and results are given below, together with an analysis of the sensitivity of the model to variations in the input data.

3.2.1 Model Inputs and Conditions

The input to the model may be broken down into three categories: source parameters, meteorological parameters and chemical parameters.

a) Source parameters: These are building size, stack height and diameter, stack gas exit velocity and temperature, and emission rate. A standard building size was adopted in the modelling study, based on information supplied by the Standards and Approvals Division of Alberta Environment's Environmental Protection Services (see Appendix A) (Powell, 1981). The height of this building was chosen as 7.0 m, and the width as 8.5 m. The depth, or downwind extent of the building is not required in the model, so these dimensions include the case of the wind blowing end on to a multiple engine building (See Figure 10). Note that the end-on wind comprises a worst case since the in-cavity concentration calculated by the model depends inversely on the cross-sectional area of building normal to the wind vector.

In fact, most compressor buildings are constructed with multiple stacks placed along the longer building face. Figure 10, therefore, illustrates the model's lack of consideration of building-stack configuration.

Stack height is an extremely important parameter. The model design therefore allows user specification of the maximum and minimum stack heights to be considered, and also the increment. A standard, representative stack diameter of 0.3 m was adopted (based on the data of Appendix A and Fanick and Dietzmann,

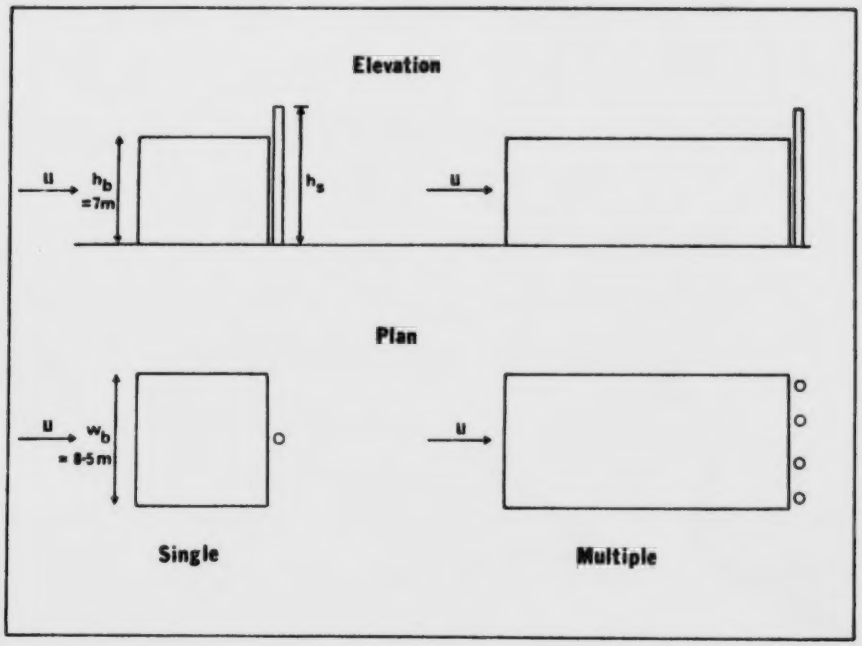

Figure 10: Configurations of the Buildings Modelled

1980). Model results are relatively insensitive to this parameter, which only enters into the flux term F, which in turn is raised to a fractional power in calculating the effective stack height. A very wide range of stack gas exit velocities has been reported, ranging from 5.9 m/s (Appendix A) to 140 m/s (Fanick and Dietzmann, 1980). Inspection of the data presented by the latter authors shows that of 66 reciprocating engines, two had stack gas velocities less than 15 m/s, 25 were between 15 and 30 m/s, 28 between 30 and 50 m/s, and 11 were greater than 50 m/s. Stack gas velocities of 20 and 40 m/s were therefore chosen for model input.

Fanick and Dietzmann (1980) also report a wide range of stack gas temperatures, i.e. 530 to 830 K. The mean of the reported values is 670 K, with a standard deviation of 45 K. Model results are relatively insensitive to this parameter since the plume rise depends on

$$\frac{T_s - T_a}{T_s}$$

raised to a fractional power. If T_a is 273 K, the term above changes from 0.48 to 0.67 as the stack gas temperature changes from 530 to 830 K.

Emission rate obviously depends on the size of the installation and its state of maintenance. It is expressed by Fanick and

Dietzmann (1980) as grams of NO_2 per hour per brake horsepower, and a representative value of 13.4 g/kW hour, with an engine of 1120 kW was adopted (i.e. 10 g/bhp hr and 1500 bhp). Downwind NO_x concentrations from the model are exactly linear in Q, the mass emission rate (the product of the two numbers quoted above) while the NO_2 concentration is approximately linear (see Section 3.2.3). Linear scaling is therefore appropriate for other installations having the same in-stack NO_2/NO_x ratio (see Section 3.2.3). Multiple stack situations are treated by lumping the emissions and assuming a single stack.

b) Meteorological Parameters: The meteorological parameters relevant to the model are ambient temperature, wind speed and stability.

Ambient temperature enters into the plume rise calculation, but sensitivity to its precise value is low. A value of 293 K was therefore adopted for this parameter, noting that a relatively high ambient temperature reduces the plume rise, thus providing a conservative estimate of ground level concentration.

Wind speed was assigned low, moderate and high values of 2, 5 and 10 m/s respectively.

Three stability classes were considered: E (slightly stable), D (neutral) and B (unstable). These classes were chosen to

ensure that the range included the most typical extremes of Alberta conditions.

c) Chemical parameters: The relevant chemical parameters are ambient ozone concentration, in-stack NO_2/NO_x ratio, and NO_2 photolysis rate. Standard values were assigned as follows:

Ambient ozone = 40 ppb

In-stack NO_2/NO_x = 0.10

NO_2 photolysis rate = $7.8 \times 10^{-3} s^{-1}$, corresponding to summer midday in Alberta (Bottenheim and Strausz, 1978)

Model sensitivity to these parameters was explored. The temperature dependence of the reaction between O_3 and NO is low, and was ignored, noting however, that the rate constant for this reaction was assigned its 298 K value. This choice provides an upper limit to the rate of NO oxidation, and thus to the NO_2 concentration.

Combination of 2 stack exit velocities, 3 wind speeds and 3 stability classes results in 18 sets of input parameters, as shown in Figure 11. However, 10 m/s winds are most unlikely with B and E stability (Turner, 1970), so 4 sets of input parameters were eliminated, as indicated by the cross hatching in Figure 11. Each of the 14 remaining conditions was modelled separately and the results are presented in the following section.

One further set of conditions was subsequently modelled, being chosen to combine a worst case stack exit velocity (5 m/s) with average meteorological conditions (D stability). This combination is expected to result in the most severe stack height requirements for maintenance of ground level NO_2 concentrations below the permissible level and was labelled Case 15.

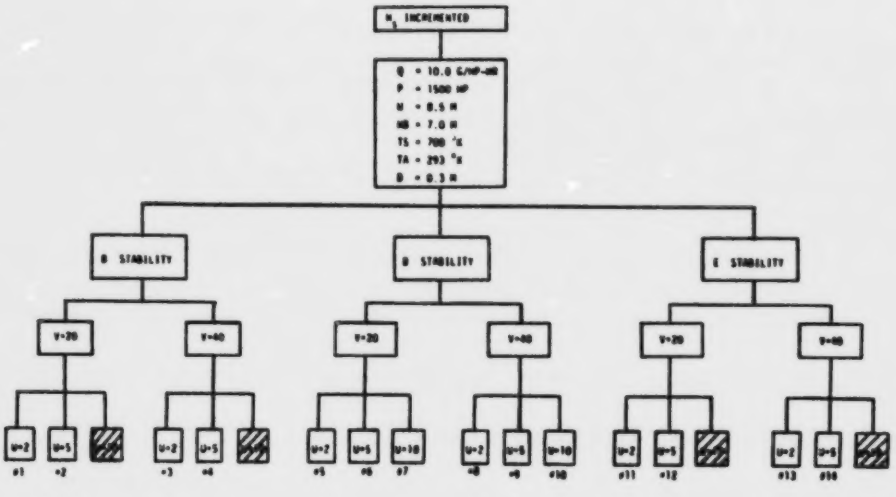

Figure 11: FLOW CHART OF MODEL INPUT PARAMETERS

3.2.2 Results

The output from a model run consists of a table of ground level NO_x and NO_2 concentrations as functions of downwind distance and plume travel time. The NO_2/NO_x ratio is also given; this is actually the concentration weighted mean of the ratios in the two parts of the plume, calculated by dividing total NO_2 concentration at the point by total NO_x concentration.

The cavity length and in-cavity NO_x concentration are also printed, as are the maximum NO_x and NO_2 concentrations downwind of the cavity, and the distances at which they occur.

Such a table is printed for each stack height specified by the user. Samples of the output are given in Appendix B for a single stack height for each of the sets of input conditions identified in Section 3.2.1. Typical results are also plotted in Figures 20 to 25 in Appendix B which display ground level NO_2 concentration as a function of downwind distance for a number of stack heights. For convenience of reference, the results for Case 1, plotted in Figure 20, from Appendix B are reproduced overleaf as Table 9 and Figure 12 respectively. These curves are plotted for Cases 1, 2, 3, 4, 7 (see Figure 11) and for the "worst likely" case. Cases which have the same ratio of V_s to $\tilde{U}$ tend to show qualitatively similar behaviour, thus

- Cases 1, 5 and 11
- Cases 2, 6, and 12
- Cases 3, 8 and 13

Table 9

Sample Of Model Output: Case 1

COMPRESSOR STATION CHEMISTRY MODEL

Q= 4.17 G/S
H= 8.50 M
HB= 7.00 M
HS= 4.00 M
U= 2.0 M/S
V= 20.0 M/S
TS= 700.0 K
TA= 283.0 K
D= 0.300 M
STAB=B
OZONE= 40.0 PPB

ALPHA=0.714
H EFF= 23.7 M

DOWNWIND DIST (M)	TRAVEL TIME (S)	NOX CONC (UG/M**3)	NO2 CONC (UG/M**3)	NO2/NOX RATIO
17.5	8.8	13050.6	1968.6	0.152
25.0	12.5	10416.2	1596.1	0.153
50.0	25.0	4850.4	766.2	0.158
75.0	37.5	2608.5	433.1	0.166
100.0	50.0	1631.8	284.7	0.181
125.0	62.5	1140.2	225.2	0.198
150.0	75.0	852.2	182.2	0.214
175.0	87.5	664.1	157.2	0.237
200.0	100.0	532.4	133.0	0.250
225.0	112.5	436.1	118.7	0.272
250.0	125.0	363.5	108.4	0.298
275.0	137.5	307.3	98.0	0.319
300.0	150.0	263.1	89.6	0.341
325.0	162.5	227.8	81.3	0.357
350.0	175.0	198.8	75.1	0.378
375.0	187.5	175.0	68.6	0.392
400.0	200.0	155.3	64.6	0.416
425.0	212.5	138.6	60.5	0.436
450.0	225.0	124.5	56.4	0.453
475.0	237.5	112.5	52.8	0.469
500.0	250.0	102.0	49.5	0.485
525.0	262.5	93.0	46.6	0.501
550.0	275.0	85.1	43.7	0.513
575.0	287.5	78.2	41.3	0.528
600.0	300.0	72.1	38.8	0.540
625.0	312.5	66.8	36.7	0.550
650.0	325.0	61.8	38.6	0.625
675.0	337.5	57.5	32.4	0.564
700.0	350.0	53.8	31.3	0.584
725.0	362.5	50.1	29.7	0.594
750.0	375.0	46.8	28.1	0.588
775.0	387.5	44.0	26.7	0.607
800.0	400.0	41.4	25.3	0.611
825.0	412.5	38.0	24.5	0.630
850.0	425.0	36.8	23.4	0.637
875.0	437.5	34.8	22.2	0.640
900.0	450.0	32.8	20.4	0.621
925.0	462.5	31.2	18.7	0.630
950.0	475.0	29.6	18.8	0.629
975.0	487.5	28.2	17.7	0.630
1000.0	500.0	26.8	17.6	0.657

CAVITY LENGTH= 17.5 M
CAVITY NOX CONC.= 50020.01 UG/M**3

MAXIMUM NOX=13050.63 UG/M**3 AT 17.5 M

MAXIMUM NO2= 1968.62 UG/M**3 AT 17.5 M

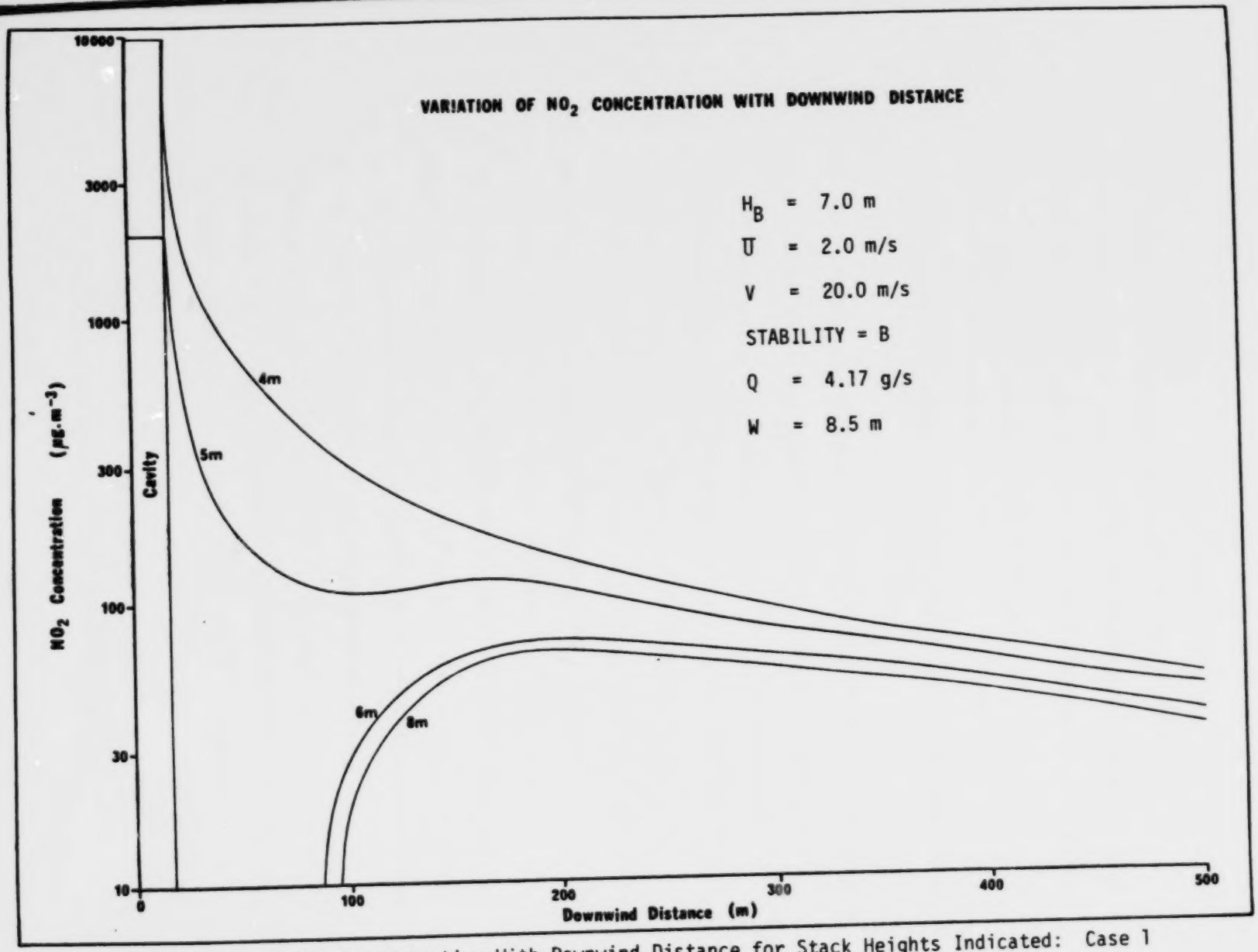

Figure 12: Variation of NO_2 Concentration With Downwind Distance for Stack Heights Indicated: Case 1

- Cases 4, 9 and 14

are similar. The differences are that with increasing stability, the downwind concentrations are higher, because of the smaller σ's.

The curves of Figures 20 to 25 show the following features, which are typical of all conditions modelled:

a) For short stacks, high in-cavity concentrations of NO_x and NO_2 are found. The upper limit for this behaviour depends on the entrainment factor, α, and thus on $V_s/\bar{U}$ as well as h_s/H_B. It corresponds typically to a stack equal to 3/4 of the building height.

b) With increasing stack height, the in-cavity concentrations drop rapidly to very low values. This feature provides the basis for stack height design, and is discussed more fully in Section 3.3. The stack height for which low concentrations are reached lies somewhere between 3/4 and 1 1/2 building heights, depending on the ratio $V_s/\bar{U}$.

c) The concentration of NO_2 downwind of the cavity shows, in many cases, a maximum value at a distance typically between 100 and 500 metres. The magnitude of this concentration and the distance at which it occurs depends on the model input parameters, but shows a low sensitivity

to stack height. The dependence is such that increasing the stack height causes the maximum concentration to decrease, and move to a greater distance. The maximum concentrations of NO_2 and NO_x generally occur within 50 metres of each other, but do not necessarily coincide.

Another feature of the results which is of great importance is the variation of the NO_2 to NO_x ratio with distance downwind. For nearly all atmospheric conditions, this ratio (which, it should be stressed, is the weighted mean of the ratios in the two parts of the plume) has an initial value of about 0.15 and shows a monotonic increase with distance. The final value reached at 1 kilometre depends on the travel time to that point, and thus on the wind speed, but generally lies in the range 0.5 to 0.7. These results indicate that the assumption of a fixed NO_2 to NO_x ratio is not appropriate.

This is further illustrated by the following example. In cases where the plume initially remains aloft for hundreds of metres, the NO_2 to NO_x ratio is initially high and decreases over the next 50 to 100 metres. Thereafter it again increases monotonically. This behaviour arises because the first contact with the ground is by the plume edge. After travelling hundreds of metres the plume edge has undergone considerable dilution, i.e. it has entrained a considerable amount of ozone, with a consequent high conversion of NO to NO_2. For further small increases in downwind distance (50 to 100 metres)

regions closer to the centre of the plume impinge on the ground. In a Gaussian plume these regions are less dilute, so that they are treated as having experienced less expansion, and thus less reaction with ozone. For greater distances still, the expansion of the whole plume becomes dominant, and increasing ozone entrainment increases the NO_2 to NO_x ratio.

In some respects this plume behaviour parallels what is known for power plant plumes, i.e. that ozone levels are highest at the plume edges, where NO to NO_2 conversion is highest, with ozone levels within the plume being very low. It should be stressed, however, that the model assumes constant ozone concentration through the plume, and the higher NO_2 to NO_x ratios at the plume edge result from the more rapid expansion experienced in those regions.

The ratio of NO_2 to NO_x will often attain a roughly constant value at relatively large downwind distances (greater than 1 kilometre). The value of this ratio is dictated by the photostationary state set up between NO, NO_2 and O_3.

Although the results shown in Figures 20 to 25 are typical, the details do vary with variation of the input parameters. The sensitivity of the model results to variation of these input parameters is considered in the next section, while the model results for a real compressor station, that at Pendant D'Oreille, will be considered in Section 3.4.

3.2.3 Model Characteristics

The dependence of the model predictions on the following input parameters has been investigated,

- Background ozone concentration
- In-stack NO_2/NO_x ratio
- In-stack NO_2 concentration
- Solar intensity
- Atmospheric stability
- Stack gas exit velocity
- Wind speed
- Stack height

Unfortunately, it was not possible to test a full matrix of the factors listed above, because of the very rapid escalation of computing costs which would have resulted. Instead, a set of inputs encompassing reasonable variations in the last four parameters was investigated (see Section 3.2.1, particularly Figure 11). Variation of each of the first four parameters was considered in isolation.

3.2.3.1 Background Ozone Concentration

Because of the rapid rate of oxidation of NO by ozone, it is to be expected that predicted NO_2 concentration will be sensitive to ambient ozone concentrations. To obtain a quantitative estimate of the

effect of changing the ozone concentration, the model was rerun for one set of atmospheric and source conditions, but with the ambient ozone concentration doubled to 80 ppb. Such high ozone concentrations are occasionally found in Alberta during the summer (Alberta Environment data). The effects of this change are shown in Table 10.

Table 10

Effect Of Increased Ambient Ozone Concentration

Downwind Distance (m)	$[NO_x]$ ($\mu g/m^3$)	$[NO_2]$ ($\mu g/m^3$)		Increase in $[NO_2]$ (%)
		$[O_3]$ = 40 ppb	$[O_3]$ = 80 ppb	
100	77.7	26.2	40.8	56
200	270.0	63.2	97.0	53
300	197.6	61.0	83.8	37
400	132.8	47.7	78.2	64

Conditions: h_s = 7.0 m

$\bar{U}$ = 2.0 m s^{-1}

V_s = 20.0 m s^{-1}

Stability = B

i.e. case 1

These results apply to a stack height of 7 metres, equal to the building height. The results for other stack heights are similar,

i.e. doubling the ambient ozone concentration increases the NO_2 concentrations in the region of the downwind maximum by up to about 60 per cent. The position of the downwind maximum is unchanged, or, for the highest stacks considered (approximately 1.5 building heights), moves 25 metres closer to the source.

The results presented in Table 10 shed some light on the magnitude of the effects to be expected when the expanding box trajectory lies wholly within the plume (see Section 3.1.4). The in-plume ozone concentration could be substantially below that of the ambient air, and the results of Table 10 indicate that the result would be a substantial decrease in NO_2 concentration. However, since no information is available on ozone concentrations in compressor station plumes, no attempt was made to model this aspect in more detail.

3.2.3.2 In-Stack Ratio of NO_2 to NO_x

The standard value of this ratio used in the modelling runs was 0.10, which is higher than the value of 0.03 reported by Angle et al (1979) for an Alberta Compressor station. However, Fanick and Dietzmann (1980) have reported values of this ratio ranging up to 0.15. The mean ratio reported by them was approximately 0.05 with a standard deviation of 0.03. Four engines out of a total of 51 had measured in-stack NO_2/NO_x ratios greater than or equal to 0.1. The standard value

of 0.1 was therefore chosen to represent a reasonable upper limit; while the effect of reducing the NO_2 to NO_x ratio to 0.05 was also tested. The comparison is shown in Table 11.

Table 11

Effect Of Decreased In-Stack NO_2/NO_x Ratio

Downwind Distance (m)	$[NO_x]$ ($\mu g/m^3$)	$[NO_2]$ ($\mu g/m^3$) $NO_2/NO_x = 0.10$	$NO_2/NO_x = 0.05$	Decrease (%)
100	77.7	26.2	23.0	12
150	241.1	60.6	50.3	17
200	270.0	63.2	54.3	14
250	238.4	65.6	63.1	4
300	197.6	61.0	55.4	9
350	161.6	46.6	39.6	15

Conditions: $h_s = 7.0$ m

$\bar{U} = 2.0$ m s^{-1}

$V_s = 20.0$ m s^{-1}

Stability = B

i.e. case 1

These results were obtained for a stack height equal to 7 metres. Similar effects are found for other stack heights and atmospheric

conditions, though larger percentage decreases (up to 25 or 30 per cent) in NO_2 concentration are found close to the source when the plume impinges there. The decrease is, of course, 50% at the source.

3.2.3.3 In-Stack NO_x Concentration, And NO_x Mass Emission Rate

Runs of the expanding box model for several different in-stack NO_x concentrations, holding NO_2/NO_x constant, revealed that the final ratio of NO_2/NO_x at all reaction times remained constant to within 10% for NO_x concentrations in the range 50 to 110 μmol l^{-1} (1200 to 2600 ppm). These concentrations cover the range expected in the exhausts from natural gas compressor stations driven by reciprocating engines (Fanick and Dietzmann, 1980).

The downwind NO_x concentration predicted by the Dual Plume Model is directly proportional to Q, the mass emission rate of NO_x. Because of the approximate constancy of NO_2/NO_x ratio with initial NO_x concentration noted above, it also follows that the downwind NO_2 concentration predicted by the CSCM will be directly proportional to Q (if all other factors remain constant).

Results presented in this report have been calculated for Q equal to 15 kg per hour. Such a value is representative of engines

of 750 to 1500 kW (1000 to 2000 horsepower) (Fanick and Dietzmann, 1980), though the actual emission rates are highly dependent on details of the engine design, and operation. Linear scaling of the calculated NO_2 concentrations should be applied for other emission rates.

3.2.3.4 Solar Intensity

Because of the photochemical nature of the reactions of NO_2, the solar intensity is a potentially important parameter in determining the extent of conversion of NO to NO_2. For most model runs the solar intensity used corresponded to solar noon in summer. The effect of varying solar intensity was tested by rerunning one set of conditions with the intensity reduced first to 50% and then to zero (see Table 12).

The effects are similar for other stack heights, and for another set of source and atmospheric conditions, namely an increase of up to about 25% for a 100% decrease in solar intensity. In practice, this figure of 25% would often be an overestimate, since production of ambient ozone also has a photochemical basis. Reduced solar intensity would thus tend to result in reduced background ozone concentrations, which, in turn, lead to lower conversion of NO to NO_2 (see Section 3.2.3.2 above). The ozone levels do not, however, drop

rapidly with a decrease in solar intensity, so the figures in the "zero" column are appropriate to night time NO_2 production in those cases where the plume still impinges on the ground.

Table 12

Effect of Reduced Solar Intensity

Downwind Distance (m)	$[NO_x]$ ($\mu g/m^3$)	$[NO_2]$ ($\mu g\ m^{-3}$) Summer Noon	0.5 Summer Noon	Zero
100	77.7	26.2	27.4	29.0
150	241.1	60.6	63.0	63.4
200	270.0	63.2	80.5	74.8
250	238.4	65.6	59.6	78.0
300	197.6	61.0	71.0	72.4
350	161.6	46.6	69.2	71.6
400	132.8	47.7	69.4	59.0

Conditions: $h_s = 7.0$ m

$\bar{U} = 2.0\ m\ s^{-1}$

$V_s = 20.0\ m\ s^{-1}$

Stability = B

i.e. case 1

The results of Table 12 indicate that relatively close to the source the production of NO_2 is largely controlled by the supply of ozone

to the plume with photolytic dissociation of NO_2 being less important. Far downwind, where mixing is complete, complete conversion to NO_2 will occur in the absence of sunlight.

3.2.3.5 Atmospheric Stability

The effect of atmospheric stability on ground level NO_2 concentration may be seen by comparing the results corresponding to the sets of Cases (1, 5, 11), (2, 6, 12), (3, 8, 13) and (4, 9, 14) (see Appendix B and Figure 11).

Calculated in-cavity concentration does not depend on stability, because of the relative simplicity of the model on which the calculation is based, and because the fairly limited basis for α does not permit a variation with stability.

The variation of downwind concentration with stability is entirely in agreement with what would be predicted qualitatively.

a) Under conditions of low plume rise (short stack and/or low V_s) increasing stability leads to increasing concentrations, because of the smaller dispersion coefficients associated with greater stability.

b) For higher stacks and/or V_s, giving greater plume rise, the plume has an increasing tendency to remain aloft as the sta-

bility increases and does not impinge on the ground until it has travelled some distance. Considerable dispersion has then taken place, and the result is that ground level concentrations tend to decrease with increasing stability.

It would appear from the results of this study (Appendix A) that the maximum effect produced on concentration by the change of stability from B to E is roughly a factor of 2. This factor can work in either direction, depending on whether the plume rise is relatively small or large, because of the two opposite effects discussed above.

3.2.3.6 Stack Velocity

The effect of stack exit velocity on ground level NO_2 concentration can be seen by inspecting the model results of Appendix B corresponding to the following pairs of cases (1 and 3), (2 and 4), (5 and 8), (6 and 9), (7 and 10), (11 and 13), and (12 and 14). In general, doubling the stack exit velocity (20 ms^{-1} to 40 ms^{-1}) causes a substantial decrease in ground level NO_2 concentration, particularly in regions of high concentration.

The dependence of concentration on stack velocity enters via two effects.

a) Plume rise is important, as discussed in Section 4.4.1, and depends on V_s or $V_s^{2/3}/\bar{U}$, depending on the atmospheric stability.

b) The entrainment coefficient, α, is a sensitive function of $V_s/\bar{U}$. This factor is probably of greater importance than that of (a) above, since a large value of α can give rise to very high in-cavity concentrations of NO_x and NO_2. It should be noted that α also depends on the stack height (more specifically on h_s/H_B) and will be discussed further under that heading.

The stack exit velocities which were used in this modelling work are somewhat larger than those of Appendix A, as was discussed in Section 3.2.1.

3.2.3.7 Wind Speed

The effect of wind speed on NO_2 concentration is revealed in the model runs based on the following sets of cases (Appendix B): (1 and 2), (3 and 4), (e, 6 and 7), (8, 9 and 10), (11 and 12), and (13 and 14).

The primary effect of wind speed arises through the dependence of α on $V_s/\bar{U}$. Through this relationship, increased wind speed causes in-

creased trapping of the plume in the cavity (i.e. increased α) and thus increased ground level concentrations of NO_x and NO_2. It also affects plume rise of the elevated portion of the plume.

In opposition to this are two further effects tending to reduce ground level NO_2 concentration as wind speed increases.

Firstly, the basic Dual Plume equation contains an inverse dependence on wind speed. Secondly, at higher wind speeds a given downwind distance corresponds to a shorter reaction time, and thus to lower conversion of NO to NO_2. The dispersion coefficients are functions of distance and stability only, so that the decreased conversion results directly in decreased NO_2 concentrations.

It is thus not possible to generalize about the effect of changes in wind speed on downwind concentration.

3.2.3.8 Stack Height

Stack height is a very important parameter in determining ground level NO_2 concentrations, which it affects both through α (via the ratio h_s/H_B) and through its effect on plume rise.

A range of stack heights was therefore considered for each of the sets of input conditions adopted for the model. Typical dependence of ground level concentration on stack height is shown in Figures

20 to 25 (Appendix B). The important features revealed in these figures are:

a) The in-cavity concentration can be very high for short stacks ($< H_B$).

b) In-cavity concentration decreases rapidly with increasing stack height. This reflects the functional dependence of α on h_s/H_B for a given $V_s/\bar{U}$.

c) The maximum concentration downwind of the cavity decreases and moves to a greater distance with increasing stack height. This dependence is fairly weak.

The precise way in which in-cavity concentration varies with stack height will depend, as noted above, on $V_s/\bar{U}$. The worst cases (i.e. highest concentrations) will be found for low $V_s/\bar{U}$. The high exhaust gas velocities characteristic of large reciprocating engines are thus of great importance.

3.2.3.9 Plume Rise

The plume rise equations used in the Dual Plume Model have definite shortcomings when applied to compressor engine plumes. These are discussed in detail in Section 2.4.4 and will not be repeated here.

The original plume rise equations have been retained in spite of these shortcomings.

To check the sensitivity of model predictions to the calculated plume rise, a calculation was carried out with the plume rise reduced to 75 per cent of the value predicted by the Plume Rise Equations. It is to be expected that this reduction will cause a significant increase in ground level concentrations, since it is equivalent in many respects to a reduction in physical stack height as discussed in the preceeding section. This expectation is confirmed by the results presented in Table 13.

Table 13

Effect Of Reducing Plume Rise By 25%

Distance (m)	Full Plume Rise $[NO_x]$ ($\mu g/m^3$)	Full Plume Rise $[NO_2]$ ($\mu g/m^3$)	Reduced Plume Rise $[NO_x]$ ($\mu g/m^3$)	Reduced Plume Rise $[NO_2]$ ($\mu g/m^3$)
50	0.0	0.0	1.1	0.3
100	77.7	26.2	246.4	50.6
150	241.1	60.6	401.7	78.3
200	270.0	63.2	358.9	77.8
250	238.4	65.6	285.6	65.5
300	197.6	61.0	223.6	57.4

Conditions: h_s = 7.0 m V_s = 20.0 m s^{-1}

$\bar{U}$ = 2.0 m s^{-1} Stability = B i.e. case 1

The results of Table 13 show that the maximum NO_x concentration increases significantly (by approximately 50%) and moves closer to the source. The maximum NO_2 concentration also moves closer to the source, and increases, but by only 20% for the case considered here. The shorter travel time to the point of maximum concentration results in lower conversion of NO to NO_2, which helps to offset the higher NO_x concentration.

3.2.3.10 Summary

The sensitivity of the CSCM to variation of the input parameters may be summarized as follows:

- Maximum ground level NO_2 concentrations are increased if the background ozone concentrations, the in-stack NO_2 to NO_x ratio, or the NO_x emission rate are increased, or if the solar intensity, the effective stack height (i.e. physical height or plume rise), or the stack gas exit velocity are decreased.

- Changes in stability and wind speed cause increases or decreases in NO_2 concentration, depending on the values of the other input parameters.

3.3 Application of Model to Stack Design

As was discussed in Section 3.2.3, stack height is one of the most important model input parameters in determining the predicted ground level concentration. In practical terms, too, stack height is important because it is directly under the control of the compressor station designer.

The generalization can be made that the maximum ground level concentration, whether it is in the cavity, or downwind of the cavity, is always reduced if the stack height is increased. The model has therefore been designed to allow the user to specify the range of stack heights to be considered to produce a plot of maximum ground level NO_2 concentration versus stack height. This then allows determination of a design stack height, which will avoid exceedence of the Alberta Provincial limit for NO_2 of 400 $\mu g/m^3$ as a 1 hour average.

This procedure was followed for the 14 cases described in Section 3.2.1, and case 7 was identified as the case in which the greatest stack height was required to avoid exceedence of the limit. Cases 2, 6 and 12 presented the next most severe situation, all three being equal. This follows because the maximum ground level concentration for these cases occurs in the cavity. Cases 2, 6 and 12 all have the same ratio of V_s to $\bar{U}$, which means that for any

given stack height they all have the same value of the entrainment coefficient, α.

The corresponding plots of maximum ground level NO_2 concentration versus stack height are shown in Figure 13 for Case 7 and Figure 14 for Cases 2, 6 and 12. The NO_2 concentrations for these two figures were calculated as twenty per cent of the NO_x concentrations. This represents a rounding up of the ratio of 0.14 derived in Section 3.1.3, and was applied to provide a margin of safety because of the simplified procedure followed by the model in calculating in-cavity concentrations.

The conclusion to be derived from Figures 13 and 14 is that a stack height of at least 7.7 metres (i.e. 1.1 building heights) will ensure against exceedence of the Alberta limit for ground level NO_2 concentrations, for all but the worst case.

The worst, Case 15, was also considered, corresponding to a low stack gas exit velocity of 5 m s^{-1}, as described in Section 3.2.1 The building configuration for this case was the same as that used for cases 1 to 14, the wind speed was 5 metres per second, and D stability was used. The graph of in-cavity NO_2 concentration (calculated assuming $NO_2 = 0.2 \times NO_x$, as above) against stack height is shown in Figure 15. For these conditions the minimum required

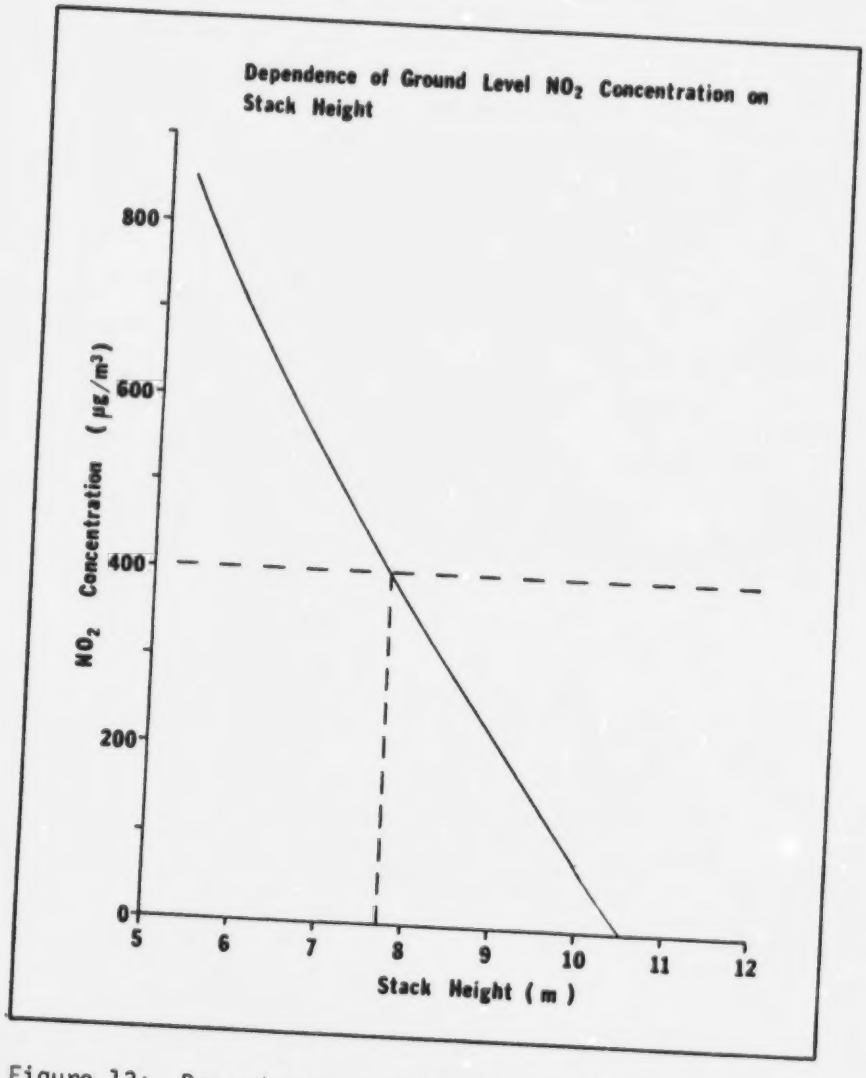

Figure 13: Dependence of Maximum Ground Level NO_2 Concentration on Stack Height

In-Cavity: Case 7:
$\bar{U}$ = 10 m/s, V_s = 20 m/s,
D Stability

Q = 4.17 g/s

H_B = 7.0 m

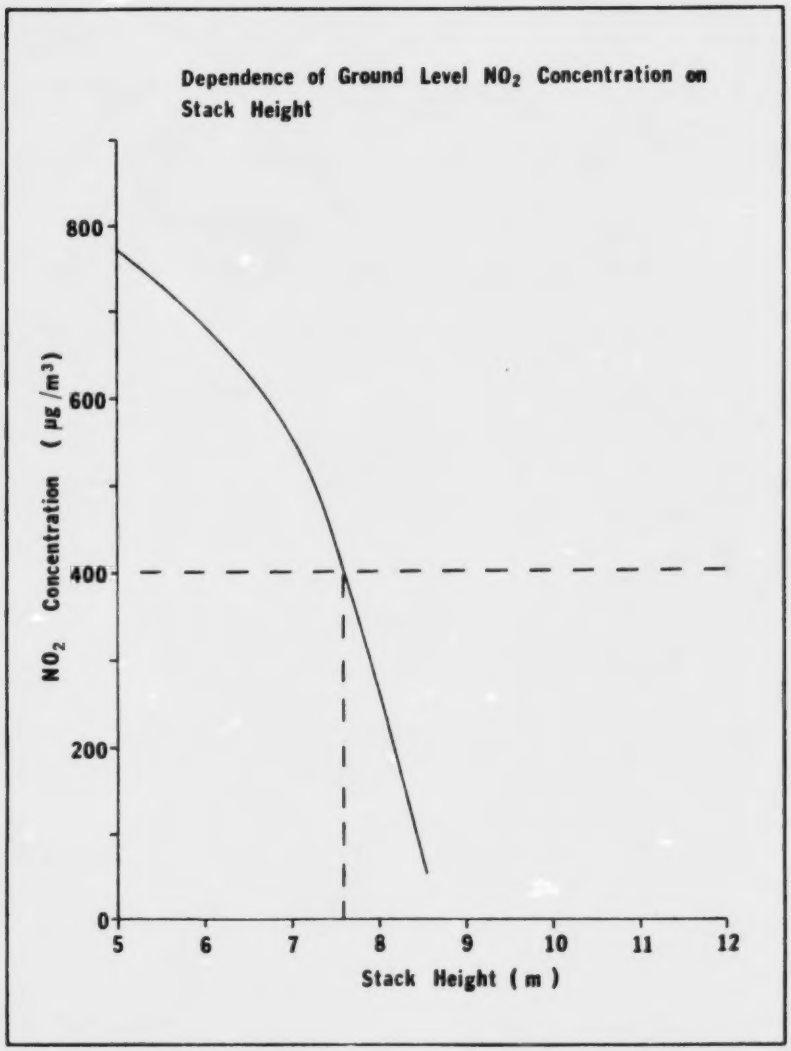

Figure 14: Dependence of Maximum Ground Level NO_2 Concentration on Stack Height

In-Cavity: Cases 2, 10 and 12:
$\bar{U}$ = 5 m/s, V_s = 20 m/s
Q = 4.17 g/s
H_B = 7.0 m
W = 8.5 m

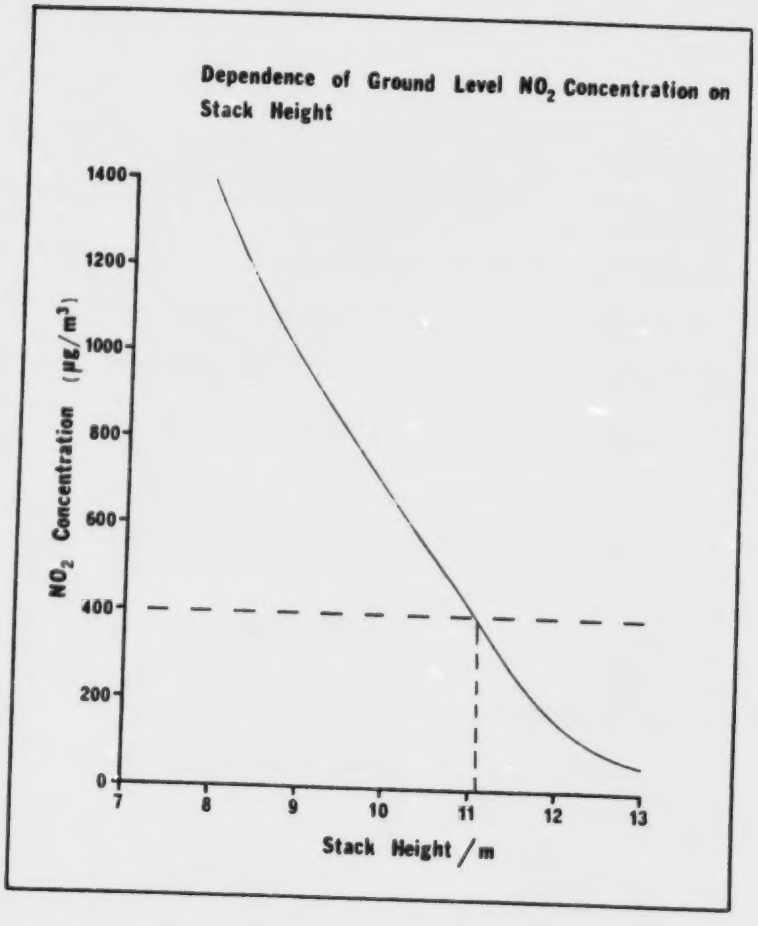

Figure 15: Dependence of Maximum Ground Level NO_2 Concentration on Stack Height.

In-Cavity: Worst likely Case:
$\bar{U}$ = 5 m/s, V_s = 5 m/s,
D Stability

Q = 4.17 g/s

H_B = 7.0 m

W = 8.5 m

stack height is 11.1 metres (1.6 building heights), underlining the importance of high stack gas exit velocities.

All discussion of minimum required stack height given above has centred on the requirement that the in-cavity NO_2 concentration be brought below 400 micrograms per cubic metre, and no mention has been made of ground level concentrations downwind of the cavity. The reason for this is that, for all cases modelled, it has been found that if the stack height is great enough to bring the in-cavity NO_2 concentration below the Alberta limit, the concentration downwind of the cavity is always brought substantially below the limit. In other words, it is the in-cavity concentration which determines how high the stack must be to avoid exceeding the 400 microgram per cubic metre limit.

It should be noted, however, that variation with stack height of the maximum concentration downwind of the cavity is much slower than the corresponding variation of in-cavity concentration. It is therefore conceivable that certain combinations of parameters could give rise to the situation where the in-cavity NO_2 concentration is below the Provincial limit, but this limit is exceeded at some point further downwind. Such a situation is likely to have a low probability of occurrence, however, since it was not encountered during this modelling study, which featured a wide range of input parameters.

For the sake of comparison, Figure 16 illustrates typical variation of maximum NO_2 concentration downwind of the cavity with stack height. The distance at which the maximum concentration occurs is also noted on the figure. Note that all of these concentrations are, as has been noted previously, substantially below the Alberta limit.

The point should be stressed again that ground level NO_2 concentrations scale approximately linearly with Q, the mass emission rate of NO_x. The conclusions derived above relating to stack height therefore apply strictly to the particular conditions being modelled, and will probably have to be modified for larger engines, or multiple-engine installations.

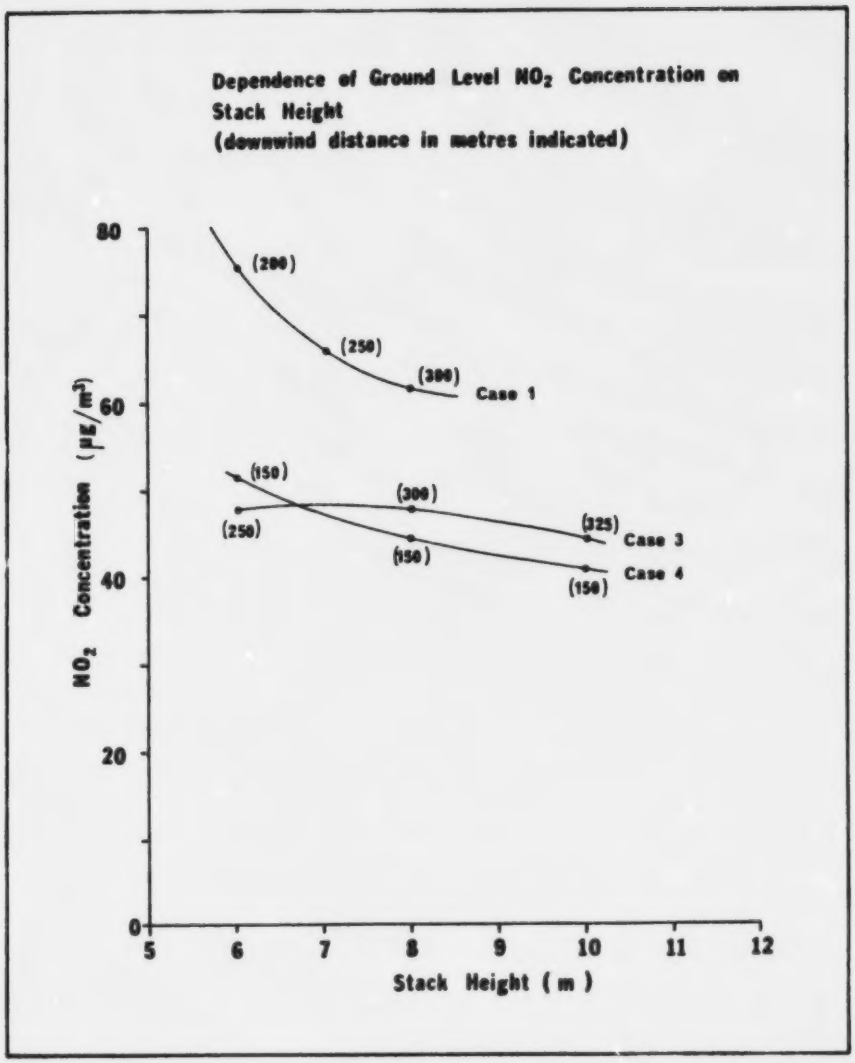

Figure 16: Dependence of Maximum Ground Level NO_2 Concentration on Stack Height

Downwind of Cavity: Case 1: $\bar{U}$ = 2 m/s, V_s = 20 m/s
Case 3: $\bar{U}$ = 2 m/s, V_s = 40 m/s
Case 4: $\bar{U}$ = 5 m/s, V_s = 40 m/s
All B Stability
Q = 4.17 g/s
H_B = 7.0 m
W = 8.5 m

3.4 Application of the CSCM to the Pendant D'Oreille Compressor Station

The CSCM was applied to the case of the Pendant D'Oreille compressor station, for which NO_2 concentration data were supplied by Alberta Environment. It is a large (3 building, 8 engine) installation, depicted in Figure 17. Emissions at each building were assumed to originate from a single stack, located at the centre of the north wall. Source conditions were as shown in Table 14.

Table 14

Source Conditions for Pendant D'Oreille Compressor Station

	Building		
	1	2	3
Stack height	5.8 m	4.3 m	14.0 m
Stack diameter	0.203 m	0.203 m	0.305 m
Exit velocity	50 m/s	56 m/s	43 m/s
Temperature	510 K	950 K	766 K
Mass emission rate	9.1 g/s	3.7 g/s	7.0 g/s
Building height	6.5 m	6.4 m	7.62 m
Building width (taken from plot plan, since tabulated data give $H_B = W$	24 m	20 m	18 m

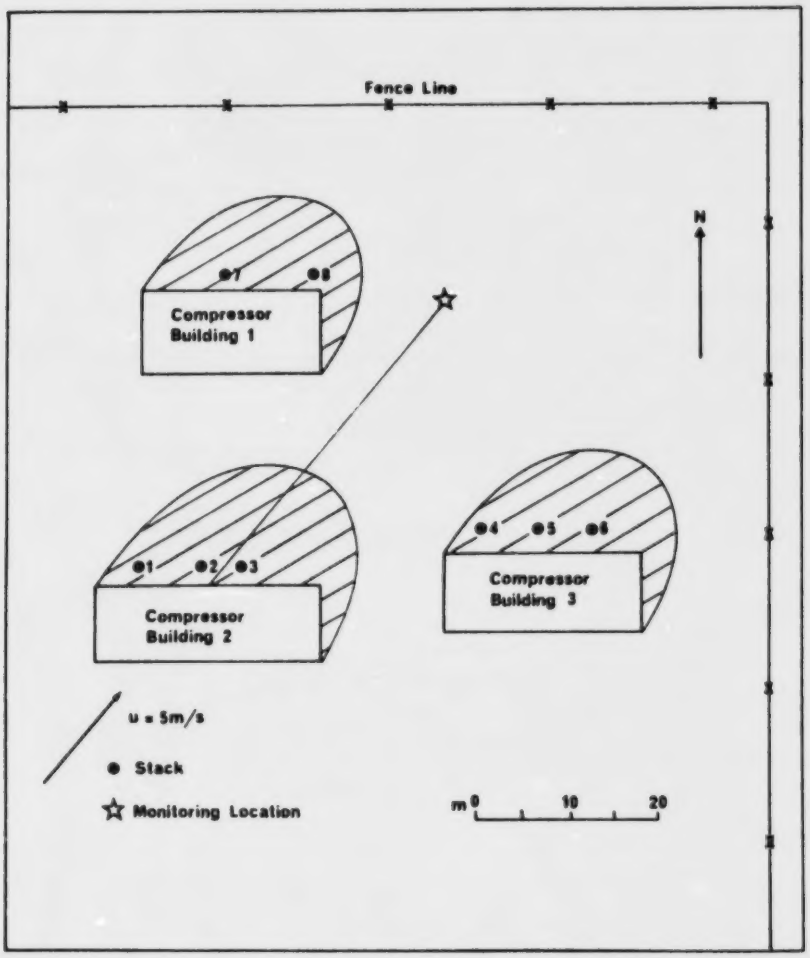

Figure 17: Pendant D'Oreille Compressor Station Plot Plan

The wind was taken as blowing from the entre of building 2 to the monitor at 5 m/s. This corresponds to a SW wind, for which 1 hour average ground level concentrations exceeding 400 $\mu g/m^3$ have frequently been measured at a distance of 40 m from Building 2. The CSCM was run to see if such large concentrations were predictable. The building width quoted in Table 15 is that normal to this wind direction. D stability was assumed.

Also included in Figure 17 are an indication of the wind direction and the approximate outline of the building cavities. It is reasonable to conclude from these and the monitor location shown in Figure 17 that emissions from Building 2 predominate at the detector. The CSCM was therefore run with Building 2 data. The results are shown in Table 15.

As can be seen from Table 14 the high stack gas exit velocities given for this station give rise to a plume which does not impinge on the ground until it has travelled more than 50 m, i.e., beyond the monitor. This model run cannot be reconciled with the observed NO_2 concentrations greater than 400 Mg/m^3.

The possibility was tested that the stack gas exit velocity was an overestimate, derived indirectly, and the model was run again with V_s set to 24 metres per second, a reduction of 50%. For this case α, the entrainment factor, is non-zero, and significant ground level NO_2 concentrations are found at the monitor location, 40 metres downwind (see Table 16).

Table 15

Model Results for Pendant D'Oreille: V=50 m/s

Q= 5.08 G/S
W= 24.00 M
WB= 6.50 M
WS= 6.20 M
U= 5.0 M/S
V= 50.0 M/S
TS= 510.0 K
TA= 253.0 K
D= 0.250 M
STAB=D
OZONE= 40.0 PPB

ALPHA=0.0
H EFF= 15.4 M

DOWNWIND DIST (M)	TRAVEL TIME (S)	NOX CONC (UG/M**3)	NO2 CONC (UG/M**3)	NO2/NOX RATIO
16.2	3.3	0.0	0.0	0.0
25.0	5.0	0.0	0.0	0.0
50.0	10.0	0.0	0.0	0.0
75.0	15.0	2.4	0.7	0.278
100.0	20.0	50.7	13.6	0.267
125.0	25.0	191.6	41.7	0.218
150.0	30.0	366.9	68.4	0.186
175.0	35.0	512.9	87.6	0.171
200.0	40.0	609.1	99.7	0.164
225.0	45.0	660.5	105.6	0.160
250.0	50.0	678.8	108.5	0.160
275.0	55.0	675.1	108.9	0.161
300.0	60.0	657.6	107.4	0.163
325.0	65.0	632.9	104.7	0.165
350.0	70.0	603.8	101.6	0.169
375.0	75.0	573.2	98.8	0.172
400.0	80.0	542.5	95.0	0.175
425.0	85.0	512.5	91.6	0.179
450.0	90.0	483.9	89.3	0.185
475.0	95.0	456.8	86.5	0.189
500.0	100.0	431.4	84.1	0.195

CAVITY LENGTH= 16.3 M
CAVITY NOX CONC.= 0.0 UG/M**3

MAXIMUM NOX= 678.77 UG/M**3 AT 250.0 M

MAXIMUM NO2= 108.90 UG/M**3 AT 275.0 M

Table 16

Model Results for Pendant D'Oreille: V= 24m/s

Q= 9.06 G/S
H= 24.00 M
HB= 6.50 M
HS= 6.20 M
U= 5.0 M/S
V= 24.0 M/S
TS= 510.0 K
TA= 293.0 K
D= 0.250 M
STAB=D
OZONE= 40.0 PPB

ALPHA=0.104
H EFF= 11.9 M

DOWNWIND DIST (M)	TRAVEL TIME (S)	NOX CONC (UG/M**3)	NO2 CONC (UG/M**3)	NO2/NOX RATIO
16.2	3.3	829.8	114.4	0.138
25.0	5.0	805.7	111.1	0.138
50.0	10.0	705.5	100.0	0.142
75.0	15.0	674.3	107.0	0.159
100.0	20.0	857.0	147.7	0.165
125.0	25.0	1160.5	181.3	0.156
150.0	30.0	1306.0	199.9	0.153
175.0	35.0	1337.1	204.0	0.153
200.0	40.0	1296.0	200.3	0.154
225.0	45.0	1224.2	192.5	0.157
250.0	50.0	1136.9	181.7	0.160
275.0	55.0	1047.7	173.6	0.166
300.0	60.0	962.4	164.2	0.171
325.0	65.0	883.4	152.7	0.173
350.0	70.0	811.4	147.0	0.181
375.0	75.0	746.6	139.5	0.187
400.0	80.0	686.4	133.1	0.193
425.0	85.0	636.3	126.0	0.198
450.0	90.0	589.6	118.8	0.202
475.0	95.0	547.7	116.2	0.212
500.0	100.0	510.0	110.2	0.216

CAVITY LENGTH= 16.3 M
CAVITY NOX CONC.= 1212.50 UG/M**3

MAXIMUM NOX= 1337.08 UG/M**3 AT 175.0 M

MAXIMUM NO2= 204.02 UG/M**3 AT 175.0 M

However, even eith this large and arbitrary reduction in the stack gas exit velocity, the calculated NO_2 concentration is only 50% of the Alberta Provincial Objective. Further adjustment of $\bar{U}$ and incorporation of emissions from Building 1 would allow the model results to be "tuned" to match the observed contraventions, but such an exercise would prove nothing, and was not carried out.

A number of reasons can be advanced for the inability of the CSCM to predict the observed exceedences of the Alberta Provincial NO_2 limit. Chief among these are the following:

1. The CSCM is designed to simulate the dispersion of pollutants emitted at a single building. The Pendant D'Oreille Station has three buildings in close proximity, which probably leads to considerable complexity in the air flows.

2. As noted in Section 3.2.3, stack gas exit velocity is a very important input to the model, and should be determined directly for each situation being modelled.

Although this has proved to be an interesting test of the model, ground level NO_2 measurements at a number of points are required to allow a characterization of model performance.

3.5 Recommendations for Model Use and Improvement

The Compressor Station Chemistry Model was developed by adding a chemistry module to an existing dispersion model. Largely as a consequence of this approach it has a number of inherent limitations. These have been discussed in detail in Section 3.1.4, and the major problems are restated briefly below.

i) Changes in the functional form of the dependence of plume volume on travel time, corresponding to the various stages of plume development, are not incorporated.

ii) The rates of reactions of order greater than one may not be correctly calculated in those regions where the two parts of the plume overlap.

iii) Ozone concentrations within the plume are assumed to be equal to those in the background air.

Three options are available for future modelling of the emissions from compressor stations.

i) Use the CSCM essentially as it is, recognizing the limitations listed above.

ii) Make changes to the CSCM to address the limitations, while retaining the existing formulation.

iii) Develop a new model integrating dispersion and chemistry drawing on the experience gained with CSCM

These options are discussed below.

3.5.1 CSCM Unchanged

This option is the least satisfactory since the inherent limitations of the model are not addressed. It is not without any merit, however, since the use of the model in stack height design normally involves only the calculation of in-cavity concentrations (see Section 3.3) for which the limitations listed above do not apply.

If this is to be the chief use of the model, it is recommended that additions be made to the output section to allow print out of a table of maximum ground level concentrations versus stack height.

3.5.2 CSCM Upgraded

It is envisaged that an improved CSCM would retain the existing formulation, i.e. consecutive calculation of dispersion and chemical reaction, with improvements being concentrated on the treatment of in-cavity NO_2 concentrations, and on ozone concentrations within the plume. In detail the recommended improvements are:

i) Use dispersion coefficients which incorporate enhancement due to the building. Note that this modification would

necessitate a recalculation of the entrainment coefficient, α, and it would be highly desirable to incorporate field study results to improve the characterization of this coefficient.

ii) Verify the in-cavity NO_2/NO_x ratio. Field study results would again be desirable, including measurement of in-cavity ozone concentrations.

iii) Measure in-plume ozone concentrations so that adjustments can be made in the model to the ambient ozone concentration entrained into the expanding box.

iv) Adjust the calculation of reaction rates where the two parts of the plume overlap. The most appropriate way to do this will probably be to check at each point in the expanding box trajectory that the ozone concentrations in the two parts of the plume are equal, and, if necessary, to adjust the lower concentration to equal the higher one. This procedure would be in line with the discussion of Section 3.1.4.

It is highly desirable that the performance of the model be verified against experimental results.

3.5.3 Development of a New Model

The separate simulation of dispersion and chemistry, as used in the CSCM, contains an inherent limitation, in that the interaction between the processes (which occurs in the real world) can not be accounted for. It is thus difficult to treat satisfactorily such features as the depletion of ozone in the plume, and the enhancement of the rates of second order reactions where the two parts of the plume overlap. The result of potential problems such as these is that the model must be validated very carefully. It is recommended that a reactive plume model, applicable to building wakes, and featuring integration of chemistry and dispersion should be developed.

In developing such a reactive plume model, a choice must be made between a Lagrangian or an Eulerian framework. At present the Lagrangian formulation is recommended, since this choice can be expected to produce a useful model within a reasonable period of time. However, there seems little doubt that many of the world's leading practitioners of mathematical modelling are now tending to favour the Eulerian approach for all spatial scales (Lamb, 1982; Seinfeld, 1982; Elliassen, 1982; Prahm, 1982). With continued improvement in mathematical techniques and computer technology an Eulerian compressor station model will probably be favoured in the future.

A Langrangian model for application to compressor stations would incorporate the following features.

i) Dual plume formulation, since this allows explicit treatment of in - and near - cavity effects. Building enhanced dispersion would be built in as discussed in Section 3.4.2 above.

ii) Each of the resulting two plumes would be segmented, as is done in a number of existing reactive plume models (see, for example, Bottenheim and Strausz, 1982; Stewart and Liu, 1980; and Melo et al, 1978). This segmentation of the plume cross-section into individual cells allows chemistry and dispersion to be advanced in step with each other, with expansion proceeding correctly through the various phases of plume development. Ozone concentrations within the plume will then be correctly treated, and, by keeping track of cell positions, the overlap of the two plumes can also be treated. It is envisaged that the concentrations of overlapping cells would be combined for the rate calculation, then repartitioned for the next dispersion step.

Again, it is important that the model be checked against good quality experimental results.

4.0 FIELD MEASUREMENT PROGRAM

This chapter presents the work carried out during the third and final stage of the Compressor Exhaust Chemistry and Wake Diffusion Study. It describes the design of an experimental field measurement program to answer 'key' questions about wake diffusion and NO to NO_2 conversion -- for example, what are the effects of building air flow distortion on ground level concentrations and NO to NO_2 conversion. The ultimate objective in answering these questions is to ensure that our understanding of chemical and dispersion processes in the vicinity of gas compressor buildings is adequate and that the Compressor Station Chemistry Model (CSCM) developed as a method of designing compressor station stack heights is based on sound principles and produces accurate predictions. The field measurement program, therefore was designed to investigate the relationship between chemistry and dispersion by testing the ability of the CSCM to model the chemistry and dispersion processes downwind of gas compressor stations.

The field program design process consisted of the following steps:

- identification of all factors in the model requiring measurement

- determination of actual measurement methods for each of these factors

- combination of the measurement methods into an actual field program

- formulation of the analyses expected from the data.

The description of the final program design reflects these steps.

In order to fulfill its objectives, the field measurement program was designed to consist of two parts, namely:

1. a model evaluation field study
2. a model verification field study.

The first part, the model validation field study has two objectives:

- to assess the predictive capability of the CSCM by comparing predictions to measurements
- to adjust the CSCM, using empirical results, to increase its predictive accuracy.

The second part of the program, the model verification study, has the objective of quantifying the predictive accuracy of the evaluated model for other gas compressor facilities. This must be done by comparing the evaluated model to at least one independent set of data.

At the end of these two studies (and their requisite analysis programs), many of the questions related to wake chemistry and diffusion should be answered and the accuracy of the CSCM for compressor station stack design should be optimized and quantified.

The balance of this chapter is devoted to the description of the proposed field measurement program. It is presented in the manner in which it was designed, i.e. by identifying what factors need to be measured (and why), by describing actual measurement techniques for these factors, and, finally, by describing the full measurement programs in the evaluation and verification studies. It is obvious that a myriad of details must be considered in designing such field studies. To keep this description to a reasonable length, it focusses only on the most important aspects of the program. Specific details have been added only where time has allowed. Expected analyses of the data are described briefly.

4.1 Required Measurements

Based on the Compressor Station Chemistry Model, the following measurements should be made:

building length, L

building width, W

building height, H_B

building orientation to the mean wind, θ

stack diameter, d

stack height, h_s

stack gas exit velocity, V_s

stack gas exit temperature, T_s

stack emission rates of NO, NO_2 and hydrocarbons

wind speed, $\bar{U}$

wind direction

solar radiation (total incoming), S

ambient temperature, T_a

cloud cover

background air ozone concentrations

background air hydrocarbon concentrations

ground level, centre-line, one hour concentrations of NO

ground level, centre-line, one hour concentrations of NO_2

plume rise, Δh

cavity length, L_c

cavity correction factor, K (see Section 2.4).

residence time of pollutants in cavity, τ_c

cavity and far-wake cross-plume entrainment of ozone

instantaneous plume position (vertical and horizontal).

It would also be useful, but not necessary, to carry out a number of special experiments to increase our detailed understanding of flow and dispersion in the vicinity of buildings. These include experiments for flow visualization, for testing different stability typing schemes, for determining actual values of the plume entrapment coefficient, α, and for measuring turbulence levels, wind speed and wind direction upwind and in the wake of buildings. Note that the measurements of the actual entrapment coefficient and the dispersion coefficients are not absolutely necessary for the model evaluation and verification studies because, in the Dual Plume (and CSCM) Model, the entrapment coefficients and the dispersion coefficients do not represent the real

values which would be measured directly in the field. To be specific, it would be possible to measure directly the fraction of mass entrapped in the building cavity from an elevated plume under differing wind speeds to determine actual values of α. However, in the model, α is an artificial calibration factor which, in theory, represents the fraction of mass entrapped in the cavity, but is, in fact, a tuning factor determined by matching measured model input conditions with measured ground level concentrations. This means that the calculated α values used in the model are dependent on the details of the model structure (eg. plume rise formulation) and do not represent the directly-measured values. Similarly, the directly-measured dispersion coefficients would not be of direct use in testing the model (when the plume is partially entrapped in the cavity) because the model uses the superposition of the elevated and ground level plumes both calculated with the Pasquill-Gifford dispersion coefficients. If changes were made in the dispersion coefficients, all of the values of α used in the model would have to be changed.

The above measurements can be separated into five distinct groups which help explain their need. They are:

Group 1 Measurements For Comparison With Model Predictions

Required here are ground-level concentration measurements which can be used to test and adjust the model's predictive

capability. For both the model evaluation and model verification studies these are one-hour, ground-level, centre-line concentrations of both NO and NO_2. Note that a centre-line concentration is defined as the peak concentration in the cross-wind direction; its position and magnitude are extremely difficult to determine unless concentrations are measured at several points across the plume axis. Also note that NO_x concentrations (i.e. NO + NO_2) can be used to test the dispersion part of the CSCM alone because NO_x is a conservative tracer on the short time scales to be considered here.

Group 2 Model Input Variables

The CSCM predictions cannot be compared to measured ground level concentration data unless the model's input variables are measured at the same time as the ground-level concentrations. The model input variables requiring measurement are:

- Building Variables
  - length, width, height and orientation to the mean wind

- Source Variables
  - stack height
  - stack diameter
  - stack gas exit velocity and temperature
  - source emission rates of NO, NO_2 and hydrocarbons
  - engine power output

- Meteorological Variables
  - wind speed and direction
  - total incoming solar radiation
  - ambient temperature
  - cloud cover

- Background Chemistry
  - ambient concentrations of ozone and hydrocarbons

Group 3 Model Parameterizations

The CSCM, like all other models, simplifies the mathematical treatment of many of the atmospheric processes by parameterizing them, based on either empirical or theoretical grounds. In order to test the reliability of the models, it is necessary to test the accuracy of the parameterizations. The main ones are:

plume rise (Briggs' formulation)

cavity length (assumed equal to 2.5 H)

cavity correction factor (K_c = 1.5 and 2 depending on h_s/H_B).

cavity-pollutant residence time

cavity and far-wake entrainment of ozone (assumed homogeneous across plume)

Each of these parameterizations should be measured experimentally and compared to the model.

Group 4 Support Measurements

A number of the measurements already discussed are very difficult to make without support measurements. For example, measuring ground-level concentrations of NO and NO_2 downwind of a compressor station is difficult without support because, near the compressor building, both gases are odourless and colourless. This makes it impossible to confirm visually whether the plume is entrained into the building cavity, whether it is impinging at ground level and where it is travelling at any given time. Individuals experienced in this type of field measurement program will recognize how useful this type of support measurement is to successful project operation. It provides the following information:

(a) where the plume is impinging at ground level

(b) where the sampling arcs should be placed or which arcs should be used

(c) which samplers should be chemically analysed

(d) whether stationarity conditions for one hour averaging times are being met

(e) whether sampling should start or end given the plume behaviour in the vertical and horizontal.

Similar information could not be gained by simply using a wind vane at a single height to guess what the plume behaviour would be.

Group 5 Other Measurements

Several other measurement programs would be useful for assessing the fundamental principles of the model. These include:

flow visualization experiments

dispersion coefficient (σ_y and σ_z) measurements

stability typing scheme (other than P-G) testing

plume entrapment coefficient (α) measurements

Turbulence and wind speed measurements upwind and on the building Wake.

Of these, flow visualization experiments would be the most useful as they provide further evidence of the cavity and far wake structure. The balance of the measurements are of low priority because they are inherent to the Dual-Plume Model and have been shown to be reasonable (Engineering Science, 1980b).

The aforementioned measurements provide a solid basis for both evaluating and verifying the Compressor Station Chemistry Model and answering many of the questions about wake chemistry and dispersion. Obviously, the ground level concentrations of NO and NO_2 represent the most important measurements of the group because they will empirically illustrate the rate of conversion of NO to NO_2 at compressor facilities. Also of high priority are measurements of stack height and the effect of changes in stack height. In fact, variable stack heights should be used in the field program to assess the sensitivity of ground level NO_2 concentrations to stack height and to allow the CSCM to be tested for its ultimate purpose - designing stack heights sufficient to prevent ground level NO_2 concentrations greater than the maximum allowable standard for Alberta.

4.2 Measurement Techniques

Instrumentation and field methods currently exist for carrying out all of the measurements discussed above. Most of the techniques have not been applied to gas compressor stations before and some require

adaptation for this type of source. The proposed methods are described in detail in this section under the categories: concentrations of NO and NO_2, model input variables, model parameterizations, support measurements and other measurements.

4.2.1 Concentrations of NO and NO_2

Ground level, centre-line concentrations of NO and NO_2 will be measured by deploying roughly 40 to 45 NO/NO_2 samplers (described later) in 4 cross-wind sampling arrays located at variable distances from the compressor building stack. Figure 18 illustrates this proposed sampling array.

Each array will form an arc, centred on the compressor stack. The distance from the stack to the arcs will depend upon the potential for entrainment of the stack plume into the building cavity. If entrainment is highly likely (high wind speeds, low stack height), the arcs will be placed at distances of 3.4, 7, 16 and 44 building heights from the stack. These distances were chosen from the CSCM tests described in Section 3.2.2 as ideal for measuring the downwind gradient of NO and NO_2. When the potential for plume entrapment in the cavity is small (CSCM suggests this occurs at wind speeds near 2 ms^{-1}), the sampling arcs should be moved further downwind to distances of roughly 15, 20, 30 and 55 building heights. Several individual samplers will also be placed within 2 building heights of the stack to measure NO and NO_2 concentrations in the building cavity.

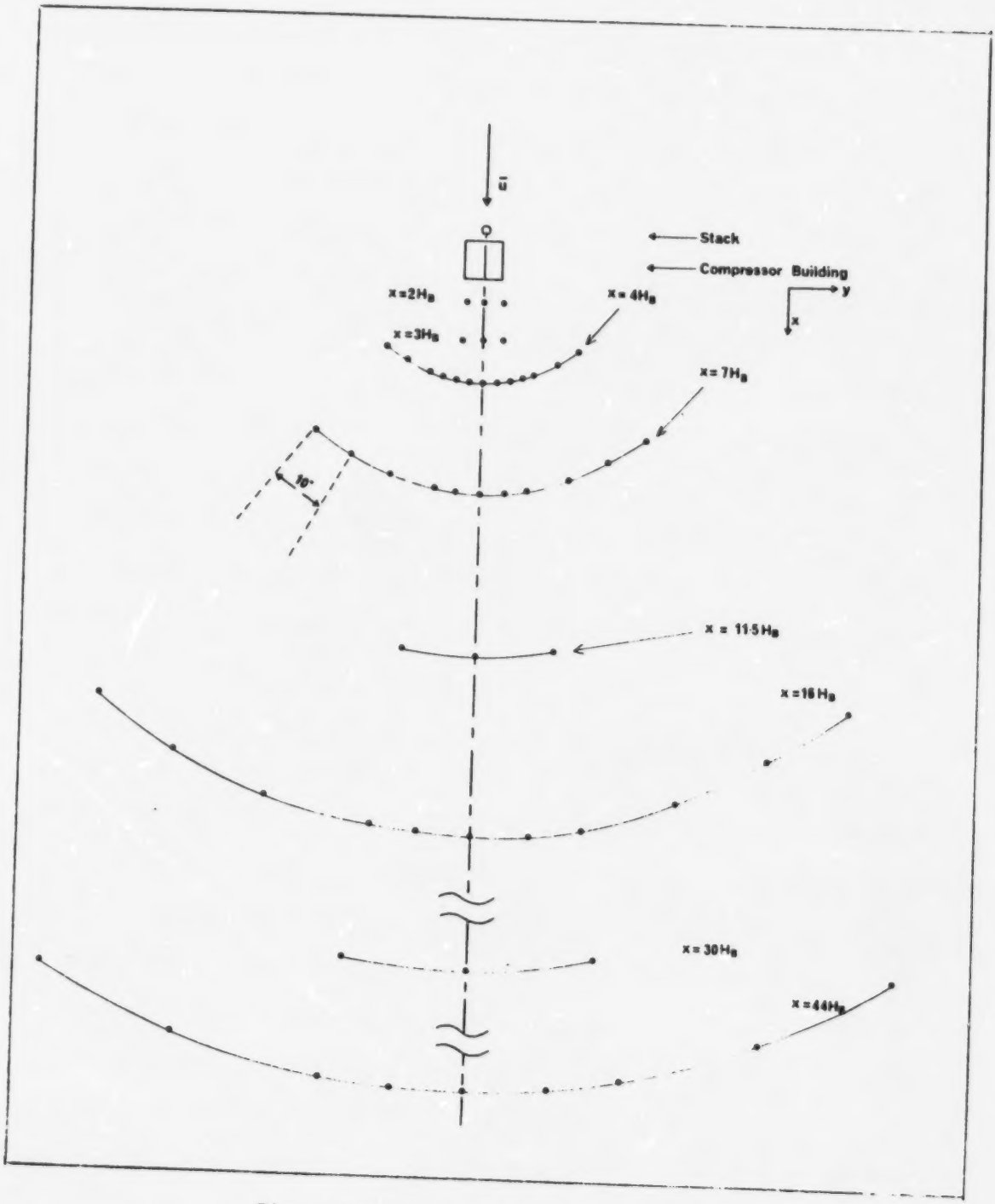

Figure 18: Proposed Sampling Array

The number of samplers deployed along each arc will depend upon the amount of windshift and plume meander predicted for each one-hour sampling interval. Typically, samplers will be placed at 10^{o} intervals along each arc to a maximum of 60 to 90^{o}. Within $\pm$ 20^{o} of the centre-line of the innermost arc and $\pm$ 10^{o} of the other arcs, extra samplers will be placed at 5^{o} intervals to give better cross-wind spatial resolution. If the wind direction is expected to be highly variable during the sampling period, the arcs can be extended as required. Also, if the building is oriented roughly 45^{o} to the mean wind direction (i.e. corner into the wind), then the arcs can be extended to account for the increased cross-wind extent of the wake.

If time permits, two partial arcs consisting of three NO/NO_2 samplers each will be placed at distances midway between the two outer arcs. This provides even better resolution of the downwind concentration gradient.

It is obvious that the success of this fixed-array sampling method depends on the design of the NO/NO_2 samplers which simultaneously measure the ambient concentrations of NO and NO_2. Obviously, to meet the need, these samplers must be inexpensive, highly sensitive to NO and NO_2, easy to handle and highly accurate. The only sampler which meets these requirements is a modified version of the personal NO/NO_2 monitor developed by Vinjamoori and Ling (1981) and subsequently tested by Concord Scientific Corporation (1982). This sampler has not yet been used for ambient measurements and requires some modification and testing

for such use. This is not seen to be a major problem.

The sampler consists of a small piece of teflon tubing packed with two sections of solid sorbent (molecular seive) impregnated with triethanolamine (TEA) for the selective absorption of NO_2. Between the two sections of sorbent is a section of oxidizing catalyst which converts NO to NO_2. The sampler works as follows:

- air is drawn through the sampler by a vacuum pump (ideally at rates between 2 and 10 l min^{-1}). The actual flow rate is controlled by a critical orifice placed in the sampling line between the pump and the sampler.

- the air stream flows through the first set of TEA-impregnated sorbent; the NO_2 in the air is selectively absorbed by the TEA.

- the air then passes through the section of oxidizing catalyst. The NO which passed freely through the first section of sorbent is converted to NO_2.

- this secondary NO_2 passes through the downstream section of sorbent and is captured by the TEA.

- separate solvent extractions of the sorbent are done followed by chemical analysis by either colorimetric methods or ion chromatography. This gives the ambient concentrations of both NO and NO_2 for the sampling period chosen. For this study, one hour sampling periods will be used.

The work of Vinjamoori et al (1981) and Concord Scientific (1982) showed that the sampler had good stability, high collection efficiency, limited sensitivity to temperature and humidity and good sensitivity to concentration (roughly 20 $\mu g/m^3$ at a flow of 10 l/min). It is inexpensive, rugged, can be prepared in the laboratory, requires no handling of the absorbing medium in the field, can be used as a plug-in, plug-out module, and is quickly changed after each experiment. In fact, it is ideal for this field application. However, as mentioned earlier, it has been used only as a personal sampler to date and requires some modification for the high flow rates and low concentrations associated with ambient air sampling. In spite of this, it is strongly recommended that the instrument be used in the field program after a proper modification and field testing program.

In the proposed sampling arrays, all of the NO/NO_2 samplers in a single arc will be operated off a single high volume pump through a multiport manifold. They will sample for a one hour period and all samplers in an arc will be started and stopped simultaneously.

It is useful at this time to point out that the only alternative to this sampling method is the use of several continuous ambient air $NO/NO_2/NO_x$ monitors (such as the Meloy NA530R) mounted on vehicles. The vehicles would continuously traverse across the plume at several downwind distances for periods of one hour. The multiple concentration profiles from the traverses would then be superimposed to form one-hour time-average plume profiles for each of the traversing arcs; the centre-line concentration could then be determined. While this 'mobile' method has general acceptance for large emission sources of SO_2 (eg. Millan et al, 1976; Weil, 1977), it has several problems in its application to NO_x emissions from gas compressor stations, namely:

1. The time response of commercial $NO/NO_2/NO_x$ monitors is of the order of 60 seconds to 90% of full scale. This means that the time for a single traverse of the plume must be very long in order for the instrument to produce accurate measurements at each point along the traverse. However, long traverse times introduce significant errors to the averaging process because the frequency of sampling at each point along the traverse is very small and because the time scale of the wind fluctuations and resultant plume position changes would be much smaller than the cross-wind sampling frequency. In fact, this method has only been used in the past with instruments having response times between one and five seconds (eg. Barringer COSPEC, Sign - X SO_2 analyser).

2. The continuous monitors are expensive (more than $10,000 each), require in-situ calibrations and require either strip-chart recorders or data acquisition systems for recording the output concentrations. The use of these instruments on several sampling arcs would be very expensive.

3. Areas designated for traversing in the plume must be accessible and in reasonable condition for vehicular traffic. Also the emissions from the vehicles on which the monitors would be mounted would interfere with the NO/NO_2 measurements further downwind.

4. Significant data handling and data analysis costs are associated with determining the time-average, cross-wind concentration profiles and the resulting centre-line concentrations.

Given these facts, the use of the sorbent NO/NO_2 samplers is strongly recommended for the field program.

4.2.2 Model Input Variables

The model input variables requiring measurement were divided into four types - building, stack, meteorology and background chemistry measurements. Their associated measurement methods are discussed below.

The building variables of interest are length, height, width and orientation to the mean wind. The first three are simple measurements and the fourth will be available from proper wind direction measurements.

Measurement of the source variables requires instrumentation and techniques which are reasonably standard for source monitoring. Dietzmann (1976) documents the instrumentation and measurement methods in "Emissions Measurement Manual for Natural Gas Pipeline Compressor Engines". The parameters requiring measurement are barometric pressure, ambient temperature, relative humidity, engine speed, horsepower, scavenging air pressure, ignition timing, fuel specific gravity, fuel high heat value, fuel temperature, orifice constant, orifice drop and static pressure, fuel flow, heat flow, air flow, air/fuel ratio, brake specific fuel consumption. In addition, exhaust velocity, exhaust temperature and concentrations of NO, NO_2 and non-methane hydrocarbons must be measured. All of these are straightforward and can be provided by groups specializing in source monitoring.

Meteorological measurements are standard as well. Wind speed and direction will be measured using a cup and vane anemometer system mounted on top of a 10 metre tower located 10 to 20 building heights from the compressor station buildings. Ambient temperature will also be measured on the tower at the 1 m, 3 m and 10 m levels using thermistors. Solar radiation (total incoming) will be measured using a

solarimeter also mounted on the tower. The output from these instruments will be recorded continuously on a multichannel digital data logger with backup from strip chart recorders. All instruments will be calibrated before and after field use. Cloud cover observations will be made manually on-site every half-hour during the sampling program.

Background concentration measurements of ozone will be made using a continuous ozone monitor (eg. Meloy OA350-2R) located upwind of the compressor stack. Hydrocarbons would be measured several times throughout each sampling day by grab samples analysed by gas chromatography.

4.2.3 Model Parameterizations

Measurements of model parameterizations often, but not always, require more complicated measurement techniques than the other measurements. Proposed methods are given below:

Cavity size - Mount wool streamers on stakes near ground level downwind of the building to indicate the flow direction. The cavity size can be determined by observing where the cavity recirculating flow meets the downwind flow.

Residence time of pollutants in the cavity - release NO_2 from a calibrated cylinder located in the building cavity. Monitor this overhead burden of NO_2 using a remote sensor such as a Barringer

Correlation Spectrometer (see Section 4.2.4). When the instrument measures a relatively constant burden, stop the release and monitor the time rate of decay of the NO_2 burden. Measure wind speed simultaneously.

Cavity K - values - deploy a set of NO/NO_2 samplers in the building cavity region to measure ground level concentrations. Release NO_2 at a known rate in the cavity. Calculate $K = \chi uA/Q$.

4.2.4 Support Measurements

Support measurements are required to provide real-time data on the vertical and horizontal position of the plume. Such measurements are required before the ground level NO/NO_2 sampling arrays are set at the proper orientation and distances. Throughout the sampling period, they are required to keep track of plume behaviour so that on-the-spot decisions can be made about extending the sampling arcs and/or starting and stopping sampling.

Two instruments are currently available for measuring the horizontal position of the plume. Both are remote-sensing spectrometers which measure the total overhead burden of NO_2 from the absorption of solar radiation at specific wavelenths. They are the Barringer COSPEC and the Moniteq MARRS Plumetracker. One of the two would be mounted on a vehicle which would continuously traverse cross-wind along one of the

sampling arcs.

Measurement of the vertical position of the plume (i.e. where it is impinging at ground level) would be done with an ambient $NO/NO_2/NO_x$ monitor located in the same vehicle as the remote sensor. It could be driven along the plume axis at different times throughout the sampling period to ensure that ground level concentrations were still detectable. Note that the long time response of the instrument would not be a factor here since any detectable signal would be sufficient to locate the plume position. Also note that the vehicle containing these instruments would have to be modified to prevent its emissions from reaching the ambient air. This is not seen to be a difficult problem for one hour sampling periods.

4.2.5 Other Measurements

Of the other measurements discussed in Section 4.1, only the flow visualization is recommended. This is easily done using a smoke generator, a camera and visual observations. Smoke releases should be made upwind of, on, beside and downwind of the compressor station. They will be particularly useful for investigating the mechanisms for entrainment and loss of air from the building cavity region.

4.3 Field Program Design

To this point the types of measurements required in the field programs have been identified and the methods of making these measurements have been described. The next step is to present the actual field program design consisting of the Model Evaluation Study and Model Verification Study. Each is discussed in turn.

4.3.1 Model Evaluation Study

As mentioned earlier, the purpose of this study is to provide data for the evaluation of the Compressor Station Chemistry Model and, generally, to provide answers to questions on wake diffusion and chemistry. The proper execution of such a study depends quite significantly on the selection of a suitable compressor station for the work. While it was not possible to select an actual station at this stage, it was possible to determine the criteria for its selection. These criteria are given below:

1. The compressor engine and building should be 'typical' of those found in the Province of Alberta. The engine should produce moderate to high emissions and a moderate to low stack gas exit velocities (this optimizes conditions for obtaining measurable ground level concentrations).

2. The compressor building should have simple geometry and its dimensions should be roughly similar to those chosen for testing the CSCM, i.e. 7 to 10 m. This simplifies many of the measurement procedures and eliminates complicated flow regimes which could make comparison of model and measurements difficult.

3. The height of the stack should be between 0.5 and 1.5 building heights. It should be positioned along one side of the building - not on a corner. Its design should be suitable for adding a variable extension to the top to measure the effect of stack height on ground level concentrations.

4. The prevailing wind direction for the site should align along the axis between the stack and the normal to the adjacent building face. The prevailing wind speed should be relatively high.

5. The topography surrounding the site should be flat with low ground cover and good access.

6. Other buildings should be located at least 100 m from the compressor building - ideally in a direction normal to the prevailing wind.

Once the site is selected, the study should be run in three phases, viz.:

1. set-up
2. routine measurements
3. special studies.

The 'set-up' phase would consist of installing the meteorological tower (and its instrumentation), the stack monitoring instrumentation and the stack extension. The remote NO_2 sensor (COSPEC or MARRS) would be installed in its vehicle, as would the ambient $NO/NO_2/NO_x$ continuous monitor. The ground level sampling arcs would be carefully surveyed and staked throughout 360^o. Sampling pumps and flow lines would be installed along the arcs. Ground level streamers would be staked out around the building. Instruments would be calibrated and a 'test run' would be carried out to familiarize the field crew with the measurement protocol.

The 'routine measurements phase' would consist of 20 to 25 successful one hour experiments during which each of the following measurements is made <u>simultaneously</u>:

- ground level concentrations of NO and NO_2 using the sorbent samplers along their pre-arranged arcs.

- stack measurements of height, diameter, exit velocity, exit temperature, concentration of NO and NO_2 (and occasionally

non-methane hydrocarbons by grab sample).

- meteorological measurements of wind speed and direction (at 10 m), solar radiation, temperature (at 1, 3 and 10 m) and cloud cover.

- upwind measurements of NO and NO_2 using the sorbent samplers, ozone using a continuous monitor and hydrocarbons using grab samples.

- cross-wind traverses of the COSPEC or MARRS and the continuous $NO/NO_2/NO_x$ monitor at variable distances downwind of the building.

- visual observation of the ground level streamers identifying the extent of the building cavity.

- ground-level NO/NO_2 concentration measurements at several points in the building cavity region.

The field organization of all these measurements is shown in Figure 19.

It is expected that, on days with good weather, 3 to 4 one-hour runs including all of these measurements could be made. If conditions remain relatively consistent throughout a given day, the stack height

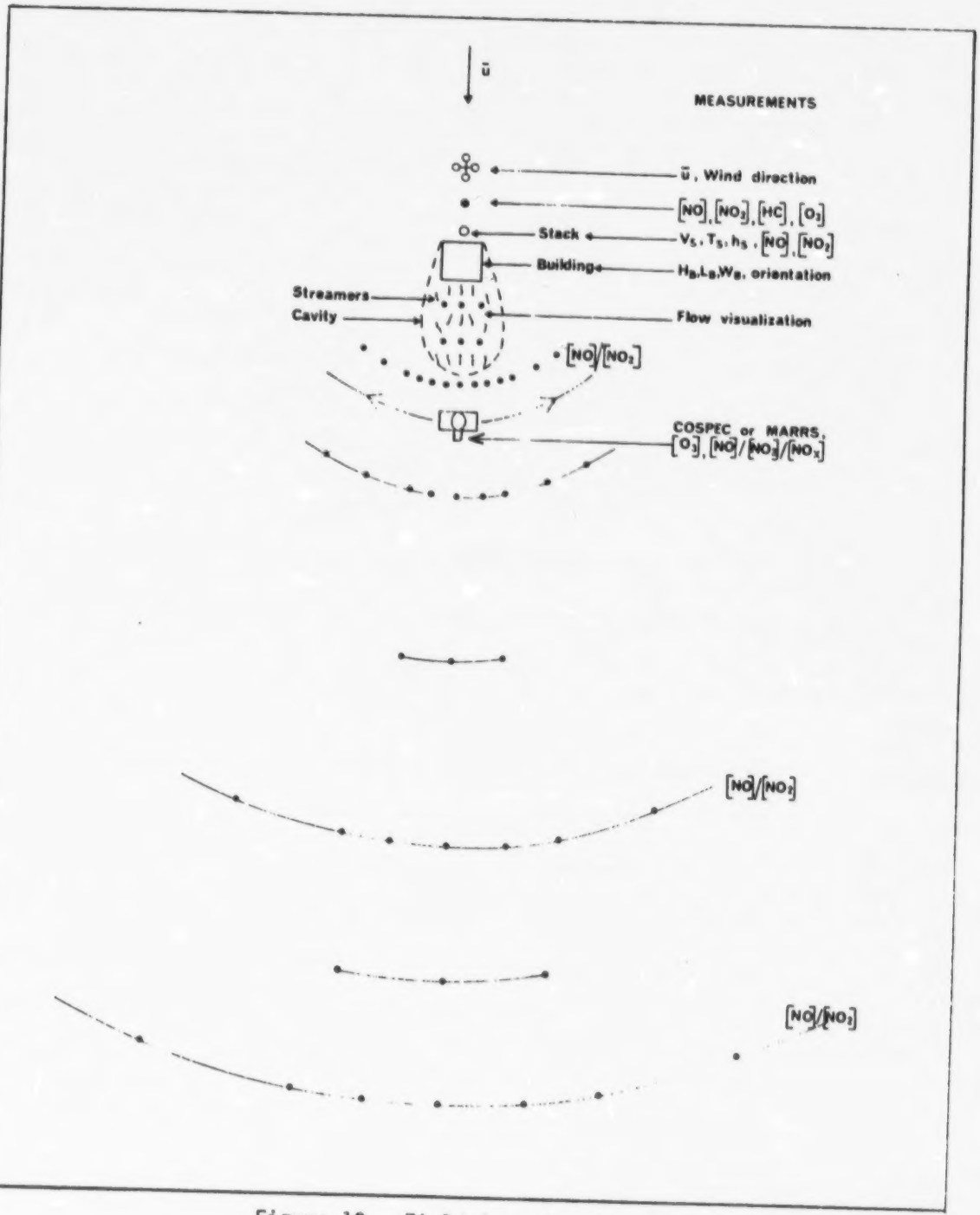

Figure 19: Field Organization of Measurements

should be changed for each run. Most experiments will be carried out during daylight hours, several will be done at dawn and dusk in order to ensure that neutral stability conditions are encountered. Also, several will be carried out at night to obtain data under stable atmospheric conditions. It should be pointed out that good communication and good weather prediction systems would be required on-site to ensure the successful operation of the program. The former would be used to coordinate the efforts of the field crews; the latter would be used to organize and design the daily sampling protocol and determine the proper sampling arcs to be used.

The last phase of the study, the 'special measurements phase' will focus on determining the adequacy of the model parameterizations. They would consist of any number of the following:

- measurements of plume rise by either plume photography or LIDAR scanning techniques. Both methods are well-established and both would be done after the injection of $TiCl_4$ or TiO_2 into the stack to make the plume visible. Both measurements would also have to be carried out simultaneously with meteorological and source measurements. The conditions under which they are made would have to be carefully chosen so that the plume was not entrained into the building cavity, thereby reducing its effective rise.

- pollutant residence time in the building cavity would have to be measured independently of the regular measurements, when the compressor station plume is definitely not being entrained into the plume cavity. Measurements of wind speed and direction would also be required.

- cross-plume entrainment of ozone into the cavity would be measured concurrently with the 'routine measurements' by moving the background ozone monitor into the plume impingement area and carrying out cross-wind traverses.

- flow visualization experiments could be carried out concurrently with the routine measurements if it can be shown that the smoke does not interfere with the NO/NO_2 measurements. Meteorological measurements would be required if the experiments were carried out on their own.

Ten to fifteen of these special measurements would be required during the field study. It is recommended that priority be given to the cavity residence time, the ozone entrainment and the flow visualization measurements. The others should be considered if financial constraints allow them as rental costs on the LIDAR are high.

This completes the description of the model evaluation field study. However, before moving on to the model verification study, it

is important to complete the design process by considering the uses of the data obtained in the measurement program. A short list of the most important is given below:

- comparison of measured ground-level concentrations of NO and NO_2 to predicted values.

- empirical adjustment of the plume entrainment factor, α, in the diffusion portion of CSCM by using measured NO_x ($NO + NO_2$) concentrations to back-calculate optimal values of α.

- comparison of measured values of cavity residence time, cavity K-values, cavity length, ozone entrainment, plume rise and plume entrainment into the cavity with values assumed in the model. This would be followed by adjustment of the model as required.

- comparison of predicted to measured NO_2/NO_x ratios and adjustment of the ozone entrainment algorithm as required.

4.3.2 Model Verification Study

The objective of this study is to produce an independent set of data to quantify the final predictive capability of the evaluated Compressor Station Chemistry Model. To fulfill this, the study must be carried out at a different site than the one used for the evaluation study. The station will be chosen using the same site selection criteria except the building will be slightly different in size and shape and multiple stacks will be considered.

The measurement program for this study will contain most of the same measurements used in the evaluation study but the focus will be on obtaining ground-level, centre-line concentrations of NO and NO_2 and the corresponding measurements of model input variables.

The study will consist of the same three phases as the evaluation study, that is, set up, regular measurements and special measurements. Both the set-up and regular measurements phase will be the same as in the evaluation study. The regular measurements will include:

- ground level measurements of NO/NO_2 concentrations along the sampling arcs
- source measurements
- meteorological measurements
- background chemistry measurements
- plume position measurements

The sampling plan will be the same as in the evaluation study, including the expected number of experiments run per day, the adjustment of stack height whenever possible and the use of both day and night-time sampling to encounter different atmospheric stability conditions. Roughly fifteen, one hour experimental runs will be made.

Special measurements in this study will consist of only the cavity-pollutant residence time measurements, the cross-plume entrainment of ozone measurements and the cavity length measurements. Only five experiments will be run for each of these measurements.

Finally, the expected uses of the data obtained in this field study are:

- comparison of cavity residence time, cavity length and ozone entrainment with those measured in the validation study and used in the evaluated CSCM.

- comparison of NO_x ground-level concentrations with those predicted from the CSCM.

- quantification of the capability of the model to predict ground level concentrations of NO, NO_2 and NO_x. (This will be done using such performance measures as predicted-to-measured ratios, regression analyses and residual analyses.)

- quantification of the model's capability to predict design stack heights.

- assessment of the sensitivity of predicted stack designs to the model input variables and parameterizations based on their measured ranges.

4.4 Summary

A field measurement program has been designed to answer many of the questions about NO/NO_2 chemistry and dispersion in the wake of gas compressor buildings. It does so by using the Compressor Station Chemistry Model as the framework for assessing the interaction between chemistry and diffusion. The program design calls for two studies - a model evaluation study and a model verification study. Each would be carried out at a different compressor station but the measurement programs would be very similar. At the end of the program, the CSCM will be empirically tuned, its predictive capabilities will be known and its suitability for designing stack heights will be demonstrated. In addition, empirical data on the effect of stack height on ground-level NO_2 concentrations downwind of gas compressor stations will be available.

The importance of this field measurement program cannot be overemphasized. Without it, there will be no scientific basis for applying the Compressor Station Chemistry Model to compressor station stack

design. With it, the capabilities and limitations of CSCM stack designs will be known.

Finally, it is implicit in the foregoing discussion that the final field study design is based on the final form of the CSCM. If the model is changed from its current form (e.g. if the recommendations for future model developments described in Section 3.5 are adopted), then a model development program would be necessary in addition to the field measurement program. This model development program has been addressed only in outline in this report but its potential requirement is noted here. Based on the recommendations for future model developments, it is expected that the current field program design will not change significantly.

5. CONCLUSIONS AND RECOMMENDATIONS

The work program carried out in Phase I of the Compressor Exhaust and Wake Diffusion Study produced the following conclusions:

1. Emission parameters (i.e. temperature, velocity and NO/NO_2 emission rates) are highly variable from engine to engine and, for the same engine, from site to site and from day to day. Measured emission parameters for a given compressor engine are often significantly different from those specified by manufacturers. This has serious implications for modelling of chemistry and diffusion in the wake of compressor buildings.

2. To date, there have been no rigorous and complete field studies addressing the interconversion of NO and NO_2 in the vicinity of buildings. Prior to this study, there has been no development of reactive chemistry models for application to building wakes.

3. The traditional concept of flow and dispersion in the vicinity of buildings (i.e. that of Halitsky, 1968) does not incorporate all of the complexities observed by recent investigators (e.g. Woo et al, 1977). These complexities

are extremely difficult to model and can have serious effects on ground-level concentrations; however, some investigators suggest that the traditional concepts are adequate for modelling purposes (Vincent, 1977).

4. Of all wake diffusion models currently available, the Huber-Snyder and Dual Plume models appear to be based on the best physical foundations and to perform best when compared against experimental data. The Dual Plume model, however, is best suited for the incorporation of reactive NO/NO_2 chemistry and adaptation to compressor station stack design.

5. Wake diffusion and NO/NO_2 chemistry have been incorporated into a single model called the Compressor Station Chemistry Model (CSCM). This model can be used to predict ground-level concentrations of NO and NO_2 and to design stack heights for gas compressor stations. Model evaluation, however, has not been carried out and awaits Phase II of the Compressor Exhaust and Wake Diffusion Study.

6. The CSCM predicts that compressor station stack heights seldom need to exceed 1.5 times the building height for a compressor station 7 m high and 8.5 m wide with a 'typical' compressor engine of approximately 1100 kW. This is mainly due to the high stack gas exit velocity characteristic of large

reciprocating compressor engines.

7. The CSCM predicts that maximum ground level concentrations of NO and NO_2 do not necessarily coincide, but generally lie within 50 metres of each other. For most source and atmospheric conditions the ratio of NO_2 to NO_x increases monotonically with downwind distance from an initial value of about 0.15 to 0.5 to 0.7 depending on wind speed. (These values are based on an in-stack ratio of 0.1) In those cases where the plume is first brought to the ground some hundreds of metres from the source, this ratio may show an initial decrease prior to the steady increase.

8. A field measurement program has been designed to answer many of the questions about wake diffusion and NO/NO_2 chemistry downwind of the compressor stations. It will also provide a data set suitable for evaluating and verifying the predictive capability of the CSCM.

The work program also produced a set of recommendations regarding model development and field measurement programs. They are:

1. Based on the literature review carried out in the first portion of this work program, it is recommended that any

field studies undertaken at compressor stations rigorously and concurrently address flow, dispersion and NO/NO_2 chemistry.

2. It is recommended that the existing Compressor Station Chemistry Model be upgraded by incorporating the following modifications:

- incorporate enhanced dispersion coefficients
- improve the ozone entrainment mechanism
- adjust the calculation of reaction rates where the two parts of the plume overlap

or by developing an integrated reactive plume model which handles chemistry and dispersion simultaneously.

3. It is recommended that Phase II of the Compressor Exhaust and Wake Diffusion Study be undertaken in order to evaluate and verify the predictive capabilities of the CSCM. Until such an exercise has been carried out, the CSCM should be used with caution.

REFERENCES

A.G.A. (1981) American Gas Association, Pipeline Research Summary, 1981.

A.G.A (1982) American Gas Association, Pipeline Research Summary, 1982.

APIGEC (1981) Request for Proposal, "Compressor Exhaust Chemistry and Wake Diffusion - Phase I", May 1981.

Anastasi, C. and Smith I.W.M. (1976) J. Chem. Soc. For. Trans. II 72, 1459 (1976).

Angle, R.P., Sandhu, H.S. and Schnitzler, W.J. (1979) "Observed and Predicted Values of NO_2/NO_x in the Exhaust Plume from a Compressor Installation". JAPCA 29, 253-255 (1979).

Barry, P.J. (1963) "Estimation of Downwind Concentration of Airborne Effluents Discharged in the Neighbourhood of Buildings". Atomic Energy of Canada Ltd., Report AECL 2043, 1963.

Baulch, D.L., Cox, R.A., Hampson, R.F. Jr., Kerr, J.A., Troe, J. and Watson, R.T. (1980) "Evaluated Kinetic and Photochemical Data for Atmospheric Chemistry". J. Phys. Chem. Ref. Data 9, 295 (1980).

Bilsky, I.L., Cunningham, J.E. and Draper, J.B. (1980) "A Study of Compressor Station NO_x Emissions". 73rd Annual Meeting of the Air Pollution Control Association, Montreal (1980).

Bottenheim, J.W. and Strausz, O.P. (1978) "Computer Modelling on Polluted Atmospheres". Report to Alberta Environment, Project 76-43, June 1978.

Bottenheim, J.W. and Strausz, O.P. (1982) "Modelling Study of a Chemically Reactive Power Plant Plume". Atm. Env. 16, 85 (1982).

Briggs, G.A. (1969) "Plume Rise". AEC Critical Review Series, U.S. Atomic Energy Commission, Office of Information Services (1969).

Briggs, G.A. (1973) "Diffusion Estimation for Small Emissions". Atm. Turb. and Diff. Lab., NOAA, Draft. Rep. May 1979.

Calvert, J.C.R. (1981) "A Brief Review of the Tropospheric Chemistry of Sulfur Dioxide and the Nitrogen Oxides". Report to Ontario Ministry of the Environment under Order Number A70782.

Caput, C., Belot, Y., Guyot, G., Samie, C. and Seguin, B. (1973) "Transport of a Diffusing Material Over a Thin Wind-Break". Atm. Env. 7, 75 (1973).

Castro, I.P. (1973) "An Experimental Investigation of the Flow Around A Surface Mounted Cube in a Uniform Free Stream". Central Electricity Generating Board (U.K.) Report R/M/N 687, August 1973.

Castro, I.P. and Robins, A.G. (1975) "The Effect of a Thick Incident Boundary Layer on the Flow Around a Small Surface Mounted Cube". Central Electricity Generating Board (U.K.) Report R/M/N 795, Jan. 1975.

Cole, H.S. and Summerhays, J.E. (1979) "A Review of Techniques Available for Estimating Short Term NO_2 Concentrations". JAPCA 29, 812 (1979).

Concord Scientific Corporation (1982) "Prototype Personal Monitor For SO_2, NO_2 and Airborne Particles". Report CSC-106. March, 1982.

Davis, W.T. (1981) (Personal Communication).

Davis, W.T. and Kolb, J.O. (1980) "Environmental Assessment of Air Quality, Noise and Cooling Tower Drift from the Jersey City Total Energy Demonstration". Oak Ridge National Lab. Report ORNL/HUD/MIUS - 52.

Demerjian, K.L., Kerr, J.A. and Calvert, J.G. (1974). "Mechanism of Photochemical Smog Formation". Adv. Env. Sci. Technol. 4, 1 (1974).

Derwent, R.G. and Hov, O. (1980) "Computer Modelling Studies of the Impact of Vehicle Exhaust Emission Controls on Photochemical Air Pollution Formation in the United Kingdom". Env. Sci. Technol. 14, 1360 (1980).

Dietzmann, H.E. and Springer, K.J. (1974) "Exhaust Emissions from Piston and Gas Turbine Engines used in Natural Gas Transmission". American Gas Asscn. Project PR-15-61, Jan. 1974.

Dietzmann, H.E. (1976) "Emissions Measurement Manual for Natural Gas Pipeline Compressor Engines". American Gas Assocn. Project PR-15-61, Aug. 1976.

Eliassen, A. (1982) Personal Communication.

Engineering-Science (1977) Workbook for Predicting Atmospheric Dispersion of Engine Exhaust Emissions from Natural Gas Compressor Stations (Preliminary Version). Am. Gas Assoc. Project PR-133-78.

Engineering-Science (1980a) Applicability of the Industrial Source Complex (ISC) Dispersion Model to Natural Gas Compressor Stations. Am. Gas Assoc. Project PR-133-122.

Engineering-Science (1980b) "Field Validation of Atmospheric Dispersion Models for Natural Gas Compressor Stations". Prepared for Pipeline Research Committee American Gas Association, PR-133-78.

Engineering-Science (1980c) "Workbook for Predicting Short-Term Atmsopheric Dispersion of Reciprocating Engine Exhaust Emissions from Natural Gas Compressor Stations". Am. Gas Assoc. Project PR-133-112.

Fanick, E.R. and Dietzmann, H.E. (1980) "Exhaust Emissions from Piston and Gas Turbine Engines used in Natural Gas Transmission. Phase II 1978-1979. Prepared for Pipeline Research Committee of the American Gas Association, Cat. No. L22280.

Frost, W. and Shahabi, A.M. (1977) "A Field Study of Wind Over a Simulated Block Building". NASA Contractor Report CR-2804, March 1977.

Gifford, F.A. (1960) "Atmospheric Dispersion Calculations Using the Generalized Gaussian Plume Model". Nuclear Safety 2.

Halitsky, J. (1968) "Gas Diffusion Near Buildings". Chapter 5.5 in Meteorology and Atomic Energy (1968) Ed. D.H. Slade, U.S. AEC, TID-24190.

Halitsky, J. (1977) "Wake and Dispersion Models for the EBR-II Building Complex". Atm. Env. 11, 577 (1977).

Hansen, A.C. and Cermak (1975) "Vortex Containing Wakes of Surface Obstacles". Colorado State University, Fluid Dynamics and Diffusion Lab Report. CER 75-76ACH-JEC16. Fort Collins, Co., 1975.

Hatcher, R.V., Meroney, R.N., Peterka, J.A. and Kothari, K. (1978) "Dispersion in the Wake of a Model Industrial Complex". U.S. Nuclear Regulatory Commission Report NUREG-0373.

Hosker, R.P.Jr. (1979) "Empirical Estimation of Wake Cavity Size Behind Block-Type Structures". Preprints of the Fourth Symposium on Turbulence Diffusion and Air Pollution, Reno, Nevada, Jan. 15-18, 1979.

Hosker, R.P.Jr. (1980a) "Flow and Diffusion Near Obstacles". A chapter to appear in "Atmospheric Science and Power Production", Ed. D. Randerson.

Hosker, R.P.Jr. (1980b) "Dispersion in the Vicinity of Buildings". 2nd Joint Conf. on Applications of Air Pollution Met. New Orleans, March, 1980.

Howroyd, G.C. and Gutfreund, P.D. (1980) "An Evaluation of the Briggs Downwash Formulation". 2nd Joint Conf. on Applications of Air Pollution Meteorology, New Orleans, March 1980.

Huber, A.H. and Snyder, W.H. (1976) "Building Wake Effects on Short Stack Effluents". Third Symposium on Atmospneric Turbulence, Diffusion and Air Quality, Raleigh, N.C.

Huber, A.H. (1977) "Incorporating Building/Terrain Wake Effects on Stack Effluents". Joint Conf. on App. of Air Pollution Met., Salt Lake City, Nov. 1977.

Hunt, J.C.R. and Mulhearn, P.J. (1973) "Turbulent Dispersion from Sources Near Two-Dimensional Obstacles". J. Fluid Mech. 61, 245 (1973).

Hunt, J.C.R., Abell, C.J., Peterka, J.A. and Woo, H. (1978a) "Kinematical Studies of the Flows Around Free or Surface-mounted Obstacles; Applying Topology to Flow Visualizaiton". J. Fluid Mech. 86, part 1, 179-200 (1978).

Hunt, J.C.R., Snyder, W.H. and Lawson, R.E. Jr. (1978b) "Flow Structure and Turbulent Diffusion Around a Three-Dimensional Hill. Fluid Modeling Study on Effects of Stratification, Part 1. Flow Structure". U.S. EPA report no. EPA-600/4-78-041.

Hunter, S.C. and Cherry, S.S. (1980) "NO_x Emissions From Petroleum Industry Operations". 73rd Annual Mtg. Air Pollution Control Assoc., Montreal, June 1980.

Kothari, K.M., Peterka, J.A. and Meroney, R.N. "The Wake Structure and Diffusion Behind a Model Industrial Complex". 5th Symposium on Turbulence, Diffusion and Air Pollution, Atlanta, March, 1981.

Koziar, K., Adamski, B. and Anderson, B. "A Sensitivity Analysis of Three Downwash Models Under Neutral Atmospheric Stability". 2nd Joint Conf. on Applications of Air Pollution Met., New Orleans, March 1980.

Lamb, R.G. (1982) Personal Communication.

McGowin, C.R. (1973) "Stationary Internal Combustion Engines in the United States". U.S. EPA Report EPA-R2-73-210, April 1973.

Melo, O.T., Lusis, M.A. and Stevens, R.D.S. (1978) "Mathematical Modelling of Dispersion and Chemical Reactions in a Plume-Oxidation of NO to NO_2 in the Plume of a Power Plant". Atmospheric Environment 12, 1231-1234 (1978).

Melo, O. and Stevens, R.D.S (1981) "The Occurrence and Nature of Brown Plumes in Ontario". Atm. Env. 15, 2523, (1981).

Millan, M.M., Gallant, A.J. and Turner, H.C. (1976) "The Application of Correlation Spectroscopy To the Study of Dispersion From Tall Stacks". Atmospheric Environment 10, 499-511.

Miller, C.W. (1981) "Comparison of Gaussian Plume Model Air Concentration Predictions Using Huber's Building Wake Effects Adjustment with Rancho Seco Observations" 5th Symposium on Turbulence, Diffusion and Air Pollution, Atlanta, March, 1981.

Milligan, R.J., Sailor, W.C., Wasilewski, J. and Kirby, W.C. (1979) "Review of NO_x Emission Factors for Stationary Fossil Fuel Combustion Sources". U.S. EPA Report EPA-450/4-79-021, September, 1979.

Moroz, W.J. Laratta, E.M. and Hoffer, A.D. "A Model For The Estimation of Contaminant Concentrations in Building Lees and Air Intakes - Darlington GS Estimates". Ontario Hydro Report 81003, Jan. 1981.

Portelli, R.V. (1974) Atmospheric Environment Services, Canada, Internal Memo.

Powell, F.C. (1981) Personal Communication.

Prahm, L.P. (1982) Personal Communication.

Puttock, J.S. and Hunt, J.C.R. (1979) "Turbulent Diffusion from Sources Near Obstacles with Separated Wakes - Part I. An Eddy Diffusivity Model". Atmospheric Environment, 13, 1-13 (1979).

Puttock, J.S. (1979) "Turbulent Diffusion from Sources Near Obstacles With Separated Wakes - Part II. Concentration Measurements Near a Circular Cylinder in Uniform Flow". Atmospheric Environment, 13, 15-22 (1979).

Sagendorf (1974) "A Program for Evaluating Atmospheric Dispersion from a Nuclear Power Station". NOAA Tech. Memo ERL-ARL-42

Salvesen, K.G. Wolfe, K.J., Chu, E., and Herther, M.A. (1978). "Emission Characterization of Stationary NO_x Sources: Vol. I Results". U.S. EPA Report, EPA-600/7-78-120a.

Seinfeld, J.H. (1982) Personal Communication.

Start, G.E., Hukari, N.F., Sagendorf, J.F., Cate, J.H. and Dickson, C.R. (1980) "EOCR Building Wake Effects on Atmospheric Diffusion" NUREG Report CR-1395.

Stewart, D.A. and Liu, M.K. (1980) "Development and Application of a Reactive Plume Model". Symposium on Plumes and Visibility, Grand Canyon, Nov. 1980.

Strom, G.H. (1976) "Transport and Diffusion of Stack Effluents". pp. 401-501 in "Air Pollution: Vol 1", Ed. A.C. Stern. Academic Press, 1976.

Thuillier, R.H. and Mancuso, R.L. (1980) "Building Effects on Effluent Dispersion from Roof Vents at Nuclear Power Plants". EPRI Report NP-1380, Research Project 1073, April, 1980.

U.S. Nuclear Regulatory Commission (1979) "Atmospheric Dispersion Models for Potential Accident Consequent Assessments at Nuclear Power Plants". Regulating Guide 1. 145.

Urban, C.M. and Springer, K.J. (1975) "Study of Exhaust Emissions from Natural Gas Pipeline Compressor Engines". American Gas Assoc. Project PR-15-61.

Vincent, J.H. (1977) "Model Experiments on the Nature of Air Pollution Transport near Buildings". Atm. Env. 11, 765-774 (1977).

Vincent, J.H. (1978) "Scalar Transport in the Near Aerodynamic Wakes of Surface-Mounted Cubes". Atm. Env. 12, 1319-1322 (1978).

Vinjamoori, D.V. and Ling, C.S. (1981) "Personal Monitoring Method for Nitrogen Dioxide and Sulfur Dioxide with Solid Sorbent Sampling and Ion Chromatographic Determination". Anal. Chem. 53, 1689-1691.

Weil, J.C. (1977) "Evaluation of the Gaussian Plume Model at Maryland Power Plants". Martin Marietta Corporation Environmental Technology Centre Report PP SP-mp-16. March, 1977.

Wilson, D.J. (1977) "Effect of Vent Stack Height and Exit Velocity on Exhaust Gas Dilution" ASHRAE Trans 83 part 1, 157-167 (1977).

Wilson, D.J. (1977) "Dilution of Exhaust Gases from Building Surface Vents". ASHRAE Trans 83 part 1, 168-176 (1977).

Wilson, D.J. and Netterville, D.D.J. (1976) "Influence of Downwind High-Rise Buildings on Stack Design". JAPCA 26, 976-980 (1976).

Wilson, D.J. and Netterville, D.D.J. (1978) "Interaction of a Roof-Level Plume with a Downwind Building". Atm. Env. 12, 1051-1059 (1978).

Wilson, D.J. (1979) "Wind Tunnel Simulation of Plume Dispersion at Syncrude Mildred Lake Site". Syncrude Env. Res. Monograph. 1979-1.

Woo, H.G.C., Peterka, J.A. and Cermak, J.E. (1977) "Wind Tunnel Measurements in the Wakes of Structures". NASA Contractor Report CR-2806, March, 1977.

APPENDIX A: Data for an Alberta Compressor Station

These data were compiled by Mr. F.C. Powell of the Standards and Approval Division of Alberta Environment, and form the basis for the "typical" Compressor Station modelled in this work.

Typical Building Dimensions: 8.5 m x 13.4 m x 6.9 m high.

Source Characteristics: See Table 17.

Table 17: Source Characteristics

Stack Height (m)	4.7	10.7	6.4	9.4	12.5	19	12
Stack Diameter (m)	.304	.25	.203	.203	.324	.355	.46
Stack Gas Temperature (^{o}C)	371	621	530	538	496	590	488
Stack Gas Exit Velocity (m/s)	5.9	38	42.4	49.5	36	38.2	33.5
Pollutant Flow Rate g NO_x/BHP hr	7	16.86	18	17	16.7	14.98	15.4
Power (BHP)	230	450	600	720	1000	1642	2145

APPENDIX B: Typical Model Output

Presented here are printouts of model runs for one stack height for each of the cases described in Section 3.2.1, and summarized in Figure 11. Graphical displays are also presented for cases 1, 2, 3, 4 and 7 and the "worst likely" case.

Parameters printed out are:

Q	-	Mass emission rate (g NO_2/s)
W	-	Building width
HB	-	Building height
HS	-	Stack height
U	-	Wind speed
V	-	Stack gas exit
TS	-	Stack gas temperature
TA	-	Ambient temperature
D	-	Stack Internal diameter
STAB	-	Stability
OZONE	-	Ozone concentration
ALPHA	-	Entrainment coefficient
H EFF	-	Effective stack height

Maximum NO_x and NO_2 refer to points downwind of the cavity.

Case #1

COMPRESSOR STATION CHEMISTRY MODEL

Q= 4.17 G/S
H= 8.50 M
HB= 7.00 M
HS= 4.00 M
U= 2.0 M/S
V= 20.0 M/S
TS= 700.0 K
TA= 283.0 K
D= 0.300 M
STAB=B
OZONE= 40.0 PPB

ALPHA=0.714
H EFF= 23.7 M

DOWNWIND DIST (M)	TRAVEL TIME (S)	NOX CONC (UG/M**3)	NO2 CONC (UG/M**3)	NO2/NOX RATIO
17.5	0.0	13050.8	1988.8	0.152
25.0	12.5	10418.2	1588.1	0.153
50.0	25.0	4850.4	765.2	0.158
75.0	37.5	2868.5	433.1	0.151
100.0	50.0	1831.8	284.7	0.181
125.0	62.5	1140.2	225.2	0.198
150.0	75.0	852.2	182.2	0.214
175.0	87.5	664.1	157.2	0.237
200.0	100.0	532.4	133.0	0.250
225.0	112.5	436.1	118.7	0.272
250.0	125.0	363.5	108.4	0.298
275.0	137.5	307.3	98.0	0.319
300.0	150.0	263.1	88.6	0.341
325.0	162.5	227.6	81.3	0.357
350.0	175.0	198.8	75.1	0.378
375.0	187.5	175.0	68.6	0.367
400.0	200.0	155.3	64.8	0.416
425.0	212.5	138.6	60.5	0.436
450.0	225.0	124.5	56.4	0.453
475.0	237.5	112.5	52.8	0.468
500.0	250.0	102.0	48.5	0.485
525.0	262.5	93.0	46.6	0.501
550.0	275.0	85.1	43.7	0.513
575.0	287.5	78.2	41.3	0.528
600.0	300.0	72.1	38.8	0.540
625.0	312.5	66.6	36.7	0.550
650.0	325.0	61.8	36.6	0.625
675.0	337.5	57.5	32.4	0.564
700.0	350.0	53.6	31.3	0.584
725.0	362.5	50.1	28.7	0.584
750.0	375.0	46.8	28.1	0.588
775.0	387.5	44.0	26.7	0.607
800.0	400.0	41.4	25.3	0.611
825.0	412.5	38.0	24.5	0.630
850.0	425.0	36.8	23.4	0.637
875.0	437.5	34.8	22.2	0.640
900.0	450.0	32.8	20.4	0.621
925.0	462.5	31.2	18.7	0.630
950.0	475.0	29.6	18.6	0.629
975.0	487.5	28.2	17.7	0.630
1000.0	500.0	26.8	17.6	0.657

CAVITY LENGTH= 17.5 M
CAVITY NOX CONC.= 90020.01 UG/M**3

MAXIMUM NOX=13050.83 UG/M**3 AT 17.5 M

MAXIMUM NO2= 1988.82 UG/M**3 AT 17.5 M

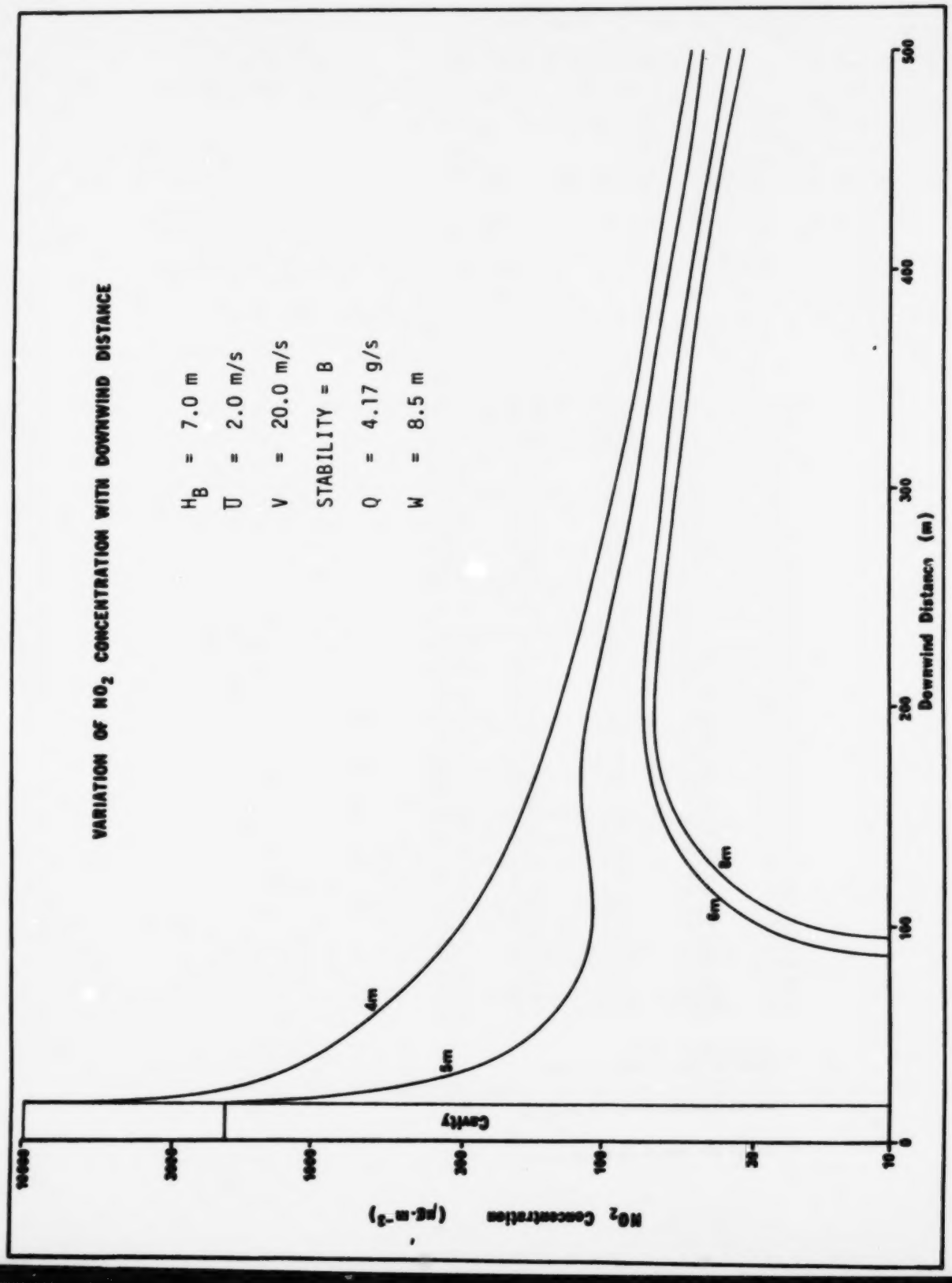

Figure 20: Variation of NO_2 Concentration With Downwind Distance for Stack Heights Indicated: Case 1

Case #2

COMPRESSOR STATION CHEMISTRY MODEL

G= 4.17 G/S
d= 0.30 M
HB= 7.00 M
HS= 7.00 M
U= 5.0 M/S
V= 20.0 M/S
TS= 700.0 K
TA= 283.0 K
D= 0.300 M
STAB=B
OZONE= 40.0 PPB

ALPHA=0.201
H EFF= 14.8 M

DOWNWIND DIST (M)	TRAVEL TIME (S)	NOX CONC (UG/M**3)	NO2 CONC (UG/M**3)	NO2/NOX RATIO
17.5	3.5	1438.7	227.4	0.155
25.0	5.0	1170.6	186.5	0.159
50.0	10.0	588.0	107.1	0.182
75.0	15.0	486.3	103.4	0.208
100.0	20.0	445.8	94.1	0.211
125.0	25.0	374.1	84.8	0.226
150.0	30.0	305.6	75.6	0.247
175.0	35.0	248.1	61.6	0.247
200.0	40.0	204.8	58.2	0.285
225.0	45.0	168.5	48.0	0.288
250.0	50.0	142.8	45.4	0.318
275.0	55.0	121.4	45.7	0.377
300.0	60.0	104.2	37.6	0.361
325.0	65.0	90.4	39.7	0.440
350.0	70.0	76.1	30.5	0.385
375.0	75.0	68.7	28.3	0.408
400.0	80.0	61.9	25.8	0.415
425.0	85.0	55.3	24.1	0.435
450.0	90.0	48.7	22.3	0.448
475.0	95.0	44.8	20.8	0.464
500.0	100.0	40.8	19.3	0.474
525.0	105.0	37.2	18.0	0.484
550.0	110.0	34.0	16.8	0.495
575.0	115.0	31.2	15.9	0.508
600.0	120.0	28.8	14.8	0.516
625.0	125.0	26.8	14.0	0.525
650.0	130.0	24.7	13.2	0.534
675.0	135.0	23.0	12.5	0.543
700.0	140.0	21.4	11.8	0.553
725.0	145.0	20.0	11.1	0.552
750.0	150.0	18.7	10.5	0.562
775.0	155.0	17.6	10.1	0.572
800.0	160.0	16.5	9.5	0.581
825.0	165.0	15.5	9.2	0.580
850.0	170.0	14.7	8.8	0.597
875.0	175.0	13.8	8.6	0.618
900.0	180.0	13.2	8.5	0.645
925.0	185.0	12.5	8.1	0.647
950.0	190.0	11.8	7.8	0.657
975.0	195.0	11.3	7.8	0.701
1000.0	200.0	10.7	7.7	0.715

CAVITY LENGTH= 17.5 M
CAVITY NOX CONC.= 2810.75 UG/M**3

MAXIMUM NOX= 1438.68 UG/M**3 AT 17.5 M

MAXIMUM NO2= 227.44 UG/M**3 AT 17.5 M

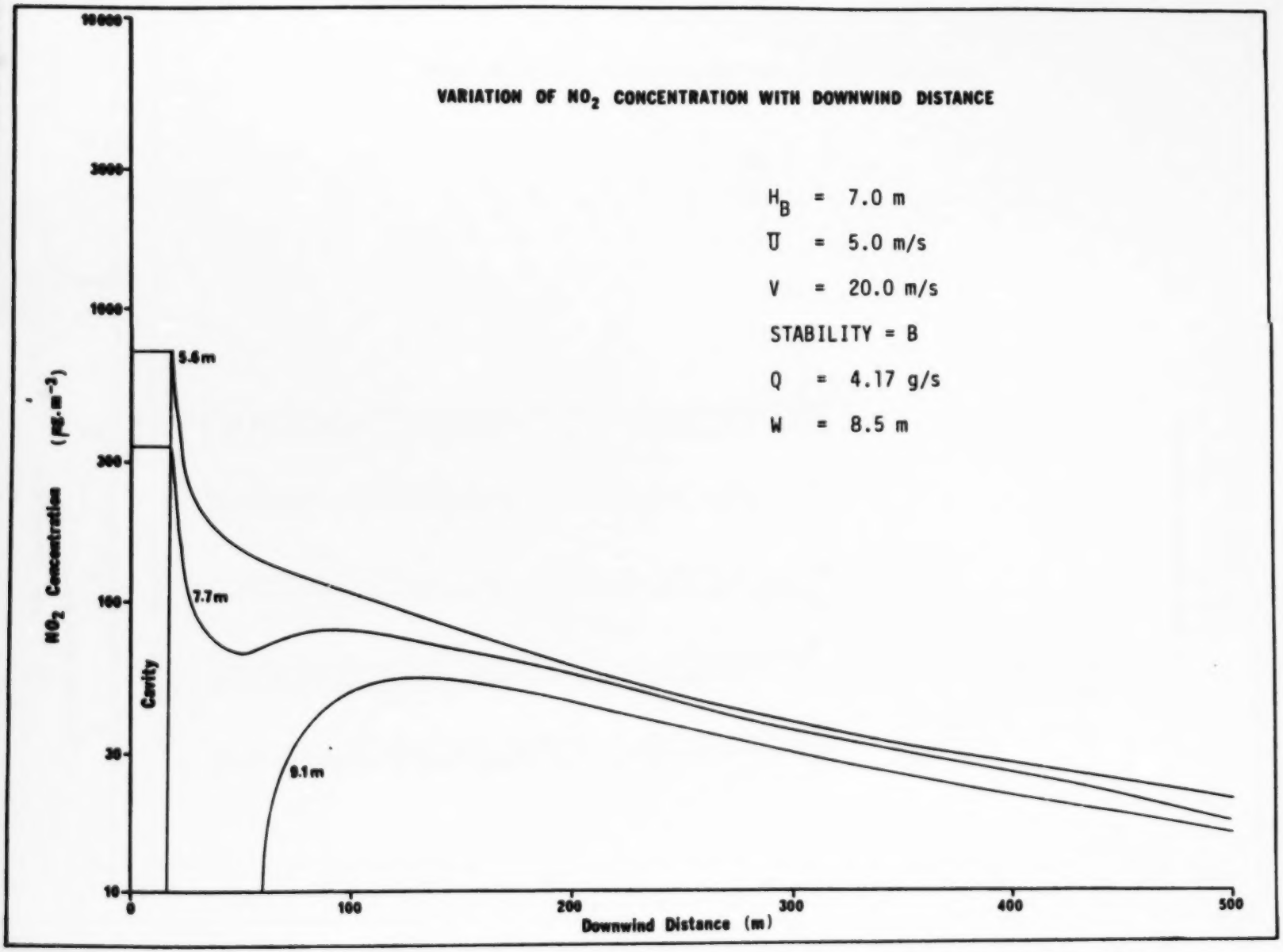

Figure 21: Variation of NO_2 Concentration With Downwind Distance for Stack Heights Indicated: Case 2

Case #3

COMPRESSOR STATION CHEMISTRY MODEL

Q= 4.17 G/S
W= 8.50 M
HB= 7.00 M
HS= 4.00 M
U= 2.0 M/S
V= 40.0 M/S
TS= 700.0 K
TA= 293.0 K
B= 0.300 M
STAB=B
OZONE= 40.0 PPB

ALPHA=0.714
H EFF= 25.2 M

BOUNDING DIST (M)	TRAVEL TIME (S)	NOX CONC (UG/M**3)	NO2 CONC (UG/M**3)	NO2/NOX RATIO
17.5	8.8	13050.8	1988.8	0.152
25.0	12.5	10416.2	1598.1	0.153
50.0	25.0	4650.3	768.2	0.158
75.0	37.5	2598.7	428.8	0.165
100.0	50.0	1587.3	278.7	0.176
125.0	62.5	1070.2	204.4	0.191
150.0	75.0	779.2	162.7	0.208
175.0	87.5	600.2	140.4	0.234
200.0	100.0	481.0	118.4	0.248
225.0	112.5	393.1	105.0	0.265
250.0	125.0	332.7	100.5	0.302
275.0	137.5	283.7	90.8	0.320
300.0	150.0	244.9	85.6	0.350
325.0	162.5	213.4	78.1	0.370
350.0	175.0	187.7	73.5	0.391
375.0	187.5	165.2	68.4	0.411
400.0	200.0	148.2	64.0	0.432
425.0	212.5	133.6	60.1	0.452
450.0	225.0	115.5	56.3	0.469
475.0	237.5	108.7	52.7	0.485
500.0	250.0	98.9	49.4	0.499
525.0	262.5	90.4	48.3	0.512
550.0	275.0	82.9	43.5	0.524
575.0	287.5	76.3	40.9	0.536
600.0	300.0	70.5	38.7	0.548
625.0	312.5	65.3	36.3	0.555
650.0	325.0	60.6	34.3	0.566
675.0	337.5	56.5	32.7	0.578
700.0	350.0	52.7	33.3	0.633
725.0	362.5	49.3	31.8	0.641
750.0	375.0	46.2	29.7	0.643
775.0	387.5	43.4	26.7	0.615
800.0	400.0	40.8	26.4	0.646
825.0	412.5	38.5	25.1	0.652
850.0	425.0	36.4	23.6	0.648
875.0	437.5	34.4	21.8	0.635
900.0	450.0	32.6	20.3	0.624
925.0	462.5	30.8	19.6	0.635
950.0	475.0	29.4	18.3	0.623
975.0	487.5	27.8	17.7	0.635
1000.0	500.0	26.6	16.9	0.636

CAVITY LENGTH= 17.5 M
CAVITY NOX CONC.= 50020.01 UG/M**3

MAXIMUM NOX=13050.83 UG/M**3 AT 17.5 M

MAXIMUM NO2= 1988.82 UG/M**3 AT 17.5 M

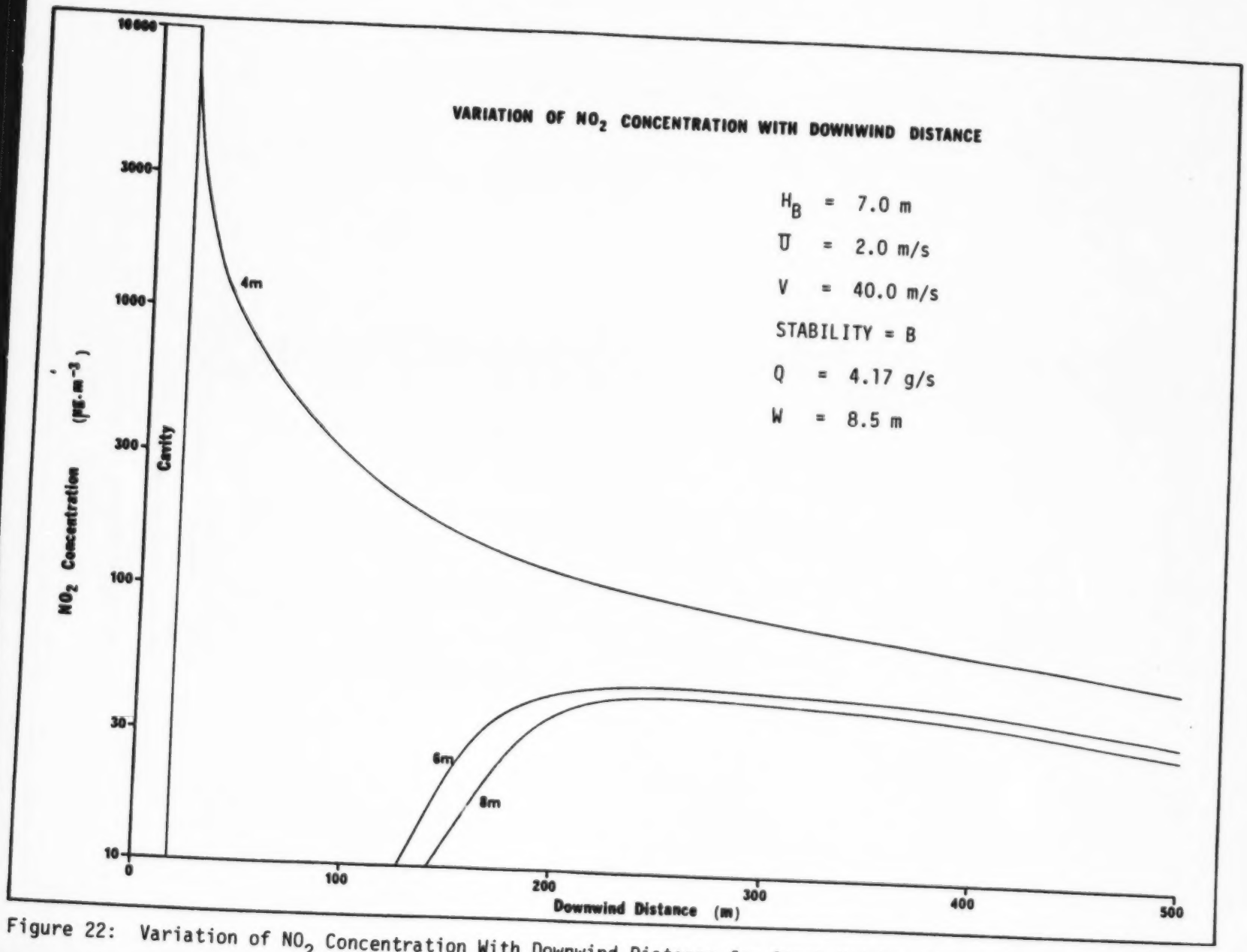

Figure 22: Variation of NO_2 Concentration With Downwind Distance for Stack Heights Indicated: Case 3

Case #4

COMPRESSOR STATION CHEMISTRY MODEL

Q= 4.17 G/S
W= 8.50 M
HE= 7.00 M
HS= 6.00 M
U= 5.0 M/S
V= 40.0 M/S
TS= 700.0 K
TA= 293.0 K
D= 0.300 M
STAB=B
OZONE= 40.0 PPB

ALPHA=0.0
H EFF= 18.5 M

DOWNWIND DIST (M)	TRAVEL TIME (S)	NOX CONC (UG/M**3)	NO2 CONC (UG/M**3)	NO2/NOX RATIO
17.5	3.5	0.0	0.0	0.0
25.0	5.0	0.0	0.0	0.0
50.0	10.0	5.4	1.0	0.184
75.0	15.0	80.4	22.5	0.249
100.0	20.0	186.3	38.6	0.207
125.0	25.0	219.3	46.6	0.212
150.0	30.0	212.8	50.8	0.238
175.0	35.0	191.5	44.8	0.234
200.0	40.0	168.0	42.7	0.254
225.0	45.0	145.6	38.4	0.264
250.0	50.0	126.2	38.5	0.305
275.0	55.0	108.7	30.8	0.282
300.0	60.0	95.8	28.8	0.301
325.0	65.0	84.2	27.8	0.330
350.0	70.0	74.4	27.8	0.375
375.0	75.0	66.1	24.3	0.367
400.0	80.0	58.1	19.1	0.323
425.0	85.0	53.1	23.6	0.444
450.0	90.0	47.9	19.8	0.412
475.0	95.0	43.5	17.4	0.400
500.0	100.0	38.6	16.4	0.415
525.0	105.0	36.2	19.0	0.526
550.0	110.0	33.2	14.0	0.422
575.0	115.0	30.6	12.8	0.423
600.0	120.0	28.2	12.2	0.432
625.0	125.0	26.2	11.5	0.440
650.0	130.0	24.3	11.0	0.453
675.0	135.0	22.8	10.6	0.468
700.0	140.0	21.1	9.9	0.468
725.0	145.0	18.7	8.4	0.478
750.0	150.0	18.5	9.0	0.486
775.0	155.0	17.4	8.6	0.492
800.0	160.0	16.4	8.2	0.501
825.0	165.0	15.4	7.8	0.508
850.0	170.0	14.6	7.3	0.503
875.0	175.0	13.8	7.6	0.548
900.0	180.0	13.1	7.1	0.541
825.0	185.0	12.4	7.3	0.581
850.0	180.0	11.8	7.0	0.581
875.0	185.0	11.2	6.1	0.545
1000.0	200.0	10.6	6.2	0.578

CAVITY LENGTH= 17.5 M
CAVITY NOX CONC.= 0.0 UG/M**3

MAXIMUM NOX= 218.31 UG/M**3 AT125.0 M

MAXIMUM NO2= 50.81 UG/M**3 AT150.0 M

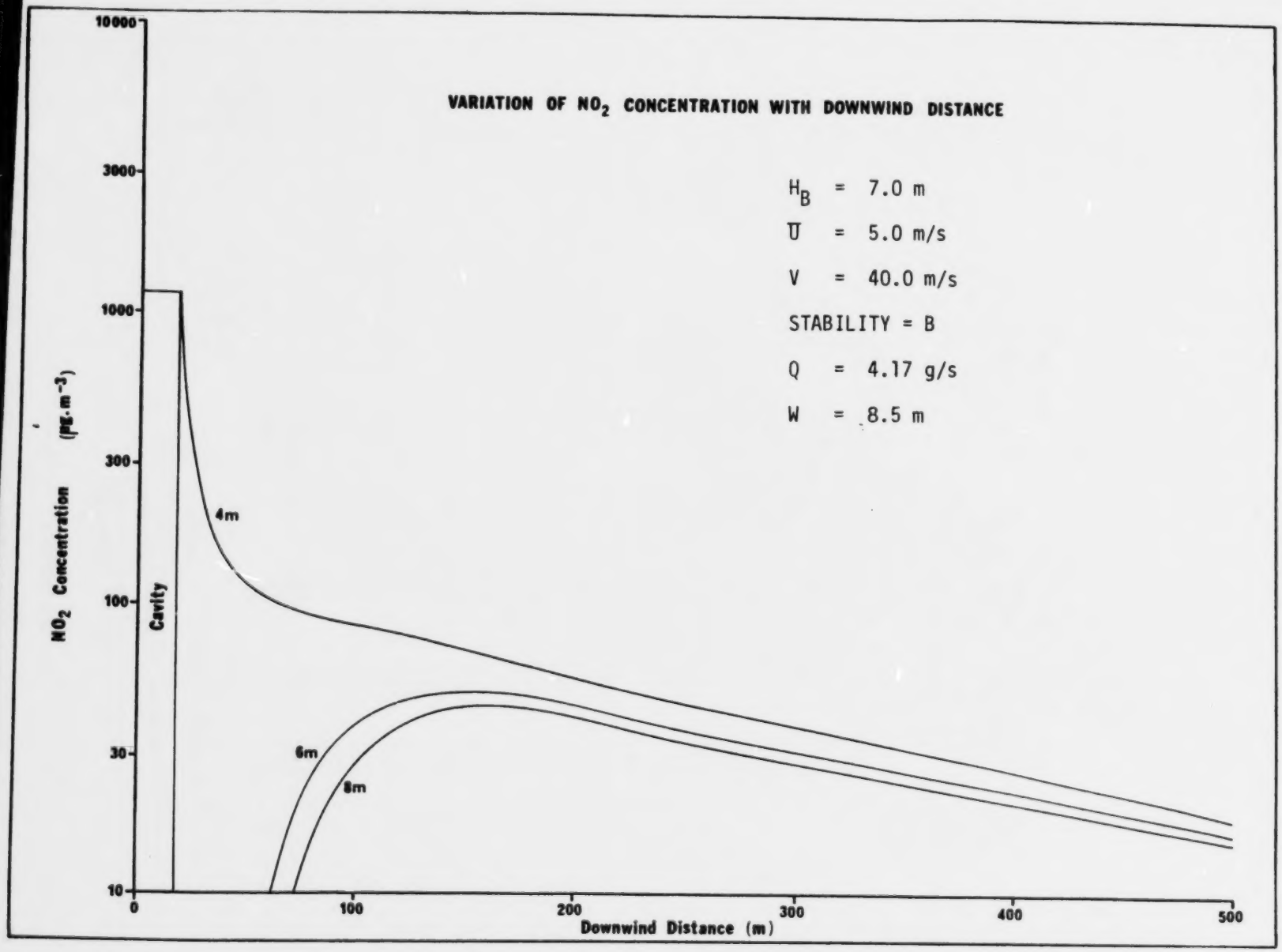

Figure 23: Variation of NO_2 Concentration With Downwind Distance for Stack Heights Indicated: Case 4

Case #5

CONNECTICUT STATION CONSTANT FLOW

G= 4.17 G/S
W= 6.50 M
HB= 7.00 M
HS= 4.00 M
U= 2.0 M/S
V= 20.0 M/S
TS= 700.0 K
TA= 293.0 K
D= 0.300 M
STAB=D
OZONE= 40.0 PPB

ALPHA=0.714
H EFF= 23.7 M

DOWNWIND DIST (M)	TRAVEL TIME (S)	NOX CONC (UG/M**3)	NO2 CONC (UG/M**3)	NO2/NOX RATIO
17.5	8.8	18372.7	2314.7	0.141
25.0	12.5	15357.5	2174.4	0.142
50.0	25.0	11422.1	1628.3	0.143
75.0	37.5	8166.4	1178.2	0.144
100.0	50.0	5932.3	858.6	0.145
125.0	62.5	4444.8	662.6	0.149
150.0	75.0	3439.3	524.3	0.152
175.0	87.5	2741.8	430.4	0.157
200.0	100.0	2245.2	365.5	0.163
225.0	112.5	1881.6	315.2	0.170
250.0	125.0	1607.8	284.2	0.177
275.0	137.5	1396.3	257.0	0.184
300.0	150.0	1228.6	235.4	0.192
325.0	162.5	1092.5	218.1	0.200
350.0	175.0	981.0	202.6	0.207
375.0	187.5	887.5	190.5	0.215
400.0	200.0	807.7	178.8	0.221
425.0	212.5	735.5	168.5	0.230
450.0	225.0	680.1	160.6	0.236
475.0	237.5	628.2	153.8	0.245
500.0	250.0	582.6	147.5	0.253
525.0	262.5	542.1	141.7	0.261
550.0	275.0	506.0	136.3	0.269
575.0	287.5	473.6	131.4	0.277
600.0	300.0	444.5	126.8	0.285
625.0	312.5	418.1	122.0	0.292
650.0	325.0	394.2	118.0	0.302
675.0	337.5	372.4	115.1	0.309
700.0	350.0	352.5	111.9	0.318
725.0	362.5	334.3	108.2	0.324
750.0	375.0	317.5	105.7	0.333
775.0	387.5	302.0	102.3	0.339
800.0	400.0	287.8	100.1	0.348
825.0	412.5	274.6	97.1	0.354
850.0	425.0	262.3	94.5	0.360
875.0	437.5	250.8	92.2	0.367
900.0	450.0	240.3	90.0	0.375
925.0	462.5	230.3	88.1	0.382
950.0	475.0	221.1	85.6	0.389
975.0	487.5	212.4	84.7	0.395
1000.0	500.0	204.2	82.2	0.402

CAVITY LENGTH= 17.5 M
CAVITY NOX CONC.= 50020.01 UG/M**3

MAXIMUM NOX=18372.70 UG/M**3 AT 17.5 M

MAXIMUM NO2= 2314.72 UG/M**3 AT 17.5 M

Case #6

COMPRESSOR STATION CHEMISTRY MODEL

Q= 4.17 G/S
W= 8.50 M
WB= 7.00 M
WS= 7.00 M
U= 5.0 M/S
V= 20.0 M/S
TS= 700.0 K
TA= 293.0 K
D= 0.300 M
STAB=D
OZONE= 40.0 PPB

ALPHA=0.201
H EFF= 14.8 M

DOWNWIND DIST (M)	TRAVEL TIME (S)	NOX CONC (UG/M**3)	NO2 CONC (UG/M**3)	NO2/NOX RATIO
17.5	3.5	1840.0	256.0	0.139
25.0	5.0	1726.0	241.7	0.140
50.0	10.0	1283.7	186.1	0.147
75.0	15.0	915.4	144.3	0.157
100.0	20.0	664.0	121.0	0.174
125.0	25.0	590.6	115.8	0.196
150.0	30.0	548.6	116.1	0.212
175.0	35.0	524.6	115.4	0.220
200.0	40.0	500.8	113.8	0.227
225.0	45.0	474.0	111.0	0.234
250.0	50.0	445.0	107.2	0.241
275.0	55.0	415.3	103.2	0.248
300.0	60.0	386.3	99.2	0.257
325.0	65.0	358.7	95.2	0.265
350.0	70.0	333.0	91.4	0.274
375.0	75.0	309.2	87.7	0.284
400.0	80.0	287.5	84.3	0.293
425.0	85.0	267.8	81.1	0.303
450.0	90.0	248.6	78.0	0.313
475.0	95.0	233.2	74.7	0.320
500.0	100.0	218.3	71.4	0.327
525.0	105.0	204.7	69.1	0.338
550.0	110.0	192.3	67.2	0.349
575.0	115.0	181.0	65.4	0.361
600.0	120.0	170.7	63.3	0.371
625.0	125.0	161.2	61.3	0.380
650.0	130.0	152.5	58.4	0.383
675.0	135.0	144.5	57.8	0.399
700.0	140.0	137.2	55.8	0.407
725.0	145.0	130.4	54.2	0.416
750.0	150.0	124.1	52.7	0.425
775.0	155.0	118.2	51.1	0.432
800.0	160.0	112.8	49.7	0.441
825.0	165.0	107.8	48.2	0.447
850.0	170.0	103.1	46.8	0.453
875.0	175.0	98.7	45.5	0.461
900.0	180.0	94.7	44.3	0.468
925.0	185.0	90.8	43.2	0.475
950.0	190.0	87.3	42.1	0.482
975.0	195.0	83.8	41.0	0.488
1000.0	200.0	80.7	40.0	0.495

CAVITY LENGTH= 17.5 M
CAVITY NOX CONC.= 2810.75 UG/M**3

MAXIMUM NOX= 1840.04 UG/M**3 AT 17.5 M

MAXIMUM NO2= 256.00 UG/M**3 AT 17.5 M

Case # 7

COMPRESSOR STATION CHEMISTRY MODEL

U= 4.17 M/S
H= 8.50 M
HB= 7.50 M
HS= 5.00 M
U= 10.0 M/S
V= 20.0 M/S
TS= 750.0 K
TA= 253.0 K
D= 0.500 M
SIGMA=0
NOINE= 40.0 PPB

K.PHA=0.664
H EFF= 8.5 M

DISTANCE DOWNWIND (M)	TIME (S)	NOX CONC (UG/M**3)	NO2 CONC (UG/M**3)	NO2/NOX
37.5	1.8	3446.2	435.8	0.126
50.0	2.5	2854.8	412.1	0.144
62.5	3.0	2425.7	357.3	0.148
75.0	3.5	2085.0	298.5	0.136
100.0	4.0	1242.6	204.5	0.165
125.0	4.5	881.8	153.8	0.174
150.0	5.0	665.5	108.5	0.165
175.0	5.5	661.3	123.4	0.186
200.0	6.0	552.6	114.4	0.207
225.0	6.5	467.2	107.5	0.215
250.0	7.0	400.4	92.8	0.231
275.0	7.5	347.0	84.5	0.244
300.0	8.0	303.7	77.8	0.256
325.0	8.5	268.3	72.1	0.268
350.0	9.0	238.8	67.2	0.281
375.0	9.5	214.1	62.8	0.294
400.0	10.0	193.2	59.2	0.306
425.0	10.5	175.3	55.8	0.318
450.0	11.0	159.9	52.8	0.330
475.0	11.5	146.6	50.1	0.342
500.0	12.0	134.8	47.7	0.354
525.0	12.5	124.6	45.5	0.365
550.0	13.0	115.5	43.5	0.376
575.0	13.5	107.5	41.8	0.387
600.0	14.0	100.3	40.3	0.398
625.0	14.5	93.8	38.9	0.408
650.0	15.0	88.0	37.7	0.418
675.0	15.5	82.7	36.6	0.428
700.0	16.0	78.0	35.4	0.437
725.0	16.5	73.8	34.1	0.447
750.0	17.0	69.7	32.5	0.456
775.0	17.5	66.0	31.7	0.464
800.0	18.0	62.7	30.6	0.472
825.0	18.5	59.8	29.8	0.480
850.0	19.0	57.1	28.6	0.488
875.0	19.5	54.2	27.7	0.496
900.0	20.0	51.7	26.5	0.467
925.0	20.5	49.5	25.0	0.502
950.0	21.0	47.4	25.2	0.510
975.0	21.5	45.4	24.3	0.514
1000.0	22.0	43.8	23.8	0.515
	100.0		22.8	0.525

CAVITY LENGTH= 17.5 M
CAVITY NOX CONC.= 9257.36 UG/M**3

MAXIMUM NOX= 3043.24 UG/M**3 AT 17.5 M

MAXIMUM NO2= 435.75 UG/M**3 AT 17.5 M

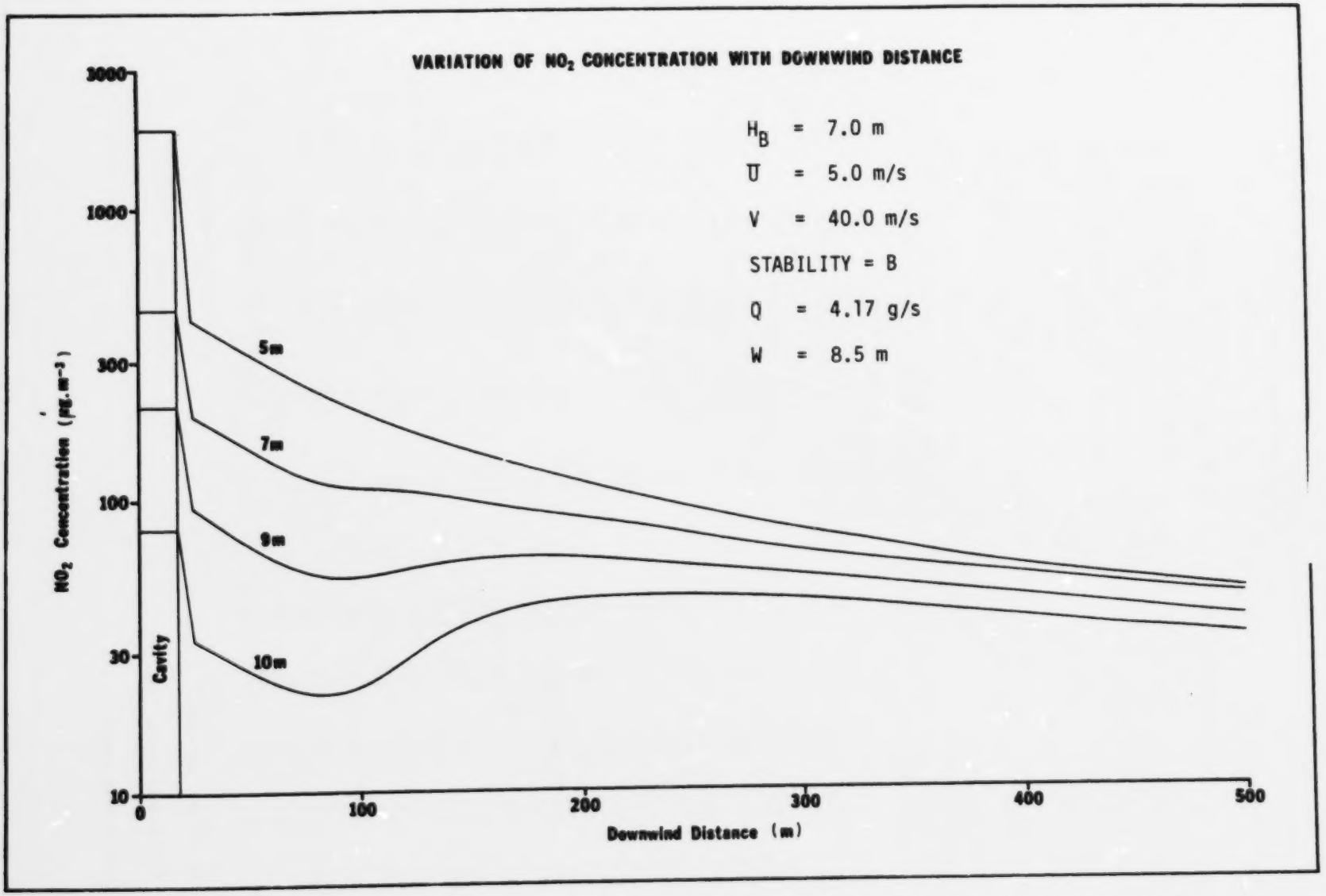

Figure 24: Variation of NO_2 Concentration With Downwind Distance for Stack Heights Indicated: Case 7

Case #8

COMPRESSOR STATION CHEMISTRY MODEL

a= 4.17 M/S
a= 8.50 M
ma= 7.00 M
mb= 6.00 M
U= 2.0 M/S
V= 40.0 M/S
TS= 700.0 K
TA= 255.0 K
B= 0.500 M
STAB=D
OZONE= 40.0 PPB

A_PAR=0.0
A EFF= 37.2 M

DISTANCE DOWNWIND FROM SOURCE (M)	TRAVEL TIME (S)	NOX CONC (UG/M**3)	NO2 CONC (UG/M**3)	NO2/NOX RATIO
17.5	8.8	0.0	0.0	0.0
25.0	12.5	0.0	0.0	0.0
50.0	25.0	0.0	0.0	0.0
75.0	37.5	0.0	0.0	0.0
100.0	50.0	0.0	0.0	0.0
125.0	62.5	0.0	0.0	0.571
150.0	75.0	0.0	0.0	0.0
175.0	87.5	0.0	0.0	0.629
200.0	100.0	0.2	0.2	0.838
225.0	112.5	1.2	0.8	0.843
250.0	125.0	3.4	2.2	0.837
275.0	137.5	7.5	4.7	0.823
300.0	150.0	13.5	8.2	0.606
325.0	162.5	21.2	12.3	0.578
350.0	175.0	30.1	15.6	0.550
375.0	187.5	38.7	20.6	0.518
400.0	200.0	48.4	24.5	0.486
425.0	212.5	58.8	28.1	0.478
450.0	225.0	67.8	30.6	0.451
475.0	237.5	76.0	33.1	0.436
500.0	250.0	85.3	35.3	0.414
525.0	262.5	88.7	37.3	0.416
550.0	275.0	85.2	37.8	0.366
66				
575.0	287.5	98.8	38.5	0.358
600.0	300.0	103.6	40.7	0.353
625.0	312.5	106.7	41.1	0.385
650.0	325.0	108.1	42.2	0.388
675.0	337.5	110.8	42.8	0.387
700.0	350.0	112.2	43.1	0.385
725.0	362.5	113.0	44.1	0.386
750.0	375.0	113.4	44.2	0.388
775.0	387.5	113.4	44.3	0.381
800.0	400.0	113.2	43.8	0.388
825.0	412.5	112.7	43.8	0.388
850.0	425.0	112.0	43.8	0.381
875.0	437.5	111.1	44.1	0.387
900.0	450.0	110.1	43.5	0.385
925.0	462.5	108.5	43.3	0.387
950.0	475.0	107.7	43.5	0.404
975.0	487.5	106.3	42.8	0.403
1000.0	500.0	104.8	42.5	0.406

CAVITY LENGTH= 17.5 M
CAVITY MAX CONC.= 0.0 UG/M**3

MAXIMUM NOX= 113.44 UG/M**3 AT 775.0 M

MAXIMUM NO2= 44.31 UG/M**3 AT 775.0 M

Case #9

COMPRESSOR STATION CHEMISTRY MODEL

U= 4.17 M/S
H= 6.50 M
HO= 7.00 M
HS= 6.00 M
W= 5.0 M/S
V= 40.0 M/S
TS= 700.0 K
TA= 283.0 K
D= 0.360 M
STAB=0
OZONE= 40.0 PPB

ALPHA=0.205
H EFF= 16.3 M

DOWNWIND DIST (M)	TRAVEL TIME (S)	NOX CONC (UG/M**3)	NO2 CONC (UG/M**3)	NO2/NOX RATIO
17.5	3.5	1880.0	274.2	0.146
25.0	5.0	1763.5	258.7	0.146
50.0	10.0	1311.5	204.1	0.156
75.0	15.0	937.3	155.7	0.166
100.0	20.0	665.8	124.4	0.186
125.0	25.0	552.0	111.1	0.201
150.0	30.0	486.2	107.7	0.222
175.0	35.0	453.5	106.8	0.235
200.0	40.0	431.4	105.5	0.245
225.0	45.0	411.0	103.5	0.252
250.0	50.0	388.1	100.6	0.258
275.0	55.0	364.1	97.8	0.268
300.0	60.0	346.1	94.5	0.273
325.0	65.0	324.6	91.2	0.281
350.0	70.0	303.5	88.0	0.290
375.0	75.0	284.5	84.8	0.298
400.0	80.0	266.3	81.7	0.307
425.0	85.0	248.4	78.6	0.316
450.0	90.0	233.6	76.0	0.325
475.0	95.0	218.5	73.5	0.336
500.0	100.0	206.3	70.8	0.343
525.0	105.0	194.2	68.4	0.352
550.0	110.0	183.1	65.1	0.361
575.0	115.0	172.8	63.2	0.366
600.0	120.0	163.4	61.9	0.378
625.0	125.0	154.7	60.2	0.389
650.0	130.0	146.7	58.2	0.397
675.0	135.0	138.3	56.6	0.408
700.0	140.0	132.5	54.8	0.413
725.0	145.0	125.1	53.3	0.423
750.0	150.0	120.2	51.8	0.431
775.0	155.0	114.7	48.7	0.436
800.0	160.0	108.6	48.8	0.448
825.0	165.0	104.8	47.3	0.451
850.0	170.0	100.4	46.3	0.461
875.0	175.0	96.5	45.1	0.468
900.0	180.0	92.4	43.9	0.475
925.0	185.0	88.7	41.8	0.472
950.0	190.0	85.3	41.7	0.488
975.0	195.0	82.1	38.8	0.485
1000.0	200.0	78.1	38.8	0.501

CAVITY LENGTH= 17.5 M
CAVITY MAX CONC.= 5743.4b UG/M**3

MAXIMUM NOX= 1879.88 UG/M**3 AT 17.5 M

MAXIMUM NO2= 274.15 UG/M**3 AT 17.5 M

Case #10

[illegible] STATION CHEMISTRY MODEL

[illegible]= 4.17 m/s
[illegible]= 8.50 m
[illegible]= 7.66 m
[illegible]= 7.66 m
[illegible]= 10.0 m/s
[illegible]= 40.0 m/s
[illegible]= 700.0 s
[illegible]= 283.0 K
[illegible]= 0.300 m
[illegible]=0
[illegible]= 40.0 PPB

[illegible]=0.28)
[illegible] Eff= 13.2 m

[illegible] DIST (m)	[illegible] TIME (s)	NOX CONC (ug/m**3)	NO2 CONC (ug/m**3)	NO2/NOX RATIO
12.5	1.0	920.0	127.6	0.138
25.0	2.5	892.0	120.4	0.135
50.0	5.0	841.8	83.1	0.145
75.0	7.5	803.5	72.2	0.156
100.0	10.0	771.6	84.2	0.175
125.0	12.5	741.2	85.0	0.180
150.0	15.0	728.4	85.8	0.203
175.0	17.5	714.4	88.8	0.213
200.0	20.0	706.4	85.7	0.222
225.0	22.5	276.0	83.7	0.231
250.0	25.0	254.6	81.3	0.240
275.0	27.5	234.5	58.7	0.250
300.0	30.0	215.4	56.1	0.261
325.0	32.5	197.4	53.8	0.272
350.0	35.0	181.9	51.2	0.282
375.0	37.5	167.5	48.0	0.288
400.0	40.0	154.7	46.5	0.300
425.0	42.5	143.1	44.8	0.314
450.0	45.0	132.8	42.9	0.322
475.0	47.5	123.5	41.4	0.335
500.0	50.0	115.1	39.8	0.346
525.0	52.5	107.5	38.4	0.357
550.0	55.0	100.7	38.6	0.383
575.0	57.5	94.5	35.6	0.377
600.0	60.0	88.8	34.2	0.385
625.0	62.5	83.8	33.0	0.394
650.0	65.0	79.1	31.9	0.403
675.0	67.5	74.8	30.8	0.413
700.0	70.0	70.8	29.9	0.422
725.0	72.5	67.2	28.9	0.430
750.0	75.0	63.8	28.0	0.438
775.0	77.5	60.6	27.1	0.448
800.0	80.0	57.8	26.3	0.455
825.0	82.5	55.3	25.6	0.462
850.0	85.0	52.8	24.8	0.470
875.0	87.5	50.5	24.1	0.477
900.0	90.0	48.4	23.3	0.484
925.0	92.5	46.4	22.6	0.488
950.0	95.0	44.8	22.2	0.488
975.0	97.5	42.8	21.8	0.509
1000.0	100.0	41.2	21.0	0.511

CAVITY LENGTH= 17.5 m
CAVITY NOX CONC.= 1400.37 ug/m**3

MAXIMUM NOX= 920.0[illegible] ug/m**3 AT 17.5 m

MAXIMUM NO2= 127.62 ug/m**3 AT 17.5 m

Case #11

COMPRESSOR STATION CHEMISTRY MODEL

Q= 4.17 G/S
W= 8.50 M
WB= 7.00 M
WS= 4.00 M
U= 2.0 M/S
V= 20.0 M/S
TS= 700.0 K
TA= 283.0 K
D= 0.300 M
STAB=E
OZONE= 40.0 PPB

ALPHA=0.714
H EFF= 30.0 M

DOWNWIND DIST (M)	TRAVEL TIME (S)	NOX CONC (UG/M**3)	NO2 CONC (UG/M**3)	NO2/NOX RATIO
25.0	12.5	16282.1	2468.1	0.152
50.0	25.0	13521.1	2058.9	0.152
75.0	37.5	10714.1	1641.7	0.153
100.0	50.0	8414.8	1298.0	0.154
125.0	62.5	6871.2	1068.1	0.156
150.0	75.0	5374.1	845.7	0.157
175.0	87.5	4404.9	701.2	0.159
200.0	100.0	3570.7	581.7	0.163
225.0	112.5	3105.1	567.4	0.183
250.0	125.0	2322.3	441.5	0.188
275.0	137.5	2310.1	388.0	0.168
300.0	150.0	2028.2	347.3	0.171
325.0	162.5	1784.3	313.8	0.175
350.0	175.0	1542.5	225.8	0.178
375.0	187.5	1443.2	263.2	0.182
400.0	200.0	1318.8	243.8	0.183
425.0	212.5	1194.2	228.3	0.191
450.0	225.0	1083.0	218.0	0.197
475.0	237.5	1011.2	203.7	0.201
500.0	250.0	897.2	182.7	0.204
525.0	262.5	872.3	187.7	0.215
550.0	275.0	815.0	178.4	0.218
575.0	287.5	734.0	168.4	0.229
600.0	300.0	718.4	162.0	0.226
625.0	312.5	677.5	156.1	0.230
650.0	325.0	640.5	150.9	0.233
675.0	337.5	606.8	150.3	0.248
700.0	350.0	578.4	144.4	0.251
725.0	362.5	548.4	138.1	0.252
750.0	375.0	522.7	135.4	0.258
775.0	387.5	498.1	131.5	0.264
800.0	400.0	477.3	125.4	0.263
825.0	412.5	457.1	125.2	0.274
850.0	425.0	438.3	121.7	0.278
875.0	437.5	420.8	131.0	0.311
900.0	450.0	404.5	118.2	0.292
925.0	462.5	388.3	113.4	0.291
950.0	475.0	375.0	112.8	0.300
975.0	487.5	361.8	108.8	0.301
1000.0	500.0	348.0	128.0	0.367

CAVITY LENGTH= 17.5 M
CAVITY NOX CONC.= 50020.01 UG/M**3

MAXIMUM NOX=18873.87 UG/M**3 AT 17.5 M

MAXIMUM NO2= 2558.87 UG/M**3 AT 17.5 M

Case #12

COMPRESSOR STATION CHEMISTRY MODEL

Q= 4.17 G/S
a= 8.50 M
HB= 7.00 M
HS= 7.70 M
U= 5.0 M/S
V= 20.0 M/S
TS= 700.0 K
TA= 283.0 K
D= 0.300 M
STAB=E
OZONE= 40.0 PPB

ALPHA=0.120
H EFF= 33.7 M

DOWNWIND DIST (M)	TRAVEL TIME (S)	NOX CONC (UG/M**3)	NO2 CONC (UG/M**3)	NO2/NOX RATIO
17.5	3.5	1137.8	174.0	0.153
25.0	5.0	1086.5	165.4	0.154
50.0	10.0	811.7	147.0	0.181
75.0	15.0	722.3	123.2	0.171
100.0	20.0	537.4	103.3	0.192
125.0	25.0	445.8	87.8	0.195
150.0	30.0	352.4	76.0	0.216
175.0	35.0	287.0	65.5	0.225
200.0	40.0	247.5	58.7	0.241
225.0	45.0	208.4	54.0	0.258
250.0	50.0	178.6	49.4	0.275
275.0	55.0	153.0	43.8	0.282
300.0	60.0	137.2	42.8	0.311
325.0	65.0	122.2	40.1	0.328
350.0	70.0	110.3	38.0	0.345
375.0	75.0	100.8	37.0	0.368
400.0	80.0	93.6	35.9	0.384
425.0	85.0	87.9	35.0	0.401
450.0	90.0	83.5	35.1	0.421
475.0	95.0	80.2	35.5	0.442
500.0	100.0	77.7	34.8	0.448
525.0	105.0	75.5	34.1	0.450
550.0	110.0	74.4	43.4	0.584
575.0	115.0	73.4	34.8	0.475
600.0	120.0	72.5	34.8	0.482
625.0	125.0	71.8	37.1	0.516
650.0	130.0	71.3	34.5	0.484
675.0	135.0	70.8	35.1	0.495
700.0	140.0	70.4	34.7	0.493
725.0	145.0	68.9	34.8	0.488
750.0	150.0	68.5	37.8	0.548
775.0	155.0	65.0	37.8	0.545
800.0	160.0	58.5	34.4	0.562
825.0	165.0	60.0	37.3	0.548
850.0	170.0	67.5	38.9	0.576
875.0	175.0	66.5	38.2	0.540
900.0	180.0	65.3	37.5	0.565
925.0	185.0	65.7	36..	0.548
950.0	190.0	63.1	33.6	0.537
975.0	195.0	34.4	32.7	0.508
1000.0	200.0	53.7	32.4	0.506

CAVITY LENGTH= 17.5 M
CAVITY NOX CONC.= 1086.46 UG/M**3

MAXIMUM NOX= 1137.83 UG/M**3 AT 17.5 M

MAXIMUM NO2= 173.98 UG/M**3 AT 17.5 M

Case #13

SCRUBBER STATION CHEMISTRY MODEL

U= 4.17 M/S
a= 8.50 M
a2= 7.00 M
a3= 6.00 M
.= 2.0 M/S
V= 40.0 M/S
TS= 700.0 K
TA= 283.0 K
D= 0.300 M
STAB-E
OZONE= 40.0 PPB

ALPHA=0.0
H EFF= 30.8 M

DOWNWIND DIST (M)	TRAVEL TIME (S)	NOX CONC (UG/M**3)	NO2 CONC (UG/M**3)	NO2/NOX RATIO
50.0	25.0	0.0	0.0	0.0
75.0	37.5	0.0	0.0	0.0
100.0	50.0	0.0	0.0	0.0
125.0	62.5	0.0	0.0	0.0
150.0	75.0	0.0	0.0	0.0
175.0	87.5	0.0	0.0	0.0
200.0	100.0	0.0	0.0	0.812
225.0	112.5	0.0	0.0	1.183
250.0	125.0	0.0	0.0	1.085
275.0	137.5	0.1	0.0	0.845
300.0	150.0	0.2	0.1	0.765
325.0	162.5	0.5	0.4	0.708
350.0	175.0	1.2	0.8	0.708
375.0	187.5	2.3	1.5	0.674
400.0	200.0	3.8	2.6	0.685
425.0	212.5	5.0	3.8	0.847
450.0	225.0	8.8	5.6	0.844
475.0	237.5	12.0	7.4	0.818
500.0	250.0	15.7	8.5	0.805
525.0	262.5	18.7	11.8	0.665
550.0	275.0	24.6	13.3	0.556
575.0	287.5	28.4	15.2	0.538
600.0	300.0	32.8	18.1	0.550
625.0	312.5	37.4	23.8	0.632
650.0	325.0	41.8	25.7	0.615
675.0	337.5	48.1	22.3	0.484
700.0	350.0	50.2	27.4	0.545
725.0	362.5	54.1	27.2	0.502
750.0	375.0	57.8	28.7	0.488
775.0	387.5	61.3	28.7	0.484
800.0	400.0	34.5	28.8	0.448
825.0	412.5	87.5	44.0	0.851
850.0	425.0	70.3	30.0	0.427
875.0	437.5	72.8	25.3	0.347
900.0	450.0	75.0	32.4	0.432
925.0	462.5	77.1	36.0	0.467
950.0	475.0	78.8	48.4	0.813
975.0	487.5	80.5	38.4	0.485
1000.0	500.0	82.0	37.8	0.458

CAVITY LENGTH= 17.5 M
CAVITY NOX CONC.= 0.0 UG/M**3

MAXIMUM NOX= 81.87 UG/M**3 AT 1000.0 M

MAXIMUM NO2= 48.37 UG/M**3 AT 550.0 M

Case #14

COMPRESSOR STATION CHEMISTRY MODEL

Q= 4.17 M/S
W= 8.50 M
WB= 7.00 M
WB= 4.00 M
U= 5.0 M/S
V= 40.0 M/S
TB= 7...3 K
TA= 283.0 K
D= ...3m3 M
STAB-E
...ONE= 40.0 PPB

...PHA=0.205
H EFF= 38.8 M

DOWNWIND DIST (M)	TRAVEL TIME (S)	NOX CONC (UG/M**3)	NO2 CONC (UG/M**3)	NO2/NOX RATIO
17.5	3.5	1527.5	305.5	0.158
25.0	5.0	1467.3	287.5	0.180
50.0	10.0	1552.5	256.1	0.165
75.0	15.0	1230.2	210.9	0.171
100.0	20.0	982.2	173.2	0.176
125.0	25.0	788.0	144.5	0.183
150.0	30.0	5.7.1	122.5	0.188
175.0	35.0	505.8	106.0	0.210
200.0	40.0	421.5	93.2	0.221
225.0	45.0	358.5	83.2	0.233
250.0	50.0	305.5	75.2	0.246
275.0	55.0	265.2	68.7	0.259
300.0	60.0	232.5	63.3	0.272
325.0	65.0	205.0	59.8	0.286
350.0	70.0	184.0	55.2	0.300
375.0	75.0	168.0	52.1	0.314
400.0	80.0	151.0	48.5	0.328
425.0	85.0	138.5	47.8	0.343
450.0	90.0	128.2	44.8	0.348
475.0	95.0	118.8	42.5	0.360
500.0	100.0	112.2	44.0	0.382
525.0	105.0	108.3	42.8	0.404
550.0	110.0	101..	42.1	0.417
575.0	115.0	98.7	41.3	0.427
600.0	120.0	95..	40.8	0.438
625.0	125.0	88.8	40.2	0.447
650.0	130.0	87.8	40.4	0.465
675.0	135.0	84.5	38.8	0.471
700.0	140.0	82.3	46.7	0.567
725.0	145.0	80.3	38.4	0.478
750.0	150.0	7..5	40..	0.511
775.0	155.0	72.8	38..	0.482
800.0	160.0	75.3	37.8	0.501
825.0	165.0	73.0	38..	0.518
850.0	170.0	72.8	37.2	0.513
875.0	175.0	71.3	37.6	0.532
900.0	180.0	70..	38.0	0.542
925.0	185.0	68.8	38.4	0.557
950.0	190.0	67.8	37.8	0.554
975.0	195.0	66.7	34.5	0.514
1000.0	200.0	65.8	36.6	0.556

CAVITY LENGTH= 17.5 M
CAVITY NOX CONC.= 5743.46 UG/M**3

MAXIMUM NOX= 1527.52 UG/M**3 AT 17.5 M

MAXIMUM NO2= 305.50 UG/M**3 AT 17.5 M

Case #15

CONFIGURATION STATION CHARACTERISTICS

U= 4.17 M/S
W= 8.50 M
HB= 7.00 M
HS= 10.00 M
UP= 5.0 M/S
VP= 5.0 M/S
TS= 700.0 K
TA= 283.0 K
D= 0.000 M
STAB=3
OZONE= 40.0 PPB

K.Prm=0.245
H EFF= 13.1 M

Downwind DIST (M)	TRAVEL TIME (S)	NOX CONC (UG/M**3)	NO2 CONC (UG/M**3)	NO2/NOX RATIO
17.5	3.5	2247.3	313.0	0.139
25.0	5.0	2106.0	255.4	0.140
50.0	10.0	1587.6	228.6	0.144
75.0	15.0	1130.8	176.0	0.156
100.0	20.0	882.1	154.7	0.175
125.0	25.0	701.7	145.5	0.188
150.0	30.0	736.7	145.8	0.198
175.0	35.0	687.8	140.3	0.204
200.0	40.0	636.5	133.6	0.210
225.0	45.0	584.8	127.5	0.218
250.0	50.0	533.0	120.6	0.225
275.0	55.0	486.5	115.4	0.236
300.0	60.0	446.1	108.4	0.245
325.0	65.0	407.5	104.1	0.255
350.0	70.0	373.8	96.6	0.264
375.0	75.0	343.5	93.7	0.273
400.0	80.0	316.1	88.4	0.280
425.0	85.0	292.0	87.1	0.298
450.0	90.0	270.4	83.0	0.307
475.0	95.0	251.0	79.5	0.318
500.0	100.0	233.7	78.8	0.337
525.0	105.0	218.1	74.0	0.339
550.0	110.0	204.0	71.1	0.348
575.0	115.0	191.3	68.7	0.359
600.0	120.0	179.8	68.1	0.378
625.0	125.0	169.5	63.5	0.377
650.0	130.0	159.7	62.1	0.389
675.0	135.0	151.0	60.5	0.401
700.0	140.0	143.0	58.6	0.411
725.0	145.0	135.8	56.1	0.414
750.0	150.0	128.8	54.4	0.422
775.0	155.0	122.5	53.5	0.437
800.0	160.0	116.7	50.6	0.435
825.0	165.0	111.4	48.3	0.443
850.0	170.0	106.4	48.4	0.455
875.0	175.0	101.7	46.7	0.459
900.0	180.0	97.4	45.3	0.465
925.0	185.0	93.4	44.0	0.472
950.0	190.0	89.6	43.0	0.480
975.0	195.0	86.1	41.8	0.485
1000.0	200.0	82.7	41.0	0.495

CAVITY LENGTH= 17.5 M
CAVITY NOX CONC.= 3432.90 UG/M**3

MAXIMUM NOX= 2247.34 UG/M**3 AT 17.5 M

MAXIMUM NO2= 313.03 UG/M**3 AT 17.5 M

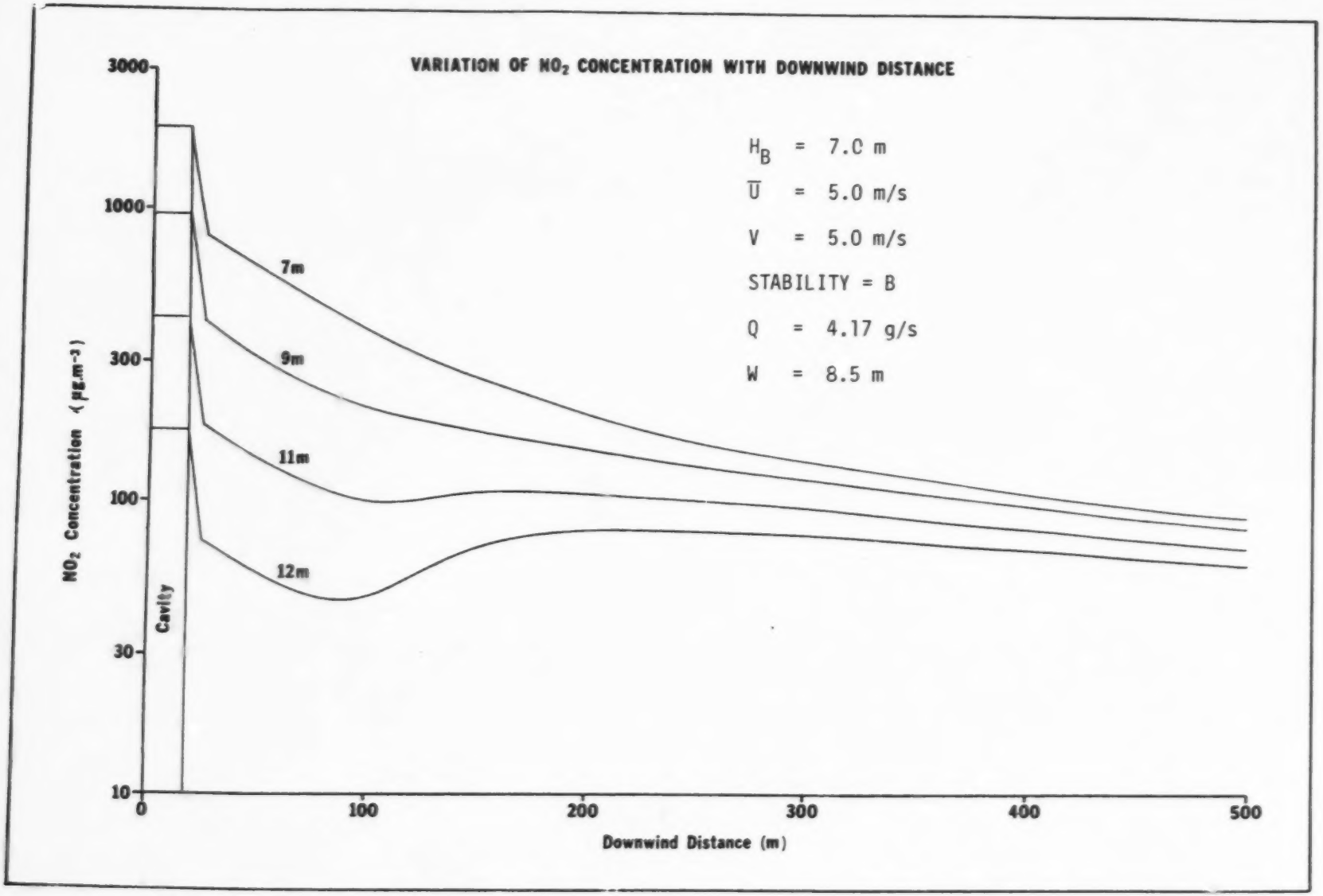

Figure 25: Variation of NO_2 Concentrations With Downwind Distance, for Stack Heights Indicated: Case 15